COMPUTER SOLUTION OF EQUATIONS
FOR THREE CENTRIFUGAL DISTRIBUTOR CONFIGURATIONS

by

Hormoz Alizadeh

Thesis submitted to the Graduate Faculty of the

Virginia Polytechnic Institute

in candidacy for the degree of

MASTER OF SCIENCE

in

Agricultural Engineering

July, 1965

Blacksburg, Virginia

TABLE OF CONTENTS

LIST OF FIGURES

LIST OF TABLES

INTRODUCTION

The use of labor saving equipment for bulk handling and application of dry granular fertilizer has become increasingly popular in recent years. Experience shows that one of the most economical and satisfactory methods of fertilizer application is with the use of centrifugal distributors. The popularity of this equipment is due to its desirable characteristics of design; economy, ease of handling and cleaning, and compactness. In addition to fertilizer, centrifugal distributors are used to apply seed and granular agricultural chemicals.

Currently, however, all centrifugal distributors, to a varying degree, have the disadvantage of uneven transverse distribution. Several studies such as those by Smith (1), and Hephard and Pascal (2), indicate that this lack of uniform distribution can seriously affect the crop yield. For profitable use of this equipment, therefore, a uniform pattern of distribution is desirable.

Such a pattern of distribution only can be obtained with equipment designed on the basis of knowledge of the principles involved. Patterson and Reece (3), Cunningham (4), and Bhagawati (5), have developed theoretical equations which accurately describe the motion of particles on the blades of centrifugal distributors. From these equations acceleration, velocity, displacement, and angle of departure may be accurately determined. The solution of these equations should, therefore, enable the designer to arrive at a satisfactory arrangement; thus insuring more uniform distribution.

Unfortunately some of the above mentioned equations are non-linear differential equations which only can be solved with computers or approximate methods. With the aid of the computer it is possible to obtain a solution with a great degree of accuracy. In addition, since the results from the computer solution may be obtained in the form of graphs, they can be used easily for any further analysis.

REVIEW OF LITERATURE

The earliest construction of centrifugal distributors for bulk fertilizer and lime dates to nearly 30 years ago. A chain on the wagon-wheel sprocket was the only source of power for this simple gravity-fed spinner. In spite of its crudeness, this machine reduced cost and labor in spreading lime and fertilizer. The machines built today are more complex than their forerunners mentioned above; nevertheless, some of the basic principles of operation remain the same.

Tests performed in 1960 and 1961 on 67 bulk spreading trucks by the Virginia Department of Agriculture (6) indicate that the amount of fertilizer collected in five-square-foot areas within a field frequently differs by several hundred per cent from the mean application rate. Many of these spreaders were equipped with centrifugal distributors. The nonuniform distribution indicates a need for further improvement of the equipment.

Field performance tests were conducted by the Virginia Agricultural Experiment Station (7) to evaluate the performance of bulk fertilizer spreader trucks as compared with the conventional tractor-drawn spreaders. The results indicate that for the same field speed, the metering of fertilizer by properly designed bulk spreaders is superior to the conventional tractor-drawn spreaders which use agitator-type metering devices. The study shows, however, that variation in truck speed, poor metering of fertilizer, and extensive variation of fertilizer physical properties are among the factors causing poor spreading.

Bhagawati (5), studying the performance of centrifugal seeders at

Ohio State University, shows that the influence of friction of seeds on distributor blades is almost negligible as compared with other distribution factors. He found that the effect of spinner speed was greater on width of coverage than on the uniformity of distribution. The distributor height measured from ground level was found to be critical. Air resistance was not studied. He concluded that the most important factor influencing uniformity is the relative feeding position of the seeds or other particles upon the rotating distributor.

Test studies conducted by Smith (1) at the University of Missouri indicate that nonuniform size, shape, and density of fertilizer material are critical factors in the mixing and spreading of dry-mixed fertilizer. Segregation of fertilizer particles due to long distances traveled, inadequately designed spreaders, and poor adjustment were also listed as problems.

The British National Institute of Agricultural Engineering (2) conducted a study on the performance of fertilizer spreading machines. Models of transverse distribution histograms were constructed on a special abacus. By forming different assumed degrees of overlap, they were able to visually estimate the variation in application rate. The performance of the centrifugal distributors was found superior to that of full-width-hopper machines. It was, however, concluded that the manufacturer should provide accurate information on the effective swath with different fertilizers and distributor rotational speeds in addition to operational information.

Crowther (8) investigated the spreading of granular fertilizer by a centrally-fed centrifugal distributor. The fertilizer was collected in radial troughs one-foot wide and having six sections, each equally spaced around the spinner. He concluded that the distribution is concentric and that the degree of segregation of the particles could be ignored in the working of the spinners. Crowther states that a centrally-fed distributor is not capable of giving even distribution.

Assuming firstly that there is no interference by the adjacent particles, and secondly that the motion of particles can be studied individually, Patterson and Reese (3) made an analysis of the motion of the fertilizer particles fed onto the center of a rotating disc. Four radial blades were mounted on the disc to form a centrifugal distributor. It was further assumed that the particles were fed onto the distributor without impact; in other words, no bouncing would occur.

It was shown that the motion of a single particle depends upon its shape and the value of the coefficient of friction between the particle and the blade. The influence of air resistance was not studied. They concluded that the final radial velocity of the particle depends on whether it would slide or roll along the blade. The study showed that in actual field operation the final speed of the particles leaving the disc was not uniform; therefore variation was caused in the final distribution pattern.

Grow (9), at Virginia Polytechnic Institute, conducted a series of tests on two centrifugal distributors, one with radial blades and the other with five-degree forward-pitched blades. The purpose of the study was to determine the proper delivery location of the fertilizer material and to correlate this variable with other parameters such as departure angle, speed of rotation, projectile path, and the pattern of distribution.

The most important variable affecting the performance was found to be the delivery location of fertilizer to the rotating distributor. The problem of material-to-blade impact was considered serious. Best results were obtained when the impact was minimized and the material was fed near the center of the distributor. The values of the coefficient of fertilizer-on-blade friction ranged between 0.3 and 0.77 in tests with triple superphosphate. Grow concluded that the centrifugal spreaders, if designed properly, have good potential for uniform distribution.

In a circular published in September, 1962, by the Agricultural Extension Service of Virginia Polytechnic Institute, the following four steps were listed as requisites to accurate spreading:

1. Accurate metering from the truck bed;
2. Proper delivery of fertilizer to the spinners;
3. Uniform distribution across the swath; and
4. Skilled operators.

OBJECTIVES

The objectives of this investigation were:

1. To solve, by electronic analog computer, equations which represent the motion of granular material on the blades of three centrifugal distributor configurations. The distinguishing component shapes identifying the three distributor configurations are (a) forward and backward-pitched, straight blades, (b) forward and backward-curved blades and, (c) concave, cone-shaped, distributor base.
2. To interpret and present the solutions in a form that a designer can obtain the desired information quickly and accurately.
3. To determine experimentally the values of granular-material-on-blade coefficient of friction for typical fertilizer and blade materials in order to establish a set of values for all design parameters.

PROCEDURE

The operating principle of the centrifugal distributor is based on the centrifugal and tangential forces imparted to the particles of the material to be distributed. Both the terms "centrifugal distributor" and "spinner" are used to designate this device. The material is fed onto the rotating distributor by various devices, such as chutes and feed rings. These methods are ideally designed to direct the flow of granular material smoothly onto the blades without appreciable impact and splattering of the material. In the computer analysis performed in this study, smooth pickup of granular material is assumed with zero initial velocity of the material with respect to the blade.

The effect of the centrifugal distributor is to impart velocity to the granular material so that its ballistic properties will be effective in carrying it through the air and depositing it across a wide band or swath. To achieve a uniform distribution pattern across this swath it is necessary that proper magnitude and direction of velocity be imparted to the material. The computer analysis to be performed is designed to supply quantitative information on how the three centrifugal distributor configurations can be used to impart a specified magnitude and direction of velocity to granular material.

Factors Involved In Study

There are many factors affecting the performance of the centrifugal distributors. Of prime importance are the following factors considered in this study:

1. Distributor configurations studied are;
    a. radial blades,
    b. forward (or backward) pitched blades,
    c. forward (or backward) curved blades, and
    d. cone-shaped distributor base.
2. Operational parameters considered include;
    a. distributor rotational velocity,
    b. position of delivery of particles to the distributor blades,
    c. and distributor blade adjustment.
3. Properties of fertilizer and fan-blade material are;
    a. coefficient of fertilizer-blade friction, and
    b. size of the particles.

Facilities

The following equipment was employed in this work:

1. Analog computer of the College of Engineering, Electronic Associates, Incorporated, Model 16-31R.
2. X-Y Recorder, Autograf Mosley, Model 2DR.
3. Centrifugal distributor apparatus including test stand and collection box.
4. Equipment and workshop of the Agricultural Engineering Department.

Derivation of Equations

As mentioned previously, there are four main distributor or distributor-blade configurations. Since the radial blade (pitch angle is equal to zero) is a special case of the straight-pitched blade, its equation of motion can be obtained easily from that of the latter. Thus, only the equations for straight-pitched blades, curved blades, and cone-shaped spinners will be derived.

While analytical and approximate solutions in general form (3,4,5) have been obtained for these configurations, long calculations are required to obtain design values. It is the purpose of the analysis and derivations that follow to arrange the problems in proper form for analog computation.

It has been noted by Patterson and Reece (3), Cunningham (4), and Bhagawati (5) that a particle on a rotating centrifugal distributor is subjected to the following three components of acceleration;

1. acceleration of the particle with respect to the path,
2. centrifugal acceleration, and
3. Coriolis acceleration which is twice the vector cross products of the angular velocity of the blade, and the particle velocity with respect to the blade.

Knowing the above components of acceleration, the reverse effective forces due to each component can be determined. In addition, the normal forces of gravity, due to the particle's mass, and friction should also be studied.

Figures 1, 2, and 3 show the particle force diagram and the top view of the straight-forward-pitched blades, forward-curved blades, and the cone-shaped spinners respectively.

According to D'Alembert's principle, the sum of the forces in the direction of the blades in Figures 1, 2, and 3 must equal zero.

The differential equations of motion with respect to the blade can now be determined. These equations are derived on the assumption that the particles will remain in contact with the blade along its length.

Symbols and Units Used in Deriving the Spinner Equations

P = displacement of the particle along the blade, feet

R = radial coordinate on distributor, feet

r = radius at which fertilizer is delivered to the blade, feet

t = time, seconds

$v = dP/dt$ = particle velocity with respect to blade, fps

a = particle acceleration with respect to blade, fps^2

w = distributor angular speed, radians per second

$\theta = wt$ = distributor angular displacement, radians

ϕ = angle of blade with respect to distributor radius, degrees

β = angle of departure of granular particle with respect to tangent to the distributor, degrees

δ = angle of blade with respect to distributor radius at r, degrees

ρ = blade's radius of curvature, feet

α = spinner cone angle, degrees

M = fertilizer particle mass, slugs

W = fertilizer particle weight, lbs

g = acceleration of gravity, fps^2

u = coefficient of fertilizer-blade friction

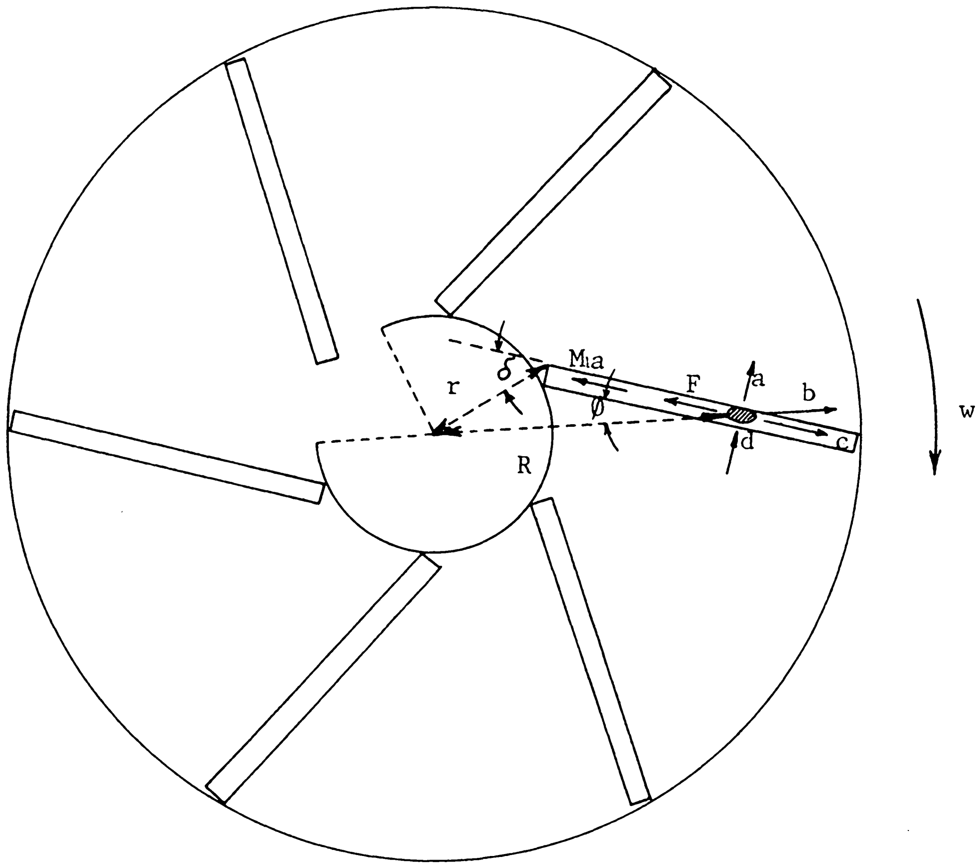

$$a = Mw^2 R \sin\emptyset$$
$$b = Mw^2 R$$
$$c = Mw^2 R \cos\emptyset$$
$$d = 2Mwv$$
$$F = u(W + 2Mwv + Mw^2 R \sin\emptyset)$$

Top View of Forward-Pitched-Bladed

Spinner Including Particle Force Diagram

Figure 1

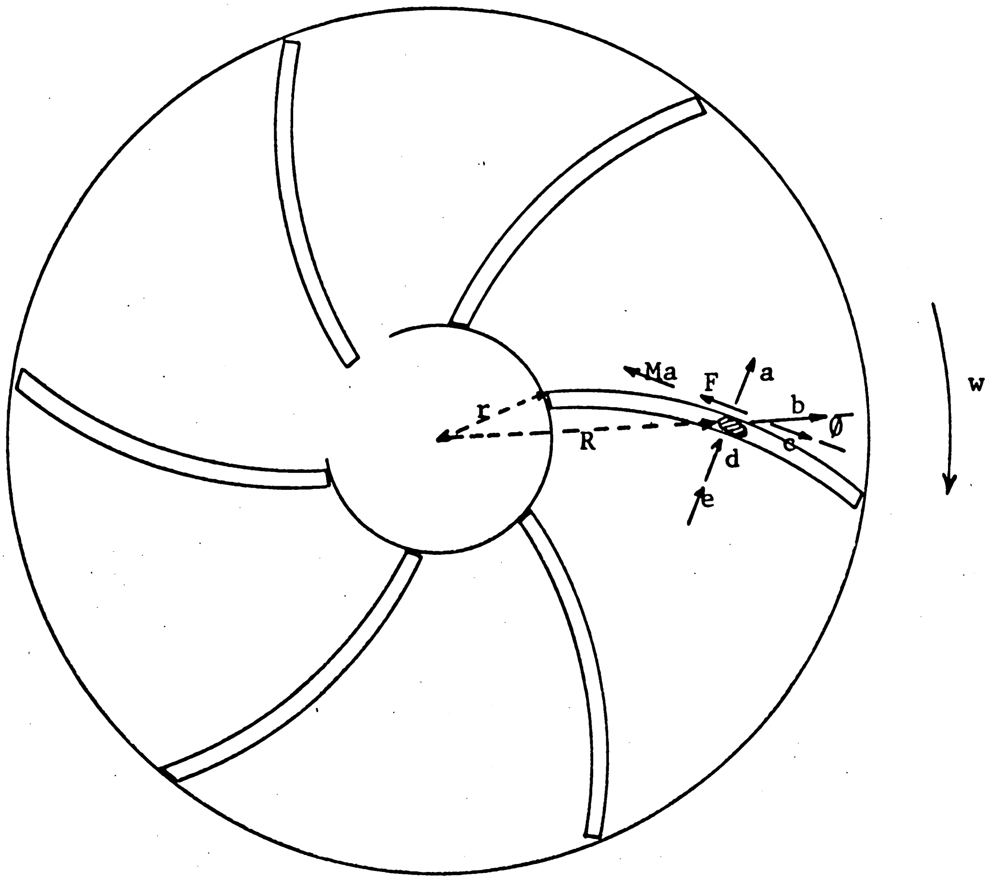

$a = Mv^2/$
$b = Mw^2R$
$c = Mw^2R \; Cos Ø$
$d = Mw^2R \; Sin Ø$
$e = 2Mwv$
$F = u(W + Mv^2/\rho + 2Mwv + Mw^2R \; Sin Ø)$

Top View of the Forward-Curved-Bladed

Spinner Including Particle Force Diagram

Figure 2

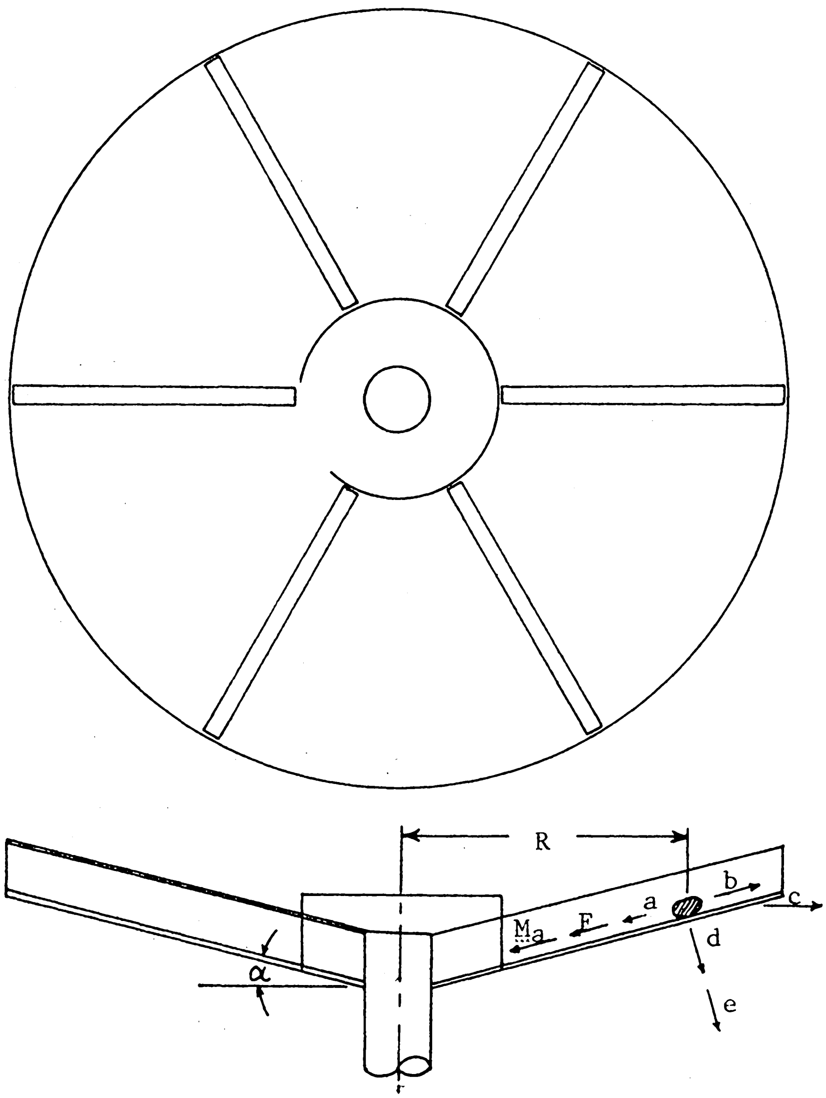

$a = W \sin\alpha$
$b = Mw^2R \cos\alpha$
$c = Mw^2R$
$d = Mw^2R \sin\alpha$
$e = W \cos\alpha$
$F = u(W \cos\alpha + 2Mwv \cos\alpha + Mw^2R \sin\alpha)$

Top and Side View of Cone-Shaped Spinner

Including Particle Force Diagram

Figure 3

Forward-Pitched Blades

The derivation of the equation of motion follows by summing the forces in the direction of the blade in Figure 1.

$$Ma + u(W + 2Mwv + Mw^2R\ Sin\emptyset) = Mw^2R\ Cos\emptyset \qquad \text{Eq. 1.1}$$

where

$$u(W + 2Mwv + Mw^2R\ Sin\emptyset) = u(\text{normal forces})$$

Using the geometrical relationships

$$R = r\ Sin\delta/Sin\emptyset$$

and

$$Cot\emptyset = (P + r\ Cos\delta)/(r\ Sin\delta)$$

in Eq. 1.1 and simplifying, the following equation is obtained:

$$d^2P/dt^2 + 2uw\ dp/dt - w^2P = w^2r\ Cos\delta - ruw\ Sin\delta - ug \qquad \text{Eq. 1.2}$$

Eq. 1.2 is the differential equation of particle motion along the blade in terms of the known parameters w, r, δ , and u. The analytical solution of this equation has been found previously (4), and is:

$$P = (Ar - ug/w^2)\left[(C + u)e^{(C-u)\theta} + (C - u)e^{-(C + u)\theta} - 2C\right]/2C$$

where

$$A = Cos\delta - u\ Sin\delta$$

$$C = \sqrt{u^2 + 1}$$

The resultant absolute velocity, V_r, of the particle as it leaves the spinner is the vector sum of the two components of velocity; namely, the tangential velocity, Rw, and the velocity with respect to the blade, V_b, as shown in Figure 4.

Therefore:

$$V_r = \sqrt{(dP/dt\ Cos\emptyset)^2 + \left[(dP/dt)\ Sin\emptyset + Rw\right]^2} \qquad \text{Eq. 1.3}$$

Eq. 1.3 can be simplified to a more convenient form involving δ and r as

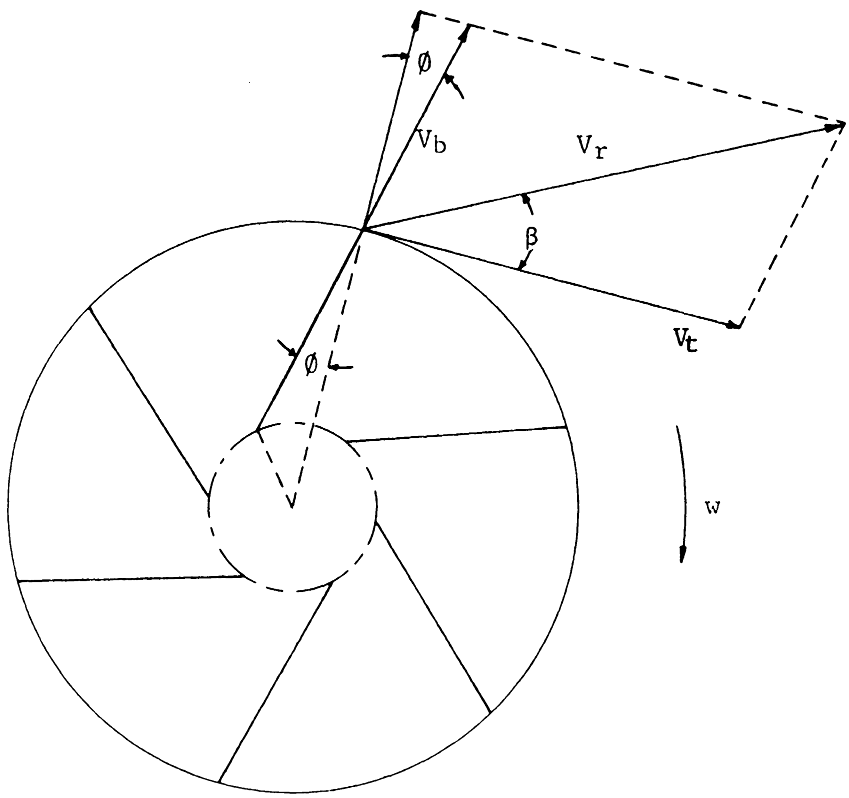

Ø = Blade Pitch
w = Disc Angular Velocity
β = Departure Angle
V_b = Velocity With Respect to Blade
V_r = Resultant Velocity
V_t = Tangential Velocity

Components of Resultant Velocity

Forward-Pitched-Bladed Spinner

Figure 4

follows:

$$V_r = \sqrt{(dP/dt)^2 + 2rw(dP/dt)\ \text{Sin}\delta + (Rw)^2} \qquad \text{Eq. 1.4}$$

If the blades are backward-pitched, changing the sign of the term $rw^2u\ \text{Sin}\delta$ will give the approximate equation of motion for this case as shown below:

$$d^2P/dt^2 + 2uw\ dP/dt - w^2P = rw^2\ \text{Cos}\delta + rw^2u\ \text{Sin}\delta - ug \qquad \text{Eq. 1.5}$$

The error in this representation of motion occurs when the material first contacts the blade. After initial contact, centrifugal acceleration occurring radially, causes momentary loss of contact with the blade. After contact has been reestablished and $2uw\ dP/dt > rw^2u\ \text{Sin}\delta$, the error vanishes.

The resultant velocity is

$$V_r = \sqrt{(dP/dt)^2 - 2rw(dP/dt)\ \text{Sin}\delta + (Rw)^2} \qquad \text{Eq. 1.6}$$

The tangent of the departure angle, β, is given below where the + sign applies to forward-pitched blades and the - sign applies to backward-pitched blades.

$$\text{Tan}\ \beta = (dP/dt\ \text{Cos}\emptyset)/\left[(Rw) \pm (dP/dt)\ \text{Sin}\emptyset)\right] \qquad \text{Eq. 1.7}$$

Forward-Curved Blades

The shape of the curved blade investigated is a logarithmic spiral. This curve has the unique characteristic of intersecting all radial lines passing through it at a constant angle, here referred to as $\emptyset$. Summing the forces in the direction tangent to the blade in Figure 2 results in the following equation:

$$Ma + u(W + Mv^2/\rho + 2Mwv + Mw^2R\ \text{Sin}\emptyset) = Mw^2R\ \text{Cos}\emptyset \qquad \text{Eq. 2.1}$$

In comparison with the equation for straight-forward-pitched blades, the term Mv^2/ρ is the only addition to this equation. This term can be converted to a simpler one invloving R and Sinϕ by using the standard formula for radius of curvature as follows:

$$\rho = (R^2 + \dot{R}^2)^{1.5}/(R^2 + 2\dot{R}^2 - R\ddot{R})$$

Since the shape of the blade is a logarithmic spiral,

then,

$$R = re^{\theta \, \mathrm{Cot}\phi}$$

$$\dot{R} = R \, \mathrm{Cot}\, \phi$$

$$\ddot{R} = R \, \mathrm{Cot}^2\phi$$

where,

R = radial coordinate,

θ = coordinate angle,

ϕ = spiral angle.

Therefore:

$$Mv^2/\rho = (Mv^2 \, \mathrm{Sin}\phi)/R$$

and

$$d^2P/dt^2 + 2uw \, dP/dt + u \, \mathrm{Sin}\phi \, (dP/dt)^2/R - Rw^2(\mathrm{Cos}\phi - u \, \mathrm{Sin}\phi) = -ug \qquad \text{Eq. 2.2}$$

Since the formula for the blade length is

$$dP = \sqrt{R^2 + \dot{R}^2} \; d\theta$$

where $\dot{R} = dR/d\theta$, then $P = (R - r)\,\mathrm{Sec}\phi$ and $dP/dt = \mathrm{Sec}\phi \, dR/dt$. Using the above relationship between P and R, Eq. 2.2 becomes:

$$d^2R/dt^2 + 2uw \, dR/dt + u \, \mathrm{Tan}\phi \, (dR/dt)^2/R - Rw^2\left[\mathrm{Cos}^2\phi - (1/2)u \, \mathrm{Sin}2\phi\right] = -ug \, \mathrm{Cos}\phi \qquad \text{Eq. 2.3}$$

Eq. 2.3 is non-linear. An approximate solution has been obtained (4), but an exact solution cannot be obtained by conventional analytical procedures.

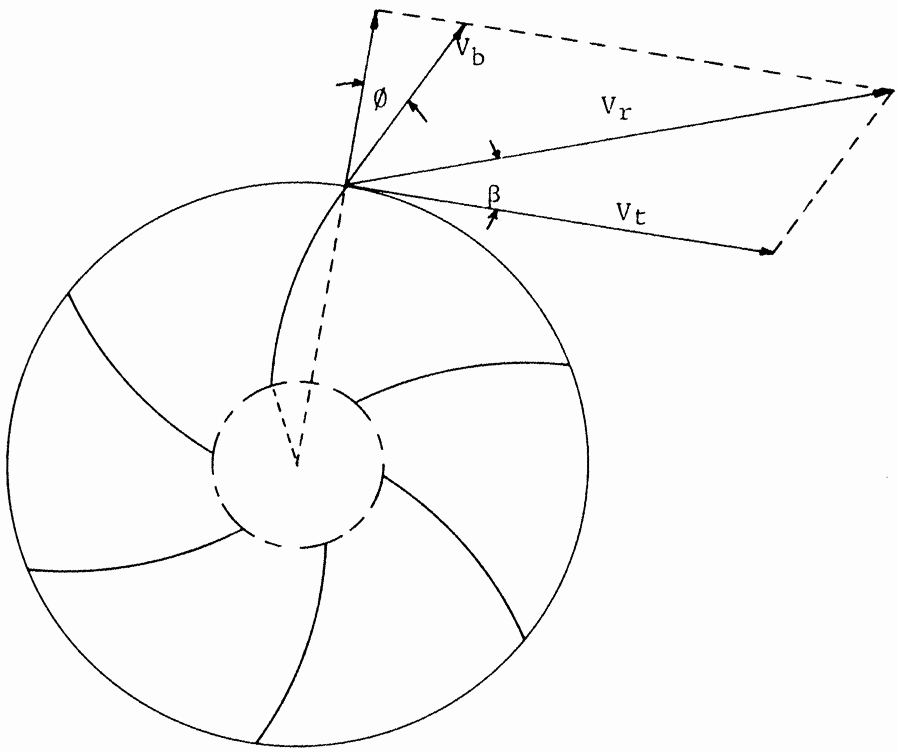

β = Departure Angle
$\emptyset$ = Angle of Blade With Respect To Spinner Radius
V_b = Velocity With Respect To Blade
V_r = Resultant Velocity
V_t = Tangential Velocity

Components of Resultant Velocity, Forward-Curved-Bladed Spinner

Figure 5

The resultant velocity of the particle as it leaves the distributor, shown in Figure 5, is

$$V_r = \sqrt{(dR/dt)^2 + \left[(dR/dt)\ Tan\emptyset + Rw\right]^2} \qquad \text{Eq. 2.4}$$

and the departure angle can be found from the following equation:

$$\beta = Arctan(dR/dt)/\left[Rw + (dR/dt)\ Tan\emptyset\right] \qquad \text{Eq. 2.5}$$

In the case of backward-curved blades the approximate differential equation of motion is:

$$d^2R/dt^2 + 2uw\ dR/dt + u\ Tan\emptyset(dR/dt)^2/R - Rw^2\left[Cos^2\emptyset + (1/2)u\ Sin2\emptyset\right] = -ug\ Cos\emptyset \qquad \text{Eq. 2.6}$$

As with the backward-pitched blades, centrifugal acceleration initially causes loss of contact with the blades. The error vanishes when $2uw\ dR/dt > (1/2)u\ Sin2\emptyset$.

The equations for resultant velocity and its departure angle are given below:

$$V_r = \sqrt{(dR/dt)^2 + (Rw - Tan\emptyset\ dR/dt)^2} \qquad \text{Eq. 2.7}$$

$$\beta = Arctan(dR/dt)/(Rw - Tan\emptyset\ dR/dt) \qquad \text{Eq. 2.8}$$

Cone-Shaped Spinner

With this type of spinner the particle is given a slight vertical component of velocity due to the shape of the distributor base or disc. Wider width-of-spread may be possible with this design.

The differential equation is obtained by summing the forces in the direction of the blade in Figure 3.

$$Ma + W\ Sin\alpha + u(W\ Cos\alpha + 2Mwv\ Cos\alpha + Mw^2R\ Sin\alpha) = Mw^2R\ Cos\alpha \qquad \text{Eq. 3.1}$$

Using the geometrical relationship, $R = P\ Cos\alpha$, the new form of Eq. 3.1 becomes:

$$d^2R/dt^2 + 2uw \operatorname{Cos}\alpha(dR/dt) + Rw^2 \left[(w/2) \operatorname{Sin}2\alpha - \operatorname{Cos}^2\alpha\right] = -ug \operatorname{Cos}^2\alpha - (1/2)g \operatorname{Sin}2\alpha \qquad \text{Eq. 3.2}$$

The analytical solution of Eq. 3.2 for zero initial velocity has been obtained by Cunningham (4):

$$R - Hg/Gw^2 = (r - Hg/Gw^2)\left[(K + u)e^{L(K - u)\theta} + (K - u)e^{-L(K + u)\theta}\right]/2K$$

where $G = \operatorname{Cos}\alpha - u \operatorname{Sin}\alpha$

$H = \operatorname{Sin}\alpha + u \operatorname{Cos}\alpha$

$K = \sqrt{u^2 + G/L}$

$L = \operatorname{Cos}\alpha$

The horizontal component of the resultant velocity, V_r, horizontal departure angle β, and the angle γ can now be obtained from Figure 6. The angle γ is the angle that the resultant velocity makes with the horizontal plane and is called the vertical departure angle.

Therefore:

$$Vr = \sqrt{(dR/dt)^2 + (Rw)^2} \qquad \text{Eq. 3.3}$$

$$\beta = \operatorname{Arctan} (dR/dt)/(Rw) \qquad \text{Eq. 3.4}$$

$$\gamma = \operatorname{Arctan} (dR/dt) \operatorname{Tan}\alpha/V_r \qquad \text{Eq. 3.5}$$

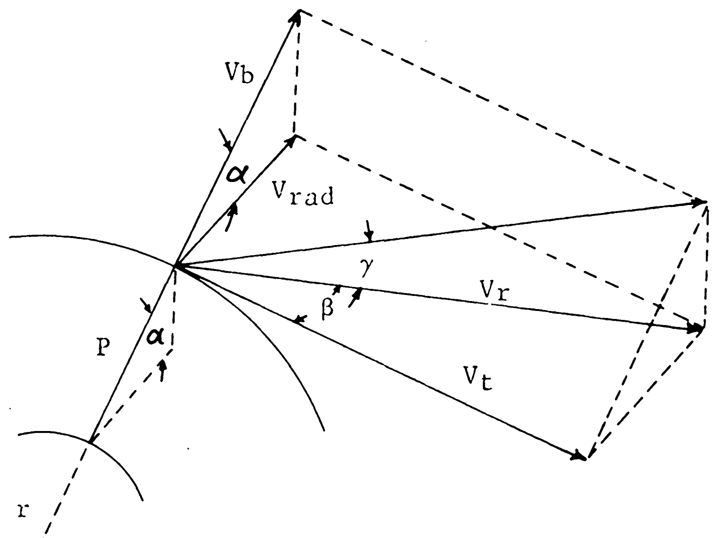

β = Horizontal Departure Angle
γ = Vertical Departure Angle
α = Cone Angle
V_b = Velocity With Respect to Blade
V_r = Component of Resultant Velocity In The Horizontal Plane
V_t = Tangential Velocity
V_{rad} = Radial Velocity

Figure 6 Components of Resultant Velocity for Cone-Shaped Spinner

Figure 6

Dimensional Analysis

Equations 1.2, 2.3, and 3.2 as they are given could be programmed for solution by the analog computer. However, since each of the parameters in the above equations has a range of values, and each individual value must be varied while the others are held constant, programming of the above equations would impose much difficulty.

In order to overcome this obstacle, dimensional analysis was employed. With dimensional analysis the above parameters are grouped into a set of dimensionless and independent quantities called pi terms (10). In this way the number of parameters is reduced considerably.

To employ dimensional analysis the total acceleration is assumed to be a function of the following parameters:

$$a = c\ P^{C1},\ r^{C2},\ R^{C3},\ t^{C4},\ V_r^{C5},\ w^{C6},\ M^{C7},\ g^{C8}$$

where c is a dimensionless function, and C1, C2, ...C8 are the appropriate exponents of the parameters previously defined. All the above parameters are expressible in terms of one or more of the following basic dimensions: time = T, length = L, and force = F.

Arranging the C exponents in terms of their basic dimensions we have:

$$L:\quad 1 = C1 + C2 + C3 + C5 - C7 + C8,$$

$$T:\quad -2 = C4 - C5 - C6 + 2C7 - 2C8,$$

$$F:\quad 0 = C7.$$

Simultaneous solution of the above equations gives:

$$C2 = 1 - C1 - C3 - C5 - C8,$$

$$C6 = C4 - C5 - 2C8 + 2.$$

Therefore:

$$a = C\ P^{C1} r^{(1-C1-C3-C5-C8)}\ R^{C3}\ t^{C4}\ V_r^{C5}\ w^{(C4-C5-2C8+2)}\ g^{C8}$$

After rearranging the terms of equal exponent and simplifying, the following equation is obtained:

$$a/rw^2 = f(P/r,\ R/r,\ V/rw,\ ug/rw^2,\ wt) \qquad \text{Eq. 4.1}$$

Inspection of the individual pi terms in the above equation indicates that they are both dimensionless and independent of other pi terms.

The differential equation of motion for the forward-pitched blades, Eq. 1.2, was shown to be:

$$d^2P/dt^2 + 2uw\ dP/dt - w^2P = w^2r\ \mathrm{Cos}\delta - uw^2r\ \mathrm{Sin}\delta - ug$$

Since $wt = \theta$ is the angular displacement of the disc through the period of time which a particle passes along the blade, the terms d^2P/dt^2 and $2uw$ dP/dt can be written as $w^2\ d^2P/d\theta^2$ and $2uw^2\ dP/d\theta$ respectively. Substituting the above two terms in Eq. 1.2 and dividing both sides by rw^2 we have the following:

$$d^2(P/r)/d\theta^2 + 2u\ d(P/r)/d\theta - (P/r) = \mathrm{Cos}\delta - u\ \mathrm{Sin}\delta - ug/rw^2 \qquad \text{Eq. 1.9}$$

where r is a parameter previously defined.

As can be seen by inspection, the terms of Eq. 1.9 are dimensionless and in accordance with Eq. 4.1. The advantage of Eq. 1.9 over Eq. 1.2 is that the three parameters u, r, and w are grouped together in the form of the dimensionless term ug/rw^2. Also, the main variable of Eq. 1.9, P/r, is dimensionless and therefore easier to handle.

Likewise, the equations of motion for the forward-curved blade and cone-shaped spinner, Eqs. 2.3 and 3.2, can be made dimensionless and are given by Eqs. 2.6 and 3.6 respectively.

$$d^2(R/r)/d\theta^2 = -2u\ d(R/r)/d\theta - u\ \mathrm{Tan}\phi\left[d(R/r)/d\theta\right]^2/(R/r) + \left[\mathrm{Cos}^2\phi - (1/2)\ u\ \mathrm{Sin}2\phi\right](R/r) - (ug/rw^2)\ \mathrm{Cos}\phi \qquad \text{Eq. 2.6}$$

and

$$d^2(R/r)/d\theta^2 = -2u\ \mathrm{Cos}\alpha\ d(R/r)/d\theta - \left[(1/2)u\ \mathrm{Sin}2\alpha - \mathrm{Cos}^2\alpha\right](R/r) - (g/2rw^2)\ \mathrm{Sin}2\alpha - (ug/rw^2)\ \mathrm{Cos}^2\alpha \qquad \text{Eq. 3.6}$$

The dimensionless forms of the equations for resultant velocity and departure angle are given by the following equations:

$$V_r = \sqrt{\left[d(P/r)/d\theta\right]^2 + 2\mathrm{Sin}\delta\ \ d(P/r)/d\theta + (R/r)^2} \qquad \text{Eq. 1.10}$$

$$\mathrm{Tan}\,\beta = \left[d(P/r)/d\theta\right]\ \mathrm{Cos}\phi/\left[R/r + \mathrm{Sin}\phi\ d(P/r)/d\theta\right] \qquad \text{Eq. 1.11}$$

for the forward-pitched blades,

$$V_r = \sqrt{\left[d(R/r)/d\theta\right]^2 + \left[\mathrm{Tan}\phi\ d(R/r)/d\theta + R/r\right]^2} \qquad \text{Eq. 2.7}$$

$$\beta = \mathrm{Arctan}\left[d(R/r)/d\theta\right]/\left[R/r + \mathrm{Tan}\phi\ d(R/r)/d\theta\right] \qquad \text{Eq. 2.8}$$

for the forward-curved blades, and

$$V_r = \sqrt{\left[d(R/r)/d\theta\right]^2 + (R/r)^2} \qquad \text{Eq. 3.7}$$

$$\beta = \mathrm{Arctan}\left[d(R/r)/d\theta\right]/(R/r) \qquad \text{Eq. 3.8}$$

$$\gamma = \mathrm{Arctan}\ \left[\mathrm{Tan}\alpha\ d(R/r)/d\theta\right]/V_r \qquad \text{Eq. 3.9}$$

for the cone-shaped spinner.

Computer Programming

Time Scaling

In actual operation of the centrifugal distributors the time required between pickup and departure of material from the blades is only a fraction of a second. Therefore, in order to accurately record the computer solution with an X-Y plotter, the speed of operation of the computer must be reduced. This is referred to as "time scaling." Since the equations to be solved are in terms of the angle θ which is a function of time, a value of $\tau = 180\ \theta/20$ was used to reduce the speed of operation. τ is the computer time in seconds. In this way one second of computer time will represent 20 degrees of the distributor rotation, θ. By using a recorder sweep rate of one inch per second, one inch on the X-axis will represent 20 degrees.

Magnitude Scaling

In order not to exceed the $\pm$ 100 volt limits imposed by the EAI 16-31R analog computer, the equations to be solved must be properly scaled. This requires a knowledge of the maximum values of the variables in the equations. Assuming that the radius in most spinners will not exceed one foot, and that the minimum feeding radius is 0.1 feet, the maximum value of R/r would equal 10.

$$R/r \Big|_{max.} = 10$$

In the case of radial blades, and neglecting any friction,

$$R/r \approx \operatorname{Cosh}\theta$$

therefore:

$$d(R/r)/d\theta \Big|_{Max.\ at\ R/r\ =\ 10} = 10$$

$$d^2(R/r)/d\theta^2 \Big]_{max.\ at\ R/r\ =\ 10} \approx 10$$

and

$$\theta \Big]_{max.\ at\ R/r\ =\ 10} = 3 \text{ radians} = 172 \text{ degrees}$$

Since $\mathcal{T} = 180\ \theta/20 = 2.8648\ \theta$ was the time scale selected, the conversion from the actual spinner time to that of computer time is found from the following relationships:

$$d(R/r)/d\theta = 2.8648\ d(R/r)/d\mathcal{T}$$

$$d^2(R/r)/d\theta^2 = (2.8648)^2\ d^2(R/r)/d\mathcal{T}^2$$

Therefore, the maximum values of $d(R/r)/d\mathcal{T}$ and $d^2(R/r)/d\mathcal{T}^2$ are

$$d(R/r)/d\mathcal{T}\Big]_{max.} = 10/2.8648 = 3.5$$

and

$$d^2(R/r)/d\mathcal{T}^2\Big]_{max.} = 10/(2.8648)^2 = 1.22$$

The magnitude scale factors can now be determined:

Scale factor for $(R/r) = 100/10 = 10$ volts/ft,

Scale factor for $d(R/r)/d\mathcal{T} = 100/3.5 \approx 30$ volts/fps,

Scale factor for $d^2(R/r)/d\mathcal{T}^2 = 100/1.22 \approx 80$ volts/fps^2.

Likewise,

Scale factor for $(P/r) = 10$ volts/ft,

Scale factor for $d(P/r)/d\mathcal{T} = 30$ volts/fps,

Scale factor for $d^2(P/r)/d\mathcal{T}^2 = 80$ volts/fps^2.

The completed scaled equations for the three distributor configurations, Eqs. 1.9, 2.6, and 3.6, are given below:

Forward-Pitched Blades;

$$(8.207/80)\left[80\ d^2(P/r)/d\mathcal{T}^2\right] = -2u(2.8648/30)\left[30\ d(P/r)/d\mathcal{T}\right] + (1/10)$$
$$(10P/r) + (\cos\delta - u\sin\delta - ug/rw^2)$$

or in the form for analog computer programming:

$$80\ d^2(P/r)/d\tau^2 = -1.862u\left[30\ d(P/r)/d\tau\right] + 0.9747(10\ P/r) + 9.747$$

$$(\cos\delta - u\ \sin\delta - ug/rw^2) \qquad \text{Eq. 1.12}$$

Forward-Curved Blades;

$$80\ d^2(R/r)/d\tau^2 = -1.862u\left[30d(R/r)/d\tau\right] - 0.899u\ \tan\phi\left[30\ d(R/r)/d\tau\right]^2/$$

$$(10/R/r) + 0.9747\left[\cos^2\phi - (1/2)u\ \sin 2\phi\right](10R/r) - 9.747(ug/rw^2)\ \cos\phi$$

$$\text{Eq. 2.9}$$

Cone-Shaped Spinner;

$$80\ d^2(R/r)/d\tau^2 = -1.862u\left[\cos\alpha\ 30d(R/r)/d\tau\right] - 0.9747\left[(1/2)u\sin 2\alpha\right.$$

$$\left.- \cos^2\alpha\right](10R/r) - 9.747(ug/rw^2)\left[\cos^2\alpha + (1/2u)\ \sin 2\alpha\right] \qquad \text{Eq. 3.10}$$

Potentiometer Settings

Since the term ug/rw^2 appears in all three of the above equations, a nomograph was constructed which gives the values of ug/rw^2 quite readily. This nomograph is shown in Figure 7. With the aid of a straight edge and the key given in the nomograph, any value of ug/rw^2 can be obtained for the given range of its parameters.

Since it is believed that the information obtained from this study is of value to designers, the largest practical range of each parameters is used. Table 1 gives the values of the parameters that were used in this analysis. Also given in Table 1 are the calculated maximum, minimum, and midpoint values of ug/rw^2.

Using the equation for the spinner with straight-forward-pitched blades, Eq. 1.12, as an example, its two parametric coefficients are 1.862 u and 9.747 ($\cos\delta$ - u $\sin\delta$ - ug/rw^2).

As shown in Table 1, the parameters u, δ, and ug/rw^2 were each given three values. Therefore, 27 combinations of these parameters are possible.

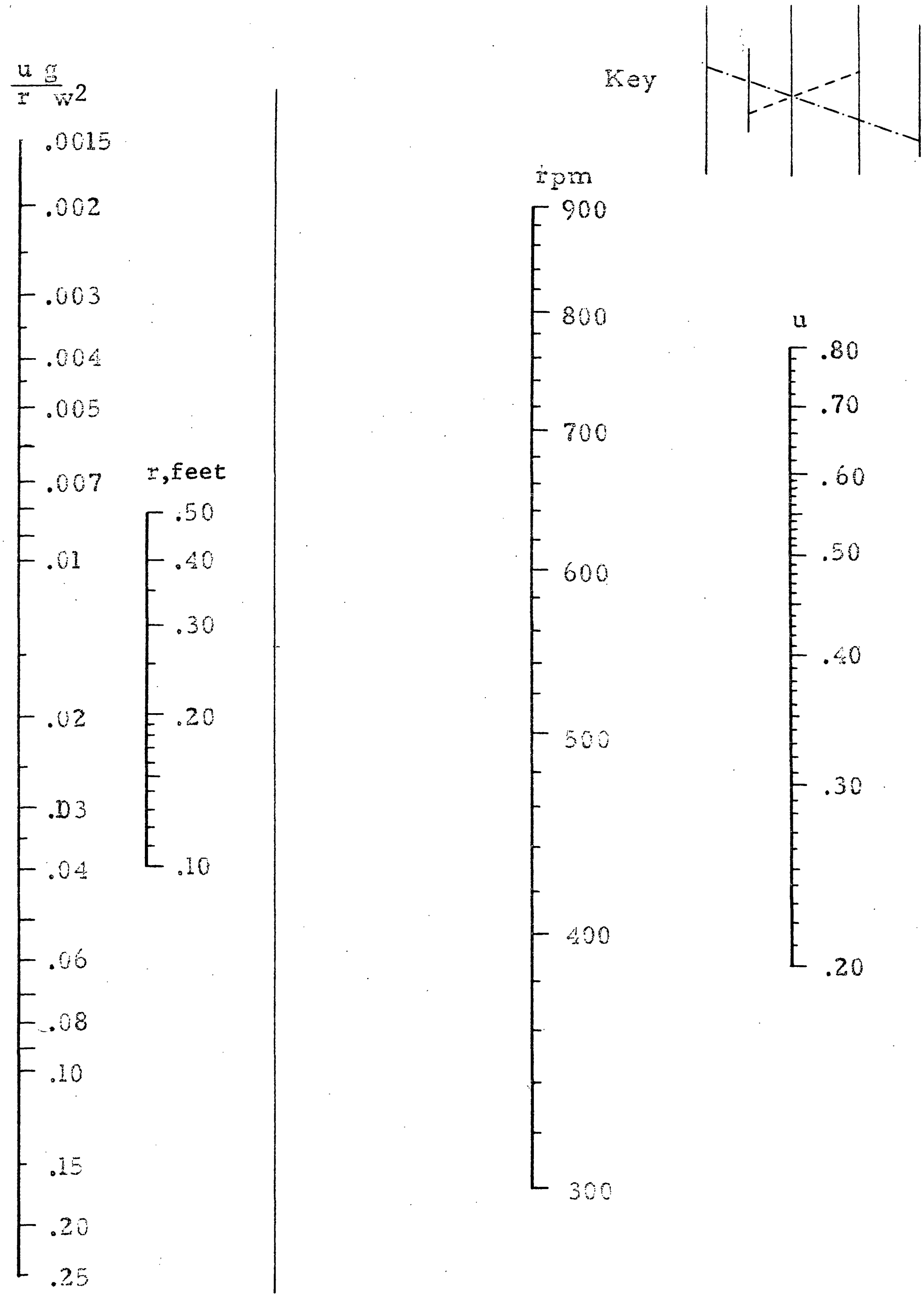

Nomograph For Determining the Values of $ug/r\,w^2$

Figure 7

These values which are the settings of the potentiometers, are given in Table 2. The potentiometer settings (the coefficients of the differential equations of motion) for the forward-curved blades and the cone-shaped distributor are given in Tables 3 and 4 respectively.

Table 1 - Values of Parameters Programmed

Blade Pitch δ Degrees	Distributor Cone Angle α Degrees	Blade Spiral Angle ϕ Degrees	Particle-Blade Coefficient of Friction u	$ug/r\omega^2$
0	10	10	0.2	0.002
30	15	20	0.5	0.126
60	20	30	0.8	0.250

Table 2 - Potentiometer Settings For Spinner With Straight-Pitched Blades

ug/rw^2	δ	u	Pot. No. 1	Pot. No. 3	Pot. No.3 Backward
0.002	0	0.2	0.1396	0.0000	-
0.126	0	0.2	0.1396	0.0046	
0.250	0	0.2	0.1396	0.0091	-
0.002	0	0.5	0.3491	0.0000	-
0.126	0	0.5	0.3491	0.0046	-
0.250	0	0.5	0.3491	0.0091	-
0.002	0	0.8	0.5584	0.0000	-
0.126	0	0.8	0.5584	0.0046	-
0.250	0	0.8	0.5584	0.0091	-
0.002	30	0.2	0.1396	0.0278	0.0352
0.126	30	0.2	0.1396	0.0234	0.0307
0.250	30	0.2	0.1396	0.0188	0.0261
0.002	30	0.5	0.3491	0.0224	0.0407
0.126	30	0.5	0.3491	0.0179	0.0361
0.250	30	0.5	0.3491	0.0134	0.0316
0.002	30	0.8	0.5584	0.0169	0.0462
0.126	30	0.8	0.5584	0.0124	0.0417
0.250	30	0.8	0.5584	0.0075	0.0371
0.002	60	0.2	0.1396	0.0118	0.0245
0.126	60	0.2	0.1396	0.0073	0.0200
0.250	60	0.2	0.1396	0.0028	0.0154
0.002	60	0.5	0.3491	0.0024	0.0340
0.126	60	0.5	0.3491	0.0021	0.0295
0.250	60	0.5	0.3491	-0.0067	0.0249
0.002	60	0.8	0.5584	-0.0071	0.0435
0.126	60	0.8	0.5584	-0.0116	0.0390
0.250	60	0.8	0.5584	-0.0161	0.0344

Table 3 - Potentiometer Settings For Spinner With Curved Blades

ug/rw^2	ø	u	Pot. No. 1	Pot. No. 2	Pot. No. 3	Pot. No. 4	Pot. No. 3 Backward
0.002	10	0.2	0.0000	0.0117	0.3419	0.1396	0.3670
0.126	10	0.2	0.0045	0.0117	0.3419	0.1396	0.3670
0.250	10	0.2	0.0090	0.0117	0.3419	0.1396	0.3670
0.002	10	0.5	0.0000	0.0294	0.3221	0.3491	0.3858
0.126	10	0.5	0.0045	0.0294	0.3221	0.3491	0.3858
0.250	10	0.5	0.0090	0.0294	0.3221	0.3491	0.3858
0.002	10	0.8	0.0000	0.0470	0.3045	0.5584	0.4042
0.126	10	0.8	0.0045	0.0470	0.3045	0.5584	0.4042
0.250	10	0.8	0.0090	0.0470	0.3045	0.5584	0.4042
0.002	20	0.2	0.0000	0.0243	0.2993	0.1396	0.3462
0.126	20	0.2	0.0043	0.0243	0.2993	0.1396	0.3462
0.250	20	0.2	0.0086	0.0243	0.2993	0.1396	0.3462
0.002	20	0.5	0.0000	0.0606	0.2640	0.3491	0.3814
0.126	20	0.5	0.0043	0.0606	0.2640	0.3491	0.3814
0.250	20	0.5	0.0086	0.0606	0.2640	0.3491	0.3814
0.002	20	0.8	0.0000	0.0971	0.2287	0.5584	0.4166
0.126	20	0.8	0.0043	0.0971	0.2287	0.5584	0.4166
0.250	20	0.8	0.0086	0.0971	0.2287	0.5584	0.4166
0.002	30	0.2	0.0000	0.0385	0.2424	0.1396	0.3057
0.126	30	0.2	0.0040	0.0385	0.2424	0.1396	0.3057
0.250	30	0.2	0.0079	0.0385	0.2424	0.1396	0.3057
0.002	30	0.5	0.0000	0.0962	0.1949	0.3491	0.3532
0.126	30	0.5	0.0040	0.0962	0.1949	0.3491	0.3532
0.250	30	0.5	0.0079	0.0962	0.1949	0.3491	0.3532
0.002	30	0.8	0.0000	0.1540	0.1475	0.5584	0.4007
0.126	30	0.8	0.0040	0.1540	0.1475	0.5584	0.4007
0.250	30	0.8	0.0079	0.1540	0.1475	0.5584	0.4007

Table 4 - Potentiometer Settings for Cone-Shaped Spinner

$ug/r\omega^2$	α	u	Pot. No. 1	Pot. No. 2	Pot. No. 3
0.002	10	0.2	0.1375	0.3419	0.0000
0.126	10	0.2	0.1375	0.3419	0.0084
0.250	10	0.2	0.1375	0.3419	0.0166
0.002	10	0.5	0.3438	0.3232	0.0000
0.125	10	0.5	0.3438	0.3232	0.0060
0.250	10	0.5	0.3438	0.3232	0.0119
0.002	10	0.8	0.5501	0.3045	0.0000
0.126	10	0.8	0.5501	0.3045	0.0054
0.250	10	0.8	0.5501	0.3045	0.0108
0.002	15	0.2	0.1349	0.3227	0.0000
0.126	15	0.2	0.1349	0.3227	0.0101
0.250	15	0.2	0.1349	0.3227	0.0201
0.002	15	0.5	0.3372	0.2953	0.0001
0.126	15	0.5	0.3372	0.2953	0.0067
0.250	15	0.5	0.3372	0.2953	0.0133
0.002	15	0.8	0.5396	0.2679	0.0000
0.126	15	0.8	0.5396	0.2679	0.0058
0.250	15	0.8	0.5396	0.2679	0.0115
0.002	20	0.2	0.1312	0.2992	0.0000
0.126	20	0.2	0.1312	0.2992	0.0115
0.250	20	0.2	0.1312	0.2992	0.0227
0.002	20	0.5	0.3280	0.2640	0.0000
0.126	20	0.5	0.3280	0.2640	0.0070
0.250	20	0.5	0.3280	0.2640	0.0139
0.002	20	0.8	0.5246	0.2286	0.0000
0.126	20	0.8	0.5246	0.2286	0.0059
0.250	20	0.8	0.5246	0.2286	0.0117

Computer Circuit Diagrams

The analog computer used in this study was the PACE 16-31R made by Electronic Associates, Incorporated, West Long Branch, New Jersey. The circuit diagram for the radial blade distributor is shown in Figure 8; for forward-pitched blades, Figure 9; for forward-curved blades, Figure 10; and for the cone-shaped distributor, Figure 11.

It was hoped that the resolver available in the computer would be used to transform the two rectangular components of the resultant velocity into their polar coordinates, thereby giving the resultant velocity and its angle of departure. However, with the pitched-straight blades, due to the non-linear equipment used in the open loop circuit of the problem, and lack of an initial condition on one component, considerable difficulty was experienced.

To overcome this difficulty, a square root circuit and a division circuit were employed to provide the resultant velocity and Tan β . Here again, due to the difficulties mentioned above, the performance of the division circuit was unsatisfactory. Consequently, as can be seen from the graphs for forward and backward-pitched blades, instead of the tangent of β, its X and Y components are given. To obtain Tanβ at any point, the value of Y read from the graph must be divided by its corresponding value of X.

Also with the forward-pitched blades, as the angle δ increases, the values of P/r and V/rw decrease. As the coefficient of friction is increased, a point is reached (δ = 60 degrees, u = 0.5, and $ug/rw^2 = 0.25$) at which the material tends to leave the feed ring in a direction opposite

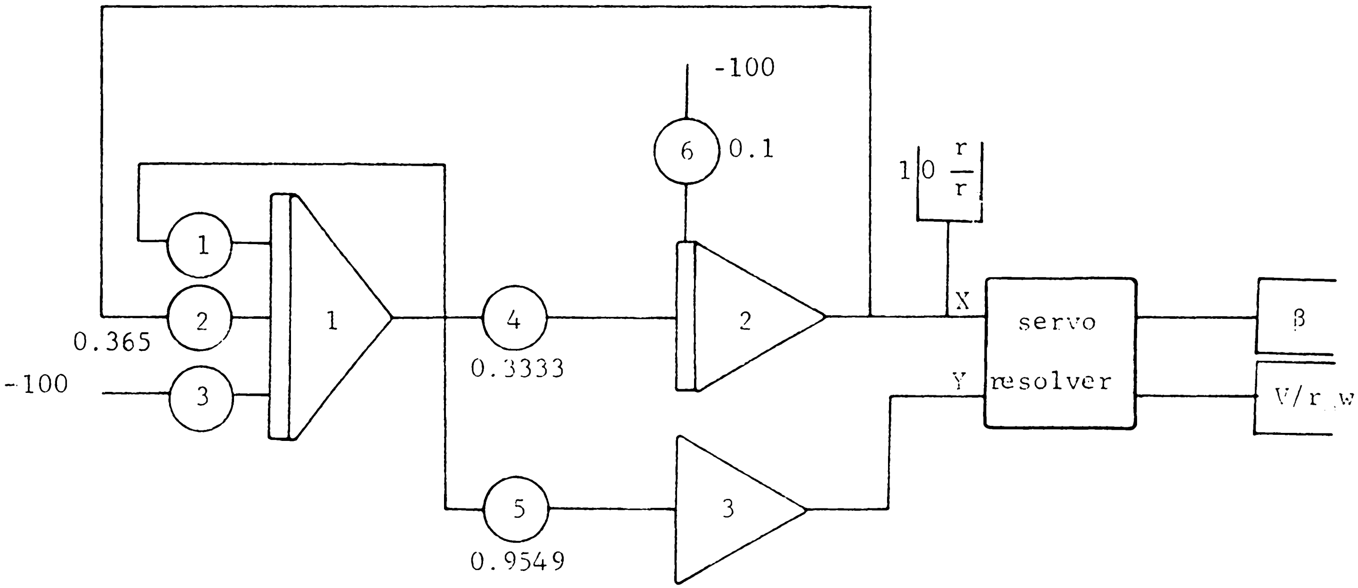

COMPUTER CIRCUIT REPRESENTING THE EQUATION FOR RADIAL BLADED SPINNER

Figure 8

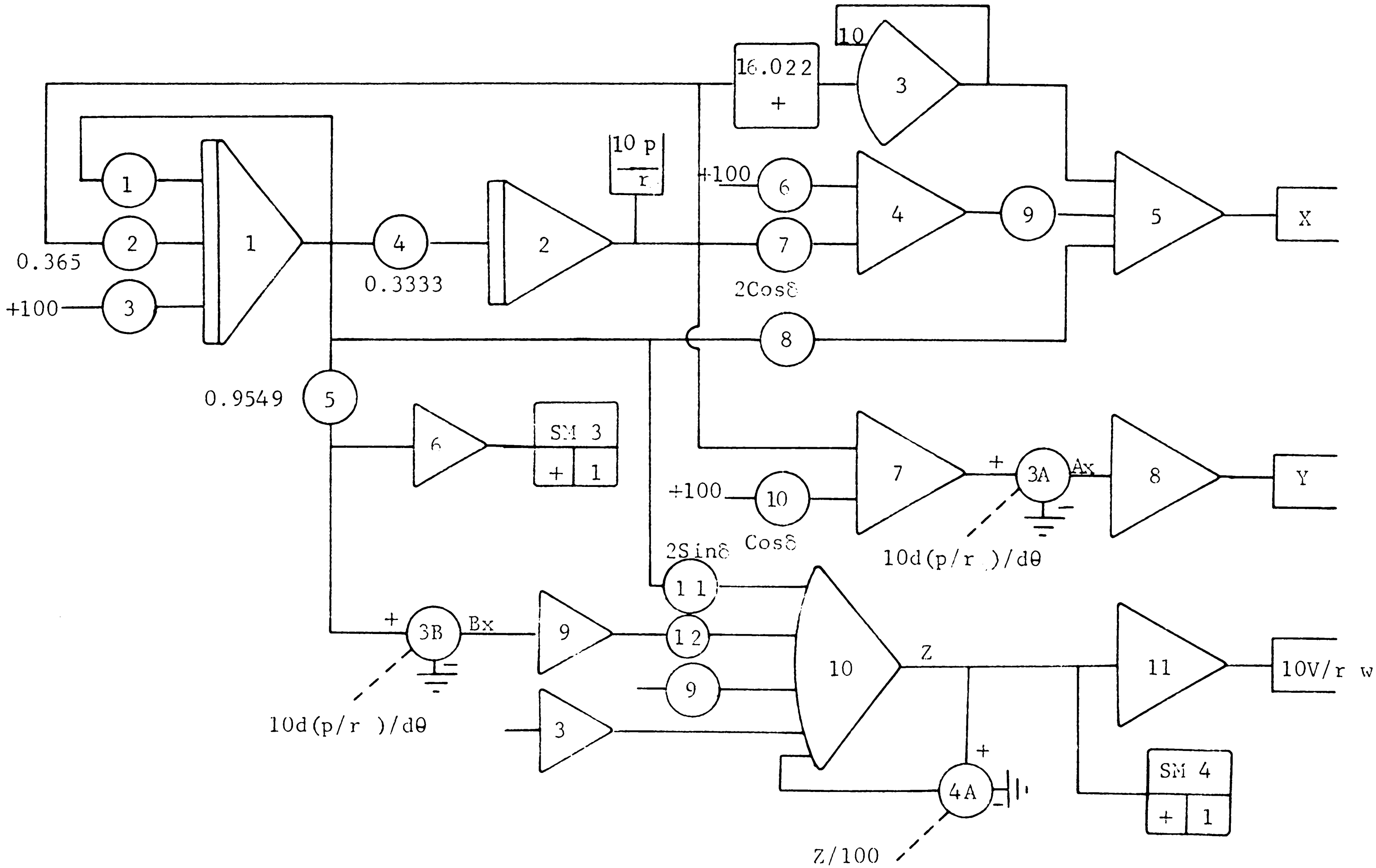

COMPUTER CIRCUIT REPRESENTING THE EQUATION FOR FORWARD-PITCHED-BLADED SPINNER

Figure 9

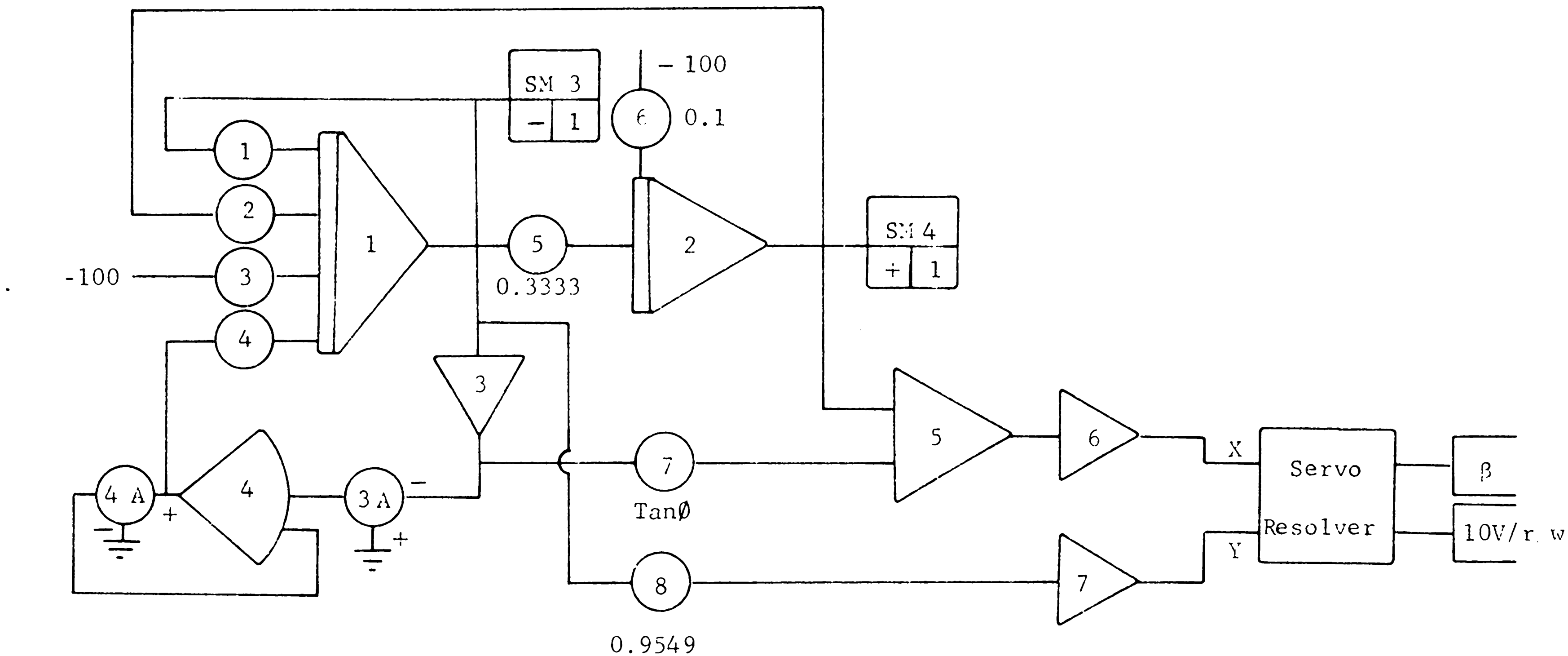

COMPUTER CIRCUIT REPRESENTING THE EQUATION FOR CURVED-BLADED SPINNER

Figure 10

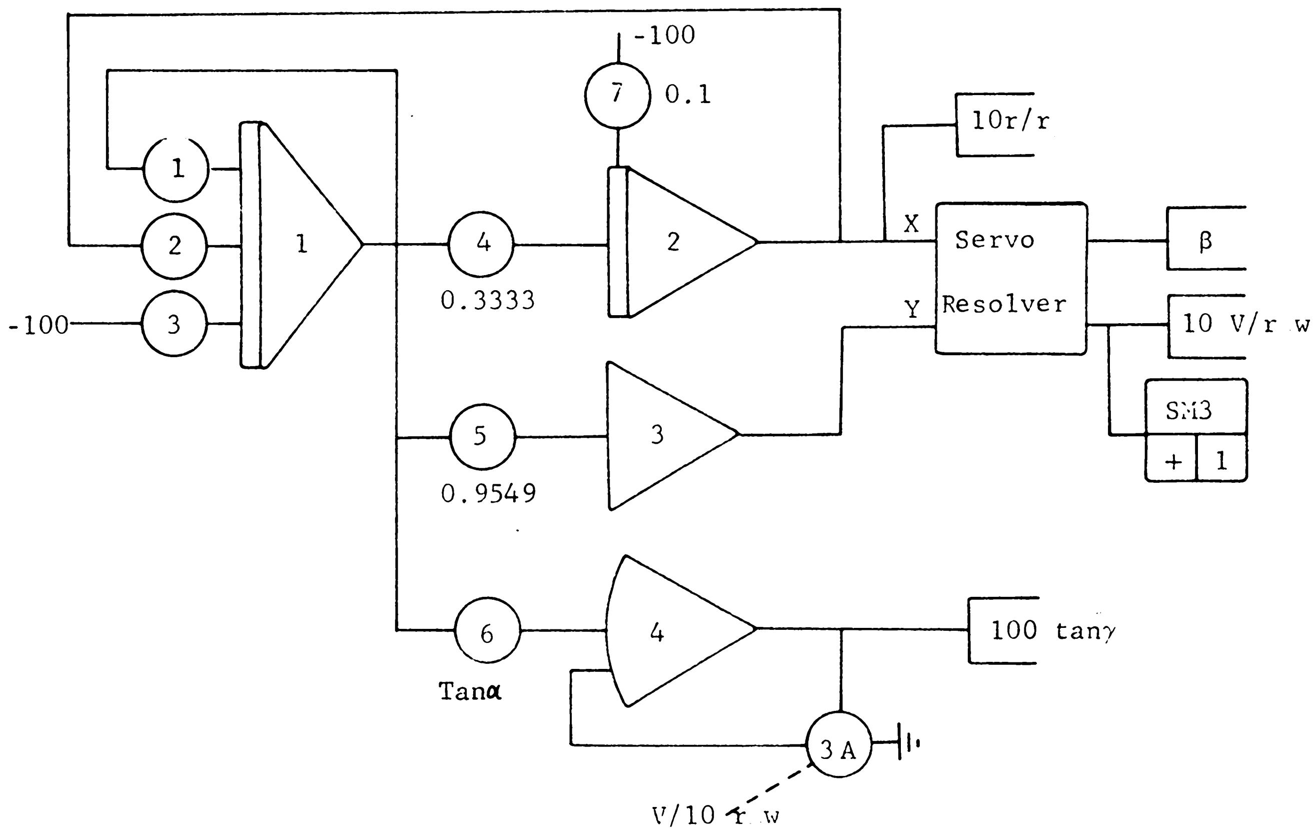

COMPUTER CIRCUIT REPRESENTING THE EQUATION FOR CONE-SHAPED SPINNER

Figure 11

to that of the blades. This is shown by the negative values of the term $9.747(\cos\delta - u \sin\delta - ug/r\omega^2)$ in Table 2. These values were not programmed because such a design was not considered to be practical.

Experimental Determination of the Coefficient of Friction

As seen from the results of the computer analysis, the coefficient of particle-blade friction has a significant influence upon the performance of the centrifugal distributors. It was, therefore, considered imperative to have an accurate knowledge of its values. If the angular displacement, θ, of the spinner between pickup and departure of fertilizer could be determined experimentally, the values of u could be found by referring to the graphs obtained from the computer.

An experiment was conducted to determine the values of the coefficient of friction as accurately as possible. The fertilizer used in this experiment was granular 46% Triple Superphosphate. The phosphate particles were irregular in shape and their bulk density obtained by the loose fill technique was 58.28 pounds per cubic foot. The distribution of particle sizes is shown in Table 5. This experiment is explained below.

Table 5 - Density and Sieve Analysis
of Granular 46% Triple Superphosphate

Density lb/ft^3	Sieve Analysis, Per Cent Retained on U. S. Sieve 8	12	16	20	Pan
58.25	5.00	33.25	47.75	11.25	2.75

Testing Procedure

The apparatus for determining the values of the coefficient of friction consisted of the following:

1. Flat distributor base or disc. Steel blades, semicircular in cross section. The center feed ring was stationary with a one-inch by one and five-eighths-inch wide opening instead of the standard 85 degree opening shown in Figure 14.
2. Fertilizer hopper with an electrical, motor-driven agitator.
3. Three phase, one-horsepower motor driving the distributor.
4. Test stand and the collection box.

Figure 12 shows the distributor and the collection box. Six steel blades were bolted to the distributor so that the blades were pitched forward with the angle $\delta = 30$ degrees.

The collection box was designed by Grow (9). A top view is shown in Figure 13. The box is a light-weight container with eight aluminum vanes which are free to rotate on their pivot pins through an angle of nearly 31 degrees. Pins are located on 23 degree intervals.

The vanes divide the collection box into nine sections. The box relative to the spinner was located in such a way that the largest percentage of the total amount of fertilizer distributed was collected in the middle sections and the smallest percentage at the end sections. This arrangement is shown in Figure 14.

The angle θ_m was found by locating the point at which the mass center of the material left the disc. However, to determine the actual amount of distributor rotation, two values must be subtracted from this angle. These two are the angle of inclination of the blades, η, and the angle θ' due to the small gap existing between the actual departure from the disc and the pickup at the collection box.

Hence,

$$\theta = \theta_m - (\eta + \theta'),$$

where

θ = the actual angular rotation of the spinner,

θ_m = measured angular location of mass center of fertilizer deposited in collection box,

η = the angle between the radius to the pickup point of the blade, r, and the radius to the tip of the blade, R.

θ' = the angle between the radius at the point of departure from the blade tip and the radius to the collection box where the fertilizer is deposited.

The formula for determining the angle θ' is given by Grow (9) as follows:

$$\text{Tan}\beta_m = \text{Tan}\theta'/2 + a/R\ \text{Sin}\theta'.$$

β_m is the observed angle of departure of the material as determined from the alignment of the vanes, and a is the distance between the blade tips and the collection box.

Table 6 gives the values of θ', θ_m, β_m, and the corrected angle of rotation, θ. The values of θ_m are based on the data given in the polar diagram of Figure 15. Knowing θ, the values of the coefficient of friction can now be determined. Since the values of $P = 6.75$ inches, $r = 3.2$ inches, and $w = 510$ rpm are known from the experiment, assuming a value of $u = 0.5$, then $ug/rw^2 = 0.021$. By referring to the graphs of the

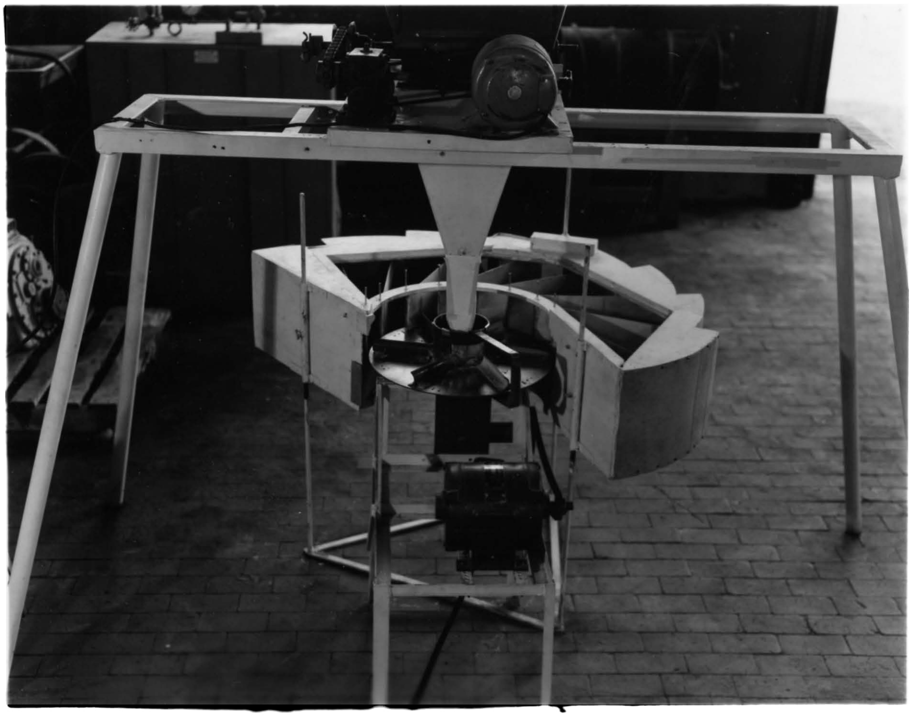

Figure 12 Distributor and Collection Box

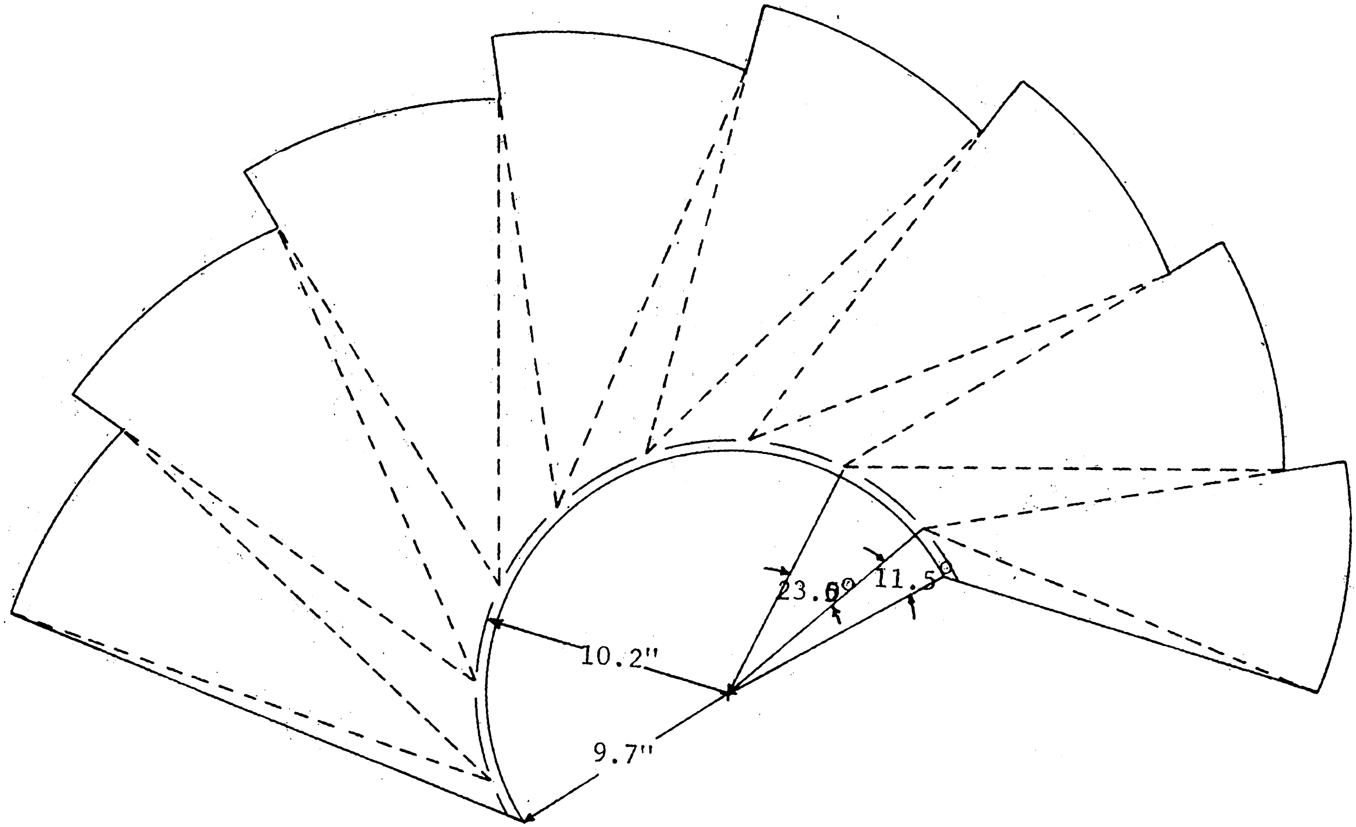

Top View of Collection Box

Figure 13

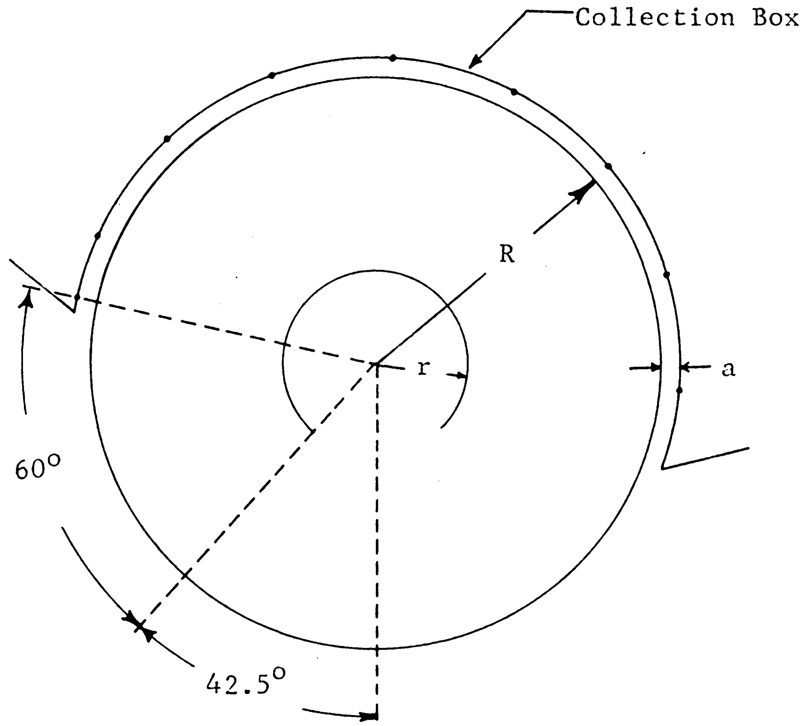

Location of Collection Box

Relative to Disc

Figure 14

forward-pitched blades obtained from the computer (for $u = 0.5$ and $\delta = 30$ degrees), a curve was interpolated for $ug/r\omega^2 = 0.021$.

Table 6 - Spinner Angular Displacement

Test No.	β_m Average	θ'	θ_m	θ	u
1	28	4	173.2	169.2	0.54
2	30	6	175.5	169.5	0.54
3	30	6	179.4	173.4	0.55
4	32	8	180.5	172.5	0.55
5	30	6	181.5	175.5	0.56

The value of $P/r = 2.11$ is known from the experiment and the corresponding value of the angular displacement, θ, was obtained from the graph for $ug/rw^2 = 0.021$. A trial and error procedure was continued until a value of u was found which resulted in agreement of the experimental and computer values of distributor rotation, θ. The values of u for the five tests are given in Table 6.

A simple test was conducted to check the values of u obtained previously. In this experiment one of the disc blades was bolted to a T-bevel which was fastened into a vice. A group of fertilizer particles, stuck to a small piece of adhesive tape to prevent rolling, was then located on the blade. The angle of the blade formed with the horizontal portion of the T-bevel was then gradually increased until a slight tapping caused the tape and the particles to slide along the blade. This angle was then measured with a protractor. The tangent of this angle is the coefficient of friction.

It is interesting to note at this point that when the blade used in this experiment was covered with fertilizer dust, which is the usual case after a few runs, the value of u is much greater than if the blades had been cleaned prior to testing. When the blade was removed from the disc and used without cleaning u = 0.6 to 0.65; whereas, when the blade was clean u = 0.4. The values of u determined by this method are in close agreement with those determined with the rotating distributor and collection box.

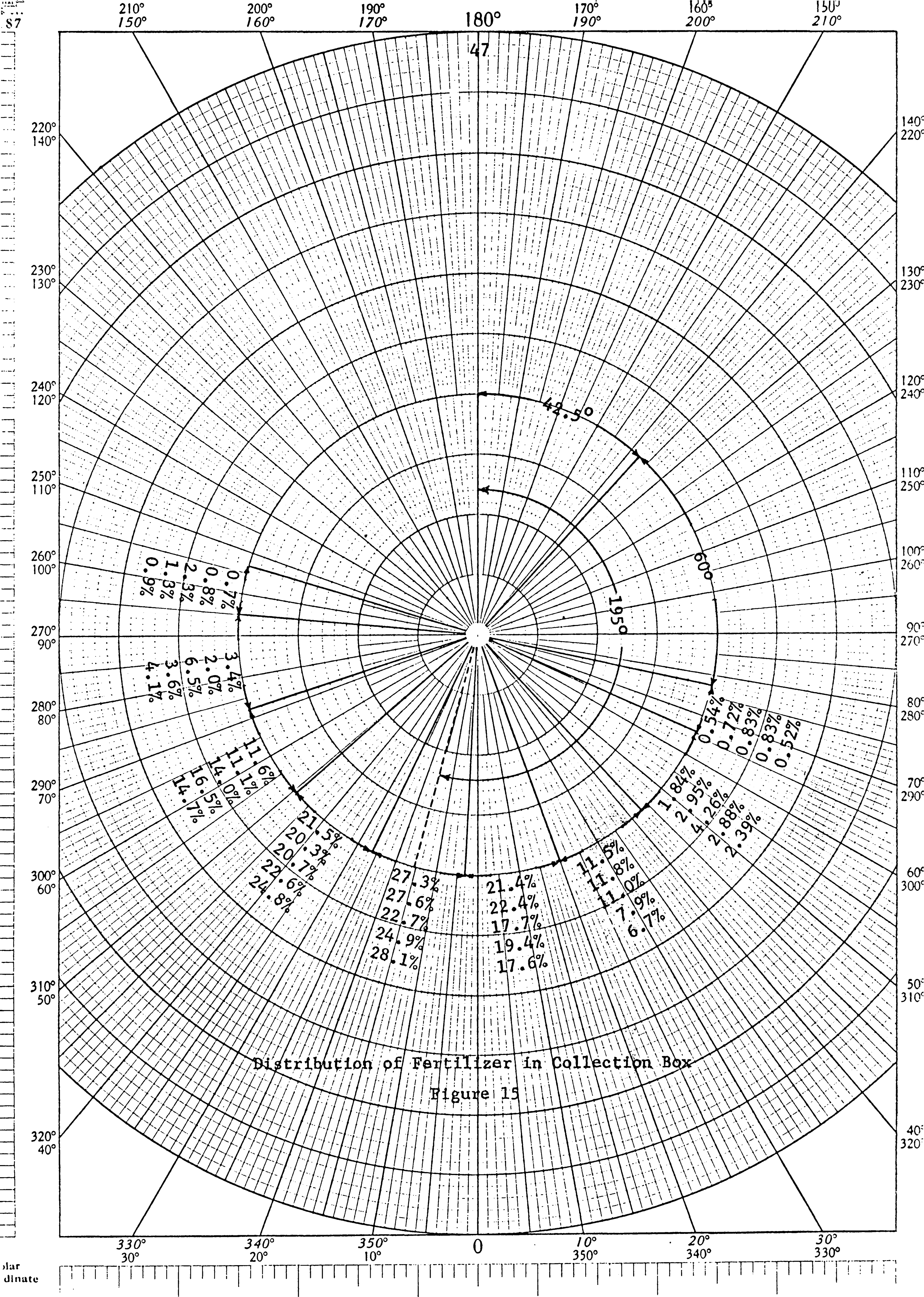

Distribution of Fertilizer in Collection Box

Figure 15

RESULTS

The results of computer analysis for the three distributor configurations are given in the Appendices, Figures 16 through 106. The curves in the figures were drawn directly by the X-Y recorder which was connected to the computer.

It was shown in the section of the potentiometer settings that for each of the three problems 27 combinations of the parameters are possible. Therefore, 27 recordings of displacement, resultant velocity, and its angle of departure are given in the appendices.

The results are in dimensionless form. Displacements, P and R, are represented by their dimensionless equivalents, P/r and R/r; and velocity, V, is represented by its dimensionless equivalent, V/rw. The graphs are suited to any problem of design analysis, since a comparison of the effects of each parameter can easily be obtained.

The fact that the parameters involved were made dimensionless will further enhance the utility of these graphs. For example, any combination of u, g, r, and w which will result in the same value of ug/rw^2 as the one desired, can be used in the analysis. For this reason, limits imposed on the range of the above parameters are broad.

As was shown in the derivation of equations for the curved-blade spinner, the term $Mv^2 \sin\phi/R$ is the only addition to the equation for the spinner with straight-pitched blades. A comparison of the graphs ($Mv^2 \sin\phi/R$ included) with the solutions obtained analytically ($Mv^2 \sin\phi/R$ neglected) shows that for the range of the parameters considered, the influence of this friction producing reverse effective force may be neglected.

The influence of the dimensionless term ug/rw^2 on R/r, V/rw and β is greatest for the spinner with the forward-curved blades. The resultant velocity, V/rw, decreases as ug/rw^2 increases. There is less decrease in the values of the resultant velocity for the spinner with backward-curved blades than there is for the spinner with forward-curved blades.

As can be seen clearly from the graphs, the influence of the coefficient of fertilizer-blade friction is significant and should not be ignored in any design or problem analysis.

The values of the coefficient of friction obtained from simple T-bevel tests were in the range of 0.60 to 0.65 for the steel blades in the condition used. These values were in close agreement with those obtained with the actual rotating distributor and collection box.

CONCLUSION

From the results of this study the following conclusions can be drawn:

1. Electronic analog computers can be used to obtain solutions of equations representing the motion of granular material on the blades of centrifugal distributors. Experimental results with forward-pitched blades verified the validity of the solutions obtained. Through the use of dimensional analysis and proper computer programming, the results obtained are in general form which may be used easily by designers of distribution equipment.
2. The value of the coefficient of granular-fertilizer-on-blade friction may be determined by a simple T-bevel test and this value may be used directly to select the particular computer solution that is applicable. It is believed that this procedure also may be satisfactory for other granular materials such as seed and granular agricultural chemicals.

SUMMARY

The application of granular materials with centrifugal distributors has become increasingly popular in recent years. Because of their desirable features, the centrifugal distributors have a great potential in the years to come.

Heretofore, the design of the spreaders has been a matter of trial and error, sometimes resulting in non-uniform distribution patterns and lower crop yields. The purpose of this study was to arrive at easily applied solutions of the basic equations representing the motion of fertilizer particles on the rotating distributor. These equations were solved with the help of an analog computer and the results are presented in the form of dimensionless graphs which are quite easy to use.

It is believed that a designer can utilize the information secured here to quickly arrive at a satisfactory distributor design to meet specific conditions.

In order to supplement the information presented in this study, values of the fertilizer-blade coefficient of friction were determined experimentally.

ACKNOWLEDGEMENTS

The author wishes to extend his deep appreciation to his major professor, Dr. F. M. Cunningham, for his unending and tireless guidance and his invaluable suggestions throughout the course of this study. Acknowledgements are due to the Engineering Mechanics Department and the computing center of Electronic Associates, Incorporated, Rockville, Maryland, for the use of their computers. He is also indebted to the entire staff of the Department of Agricultural Engineering for their cooperation in the writing of this thesis.

LITERATURE CITED

1. Smith, George, E., Bulk Blended Fertilizers, Proceedings of the 11th Annual Meeting, Fertilizer Industry Round Table, 1961, pps. 90-97.

2. Hephard, R. Q. and J. A. Pascal, The Transverse Distribution of Fertilizer by Conventional Methods, Journal of Agricultural Engineering Research 3-2:95-1-7, 1958.

3. Patterson, D. E. and A. R. Reece, The Theory of the Centrifugal Distributor. I: Motion on the Disc, Near-Center Feed. Journal of Agricultural Engineering Research, 7, (3) p. 232, 1962.

4. Cunningham, F. M., Performance Characteristics of Bulk Distributors for Granular Fertilizer. Transactions of the American Society of Agricultural Engineers, 6, (2) pps. 108-114, 1963.

5. Bhagawati, S. R., Theoretical Analysis and Performance of Centrifugal Seeders, Unpublished Master of Science Thesis, Ohio State University, 1961.

6. Virginia Department of Agriculture, Division of Food and Chemistry, Fertilizer Consumption and Results of Inspection. Virginia, 1959-1960.

7. Cunningham, F. M., Field Performance of Bulk Fertilizer Spreaders, Proceedings of the Association of Southern Agricultural Workers, Inc., 59th Annual Convention, Jacksonville, Florida, 1962.

8. Crowther, A. J., The Distribution of Particles by a Spinning Disc. Journal of Agricultural Engineering Research, 3 (4), p. 288, 1958.

9. Grow, H. F., Centrifugal Spreaders for Granular Fertilizers, Unpublished Master of Science Thesis, Virginia Polytechnic Institute, 1963.

10. Murphy, Glenn, Similitude in Engineering, Ronald Press Company, New York, 1950.

11. Davis, Dale S., Nomography and Empirical Equations, Reynold Publishing Corporation, New York.

12. Jackson, Albert, Analog Computation, McGraw-Hill Book Company, Incorporated, 1960.

The vita has been removed from the scanned document

APPENDICES

Appendix I

Dynamic Characteristics for Spinner With Radial Blades

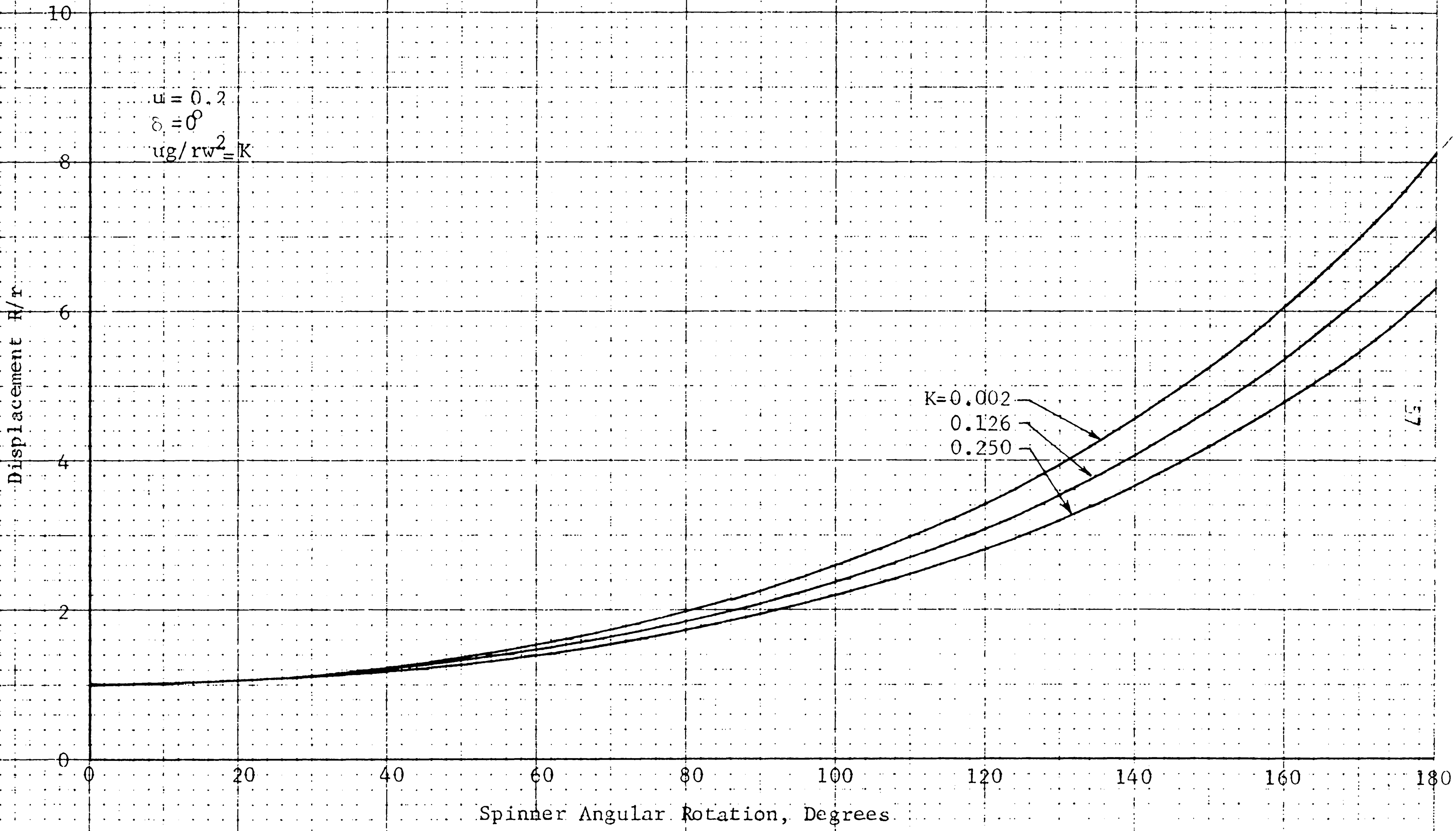

Figure 16 Dynamic Characteristics for Spinner With Radial Blades

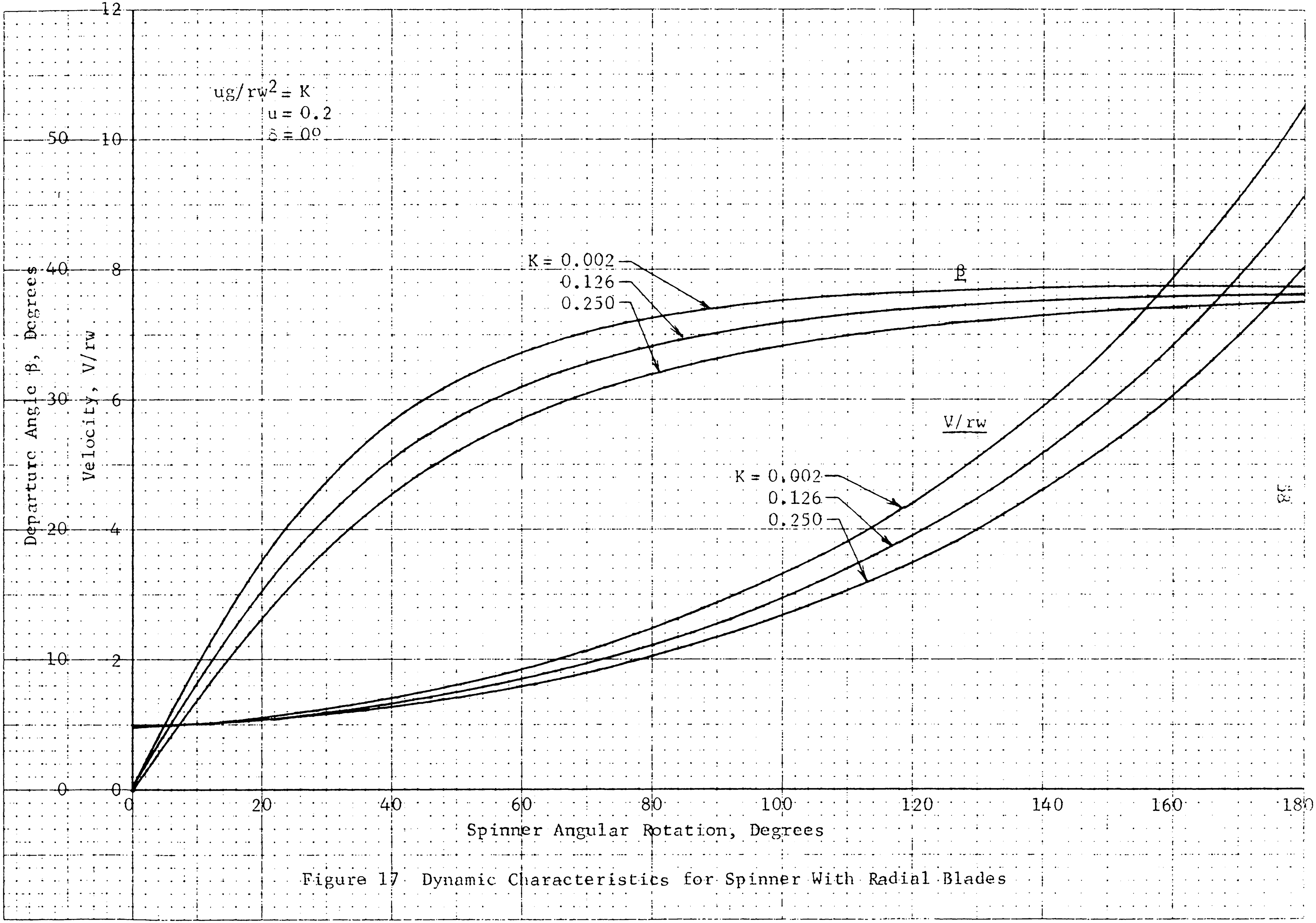

Figure 17 Dynamic Characteristics for Spinner With Radial Blades

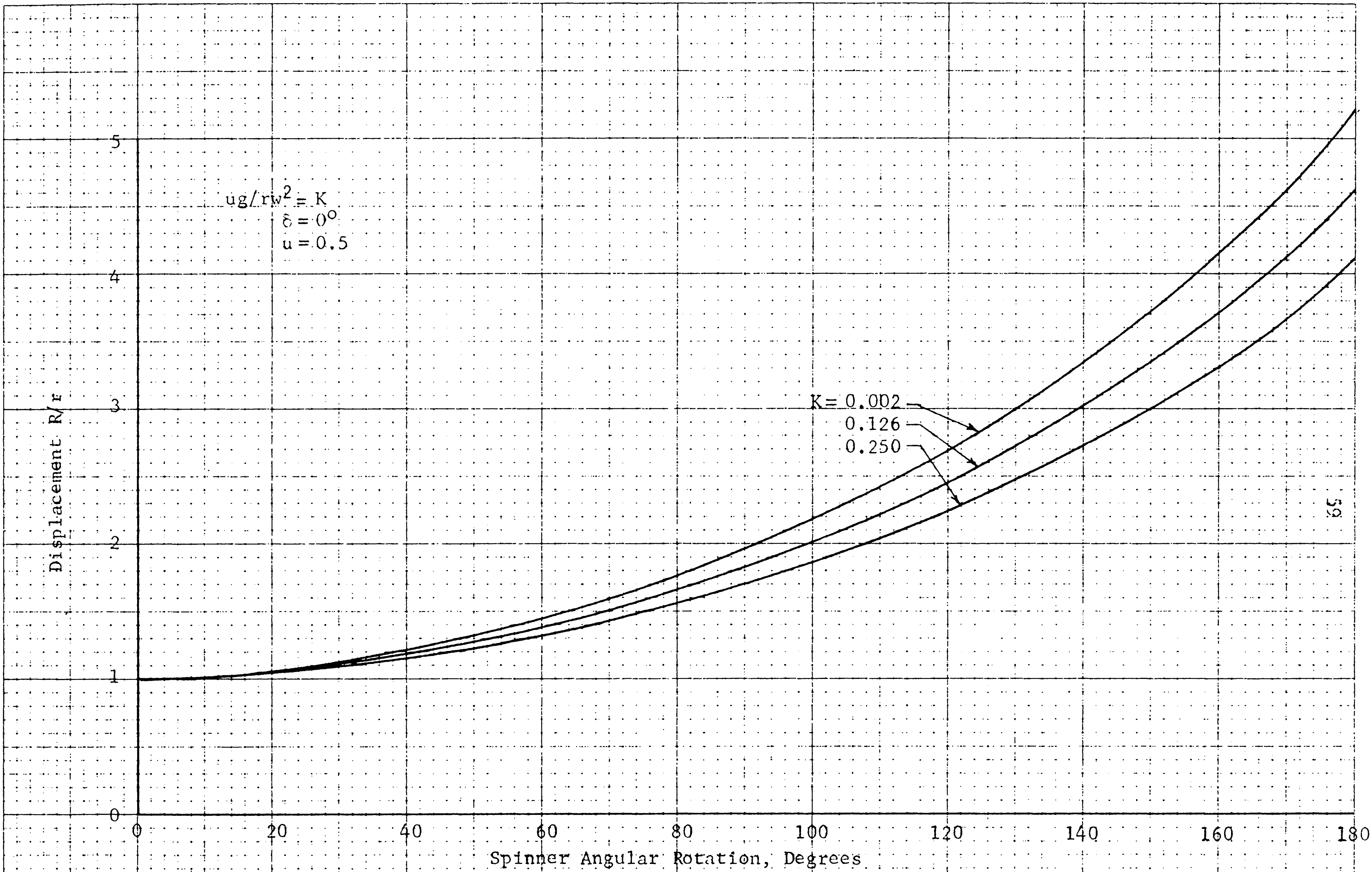

Figure 18 Dynamic Characteristics for Spinner With Radial Blades

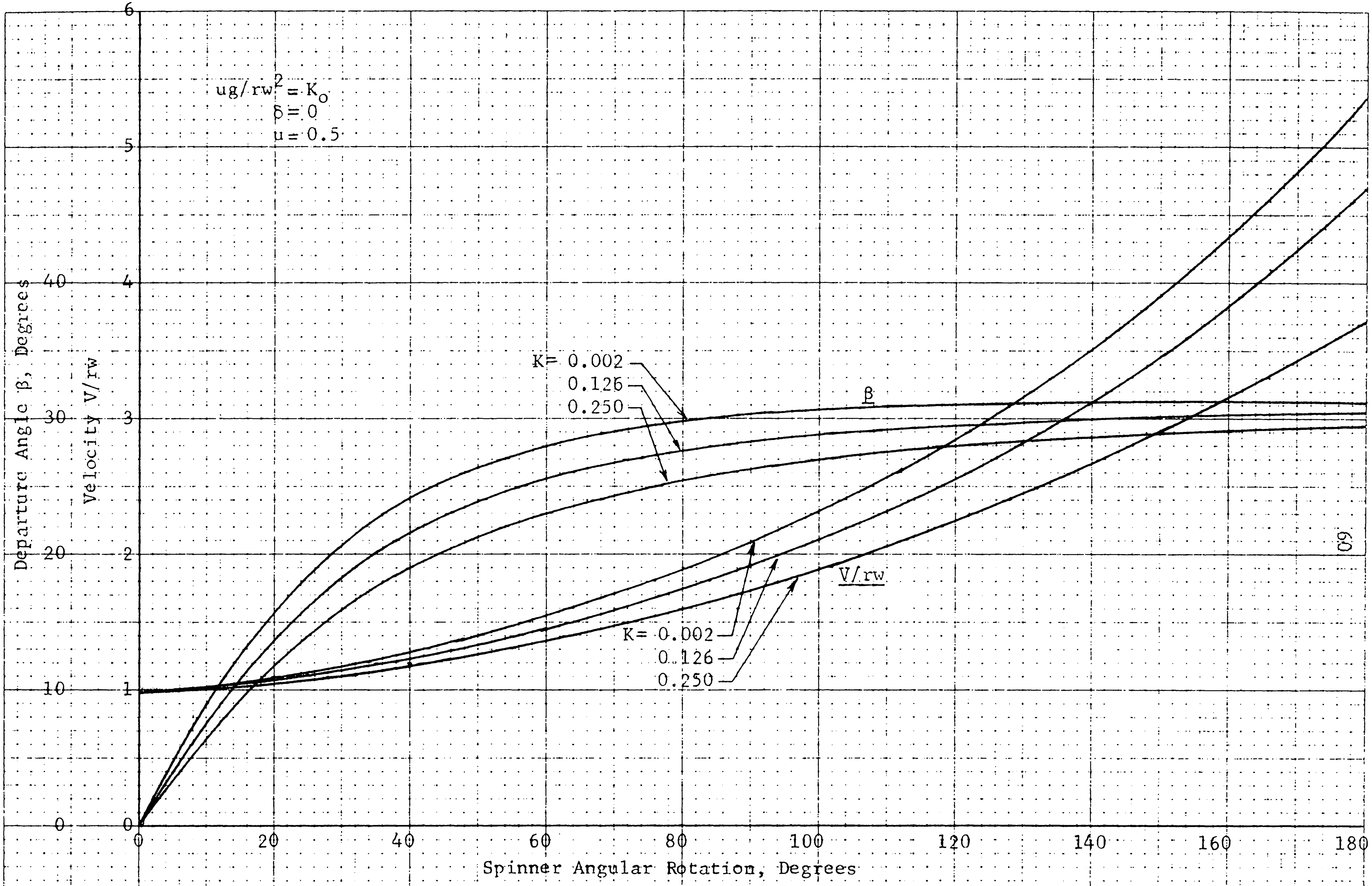

Figure 19 Dynamic Characteristics for Spinner With Radial Blades

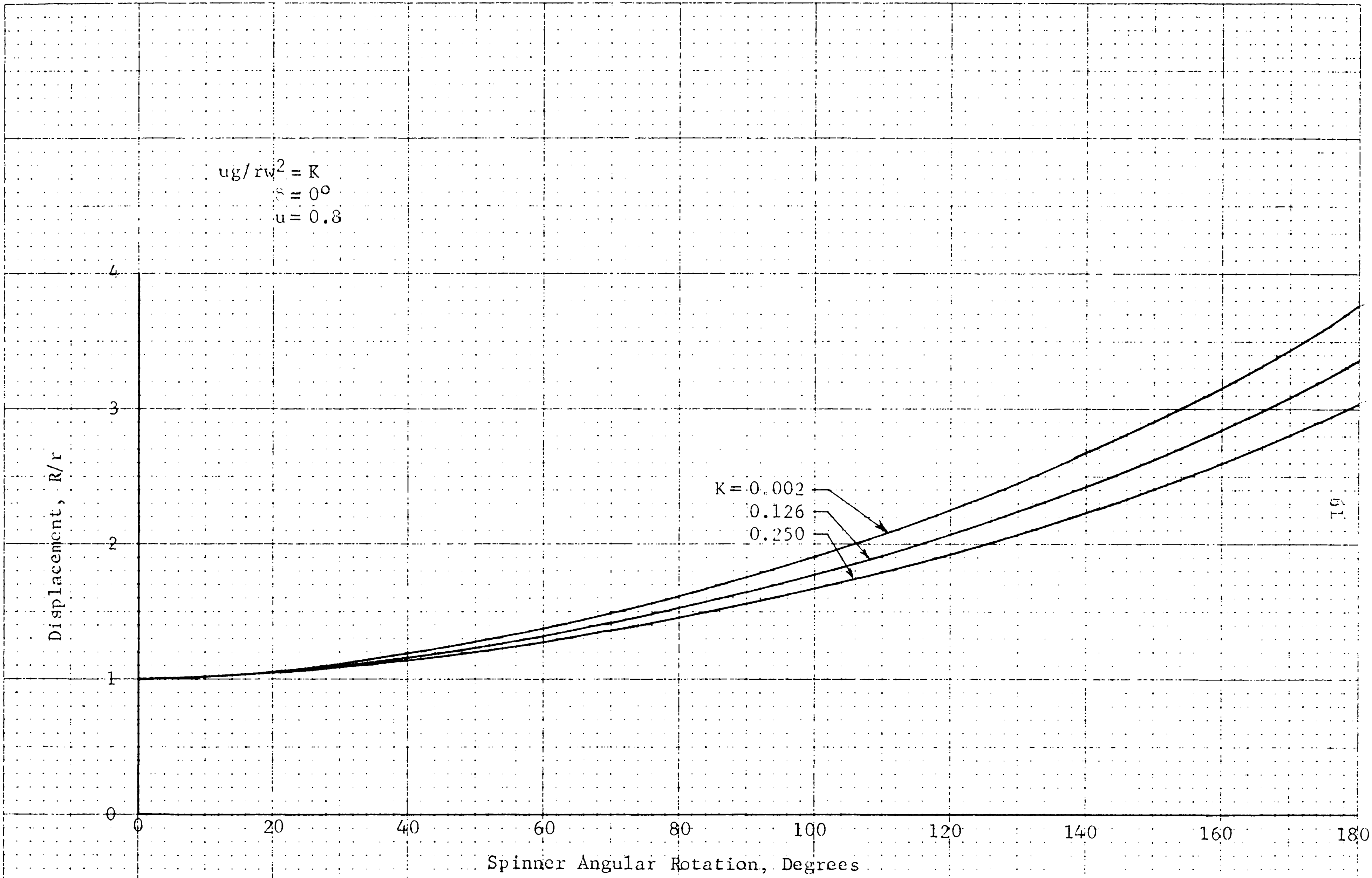

Figure 20 Dynamic Characteristics for Spinner With Radial Blades

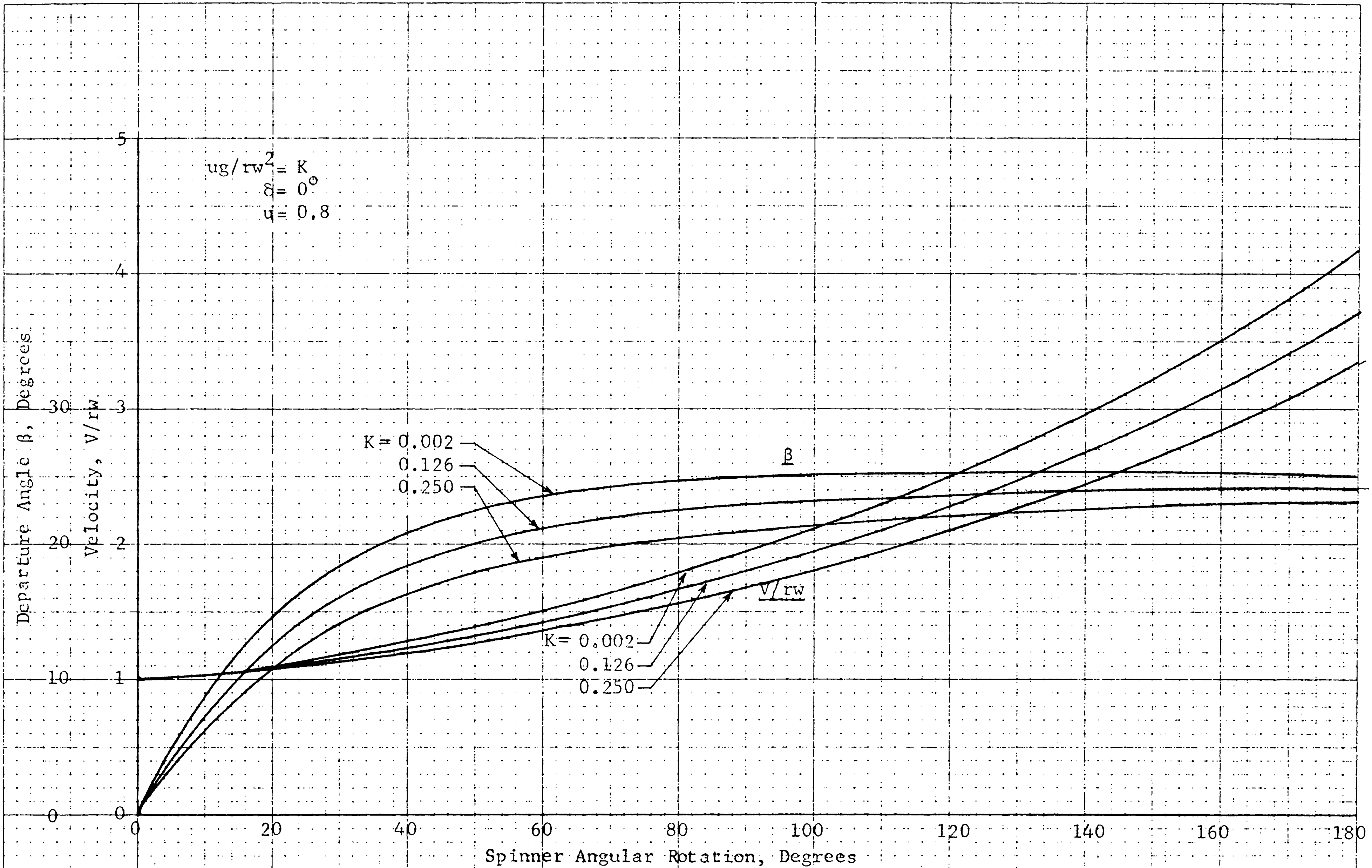

Figure 21 Dynamic Characteristics for Spinner With Radial Blades

Appendix II

Dynamic Characteristics for Spinner With Forward and Backward-Pitched Blades

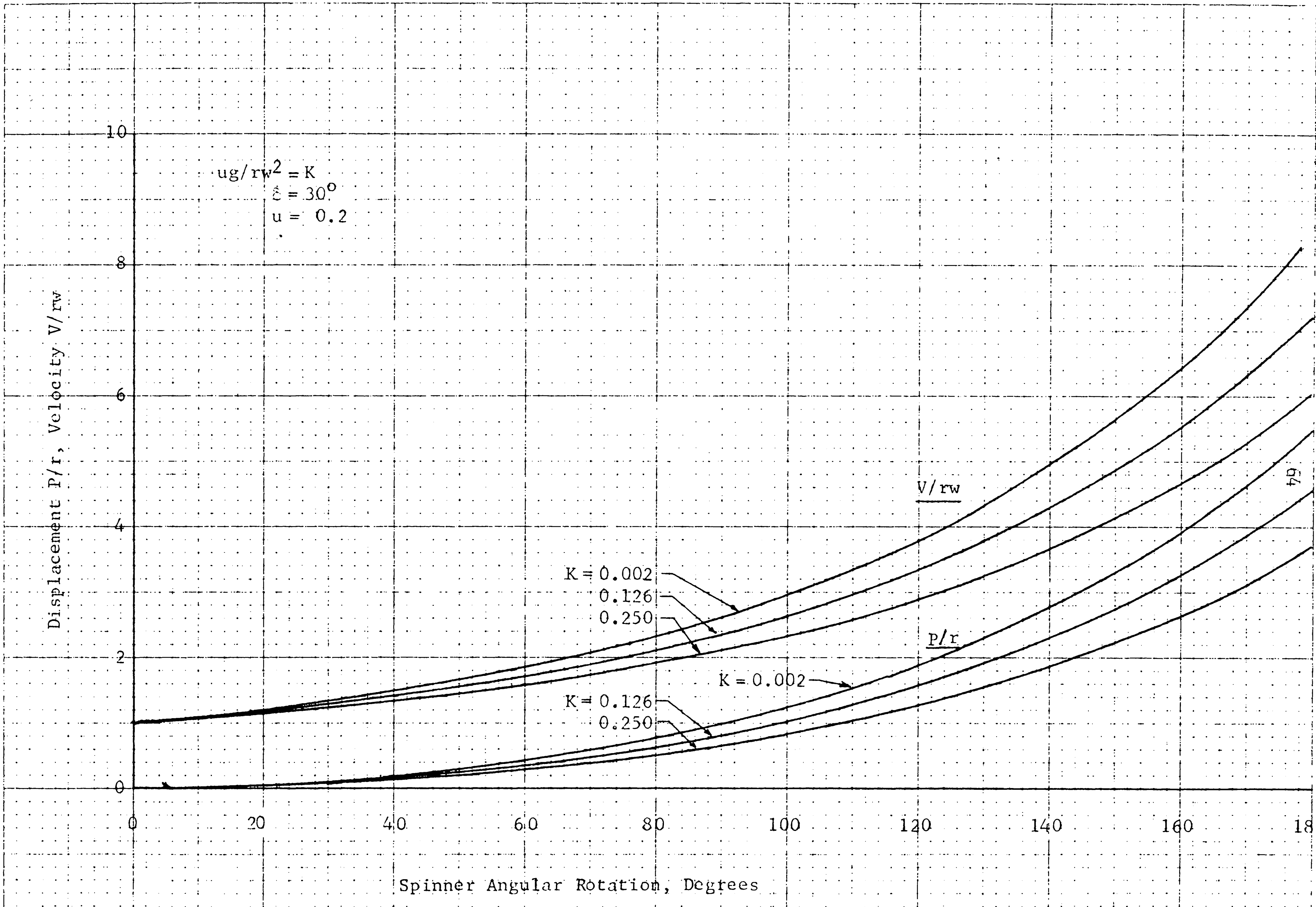

Figure 22 Dynamic Characteristics for Spinner With Forward-Pitched Blades

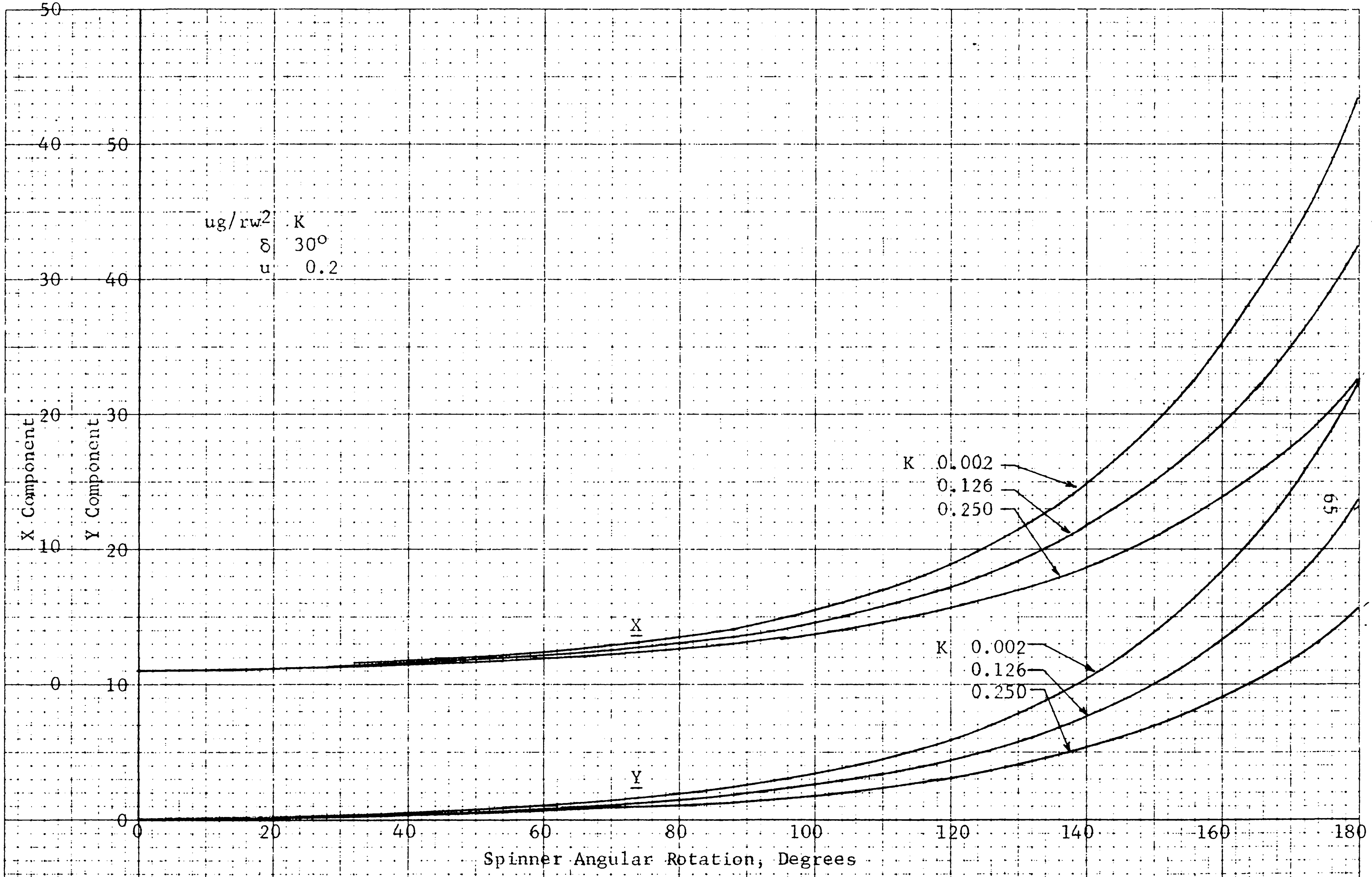

Figure 23 Dynamic Characteristics for Spinner With Forward-Pitched Blades.
Components of Tangent of Departure Angle

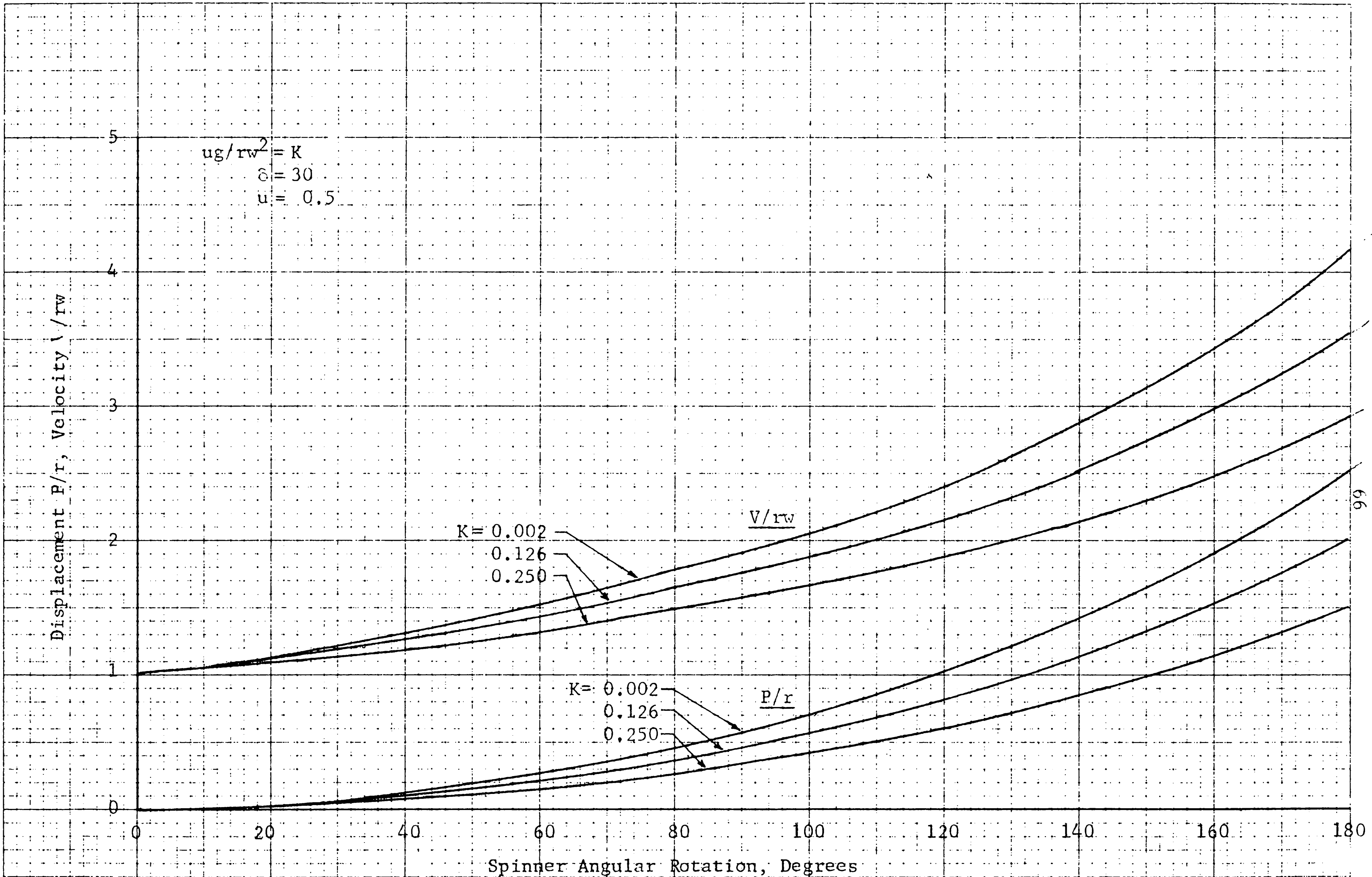

Figure 24 Dynamic Characteristics for Spinner With Forward-Pitched Blades

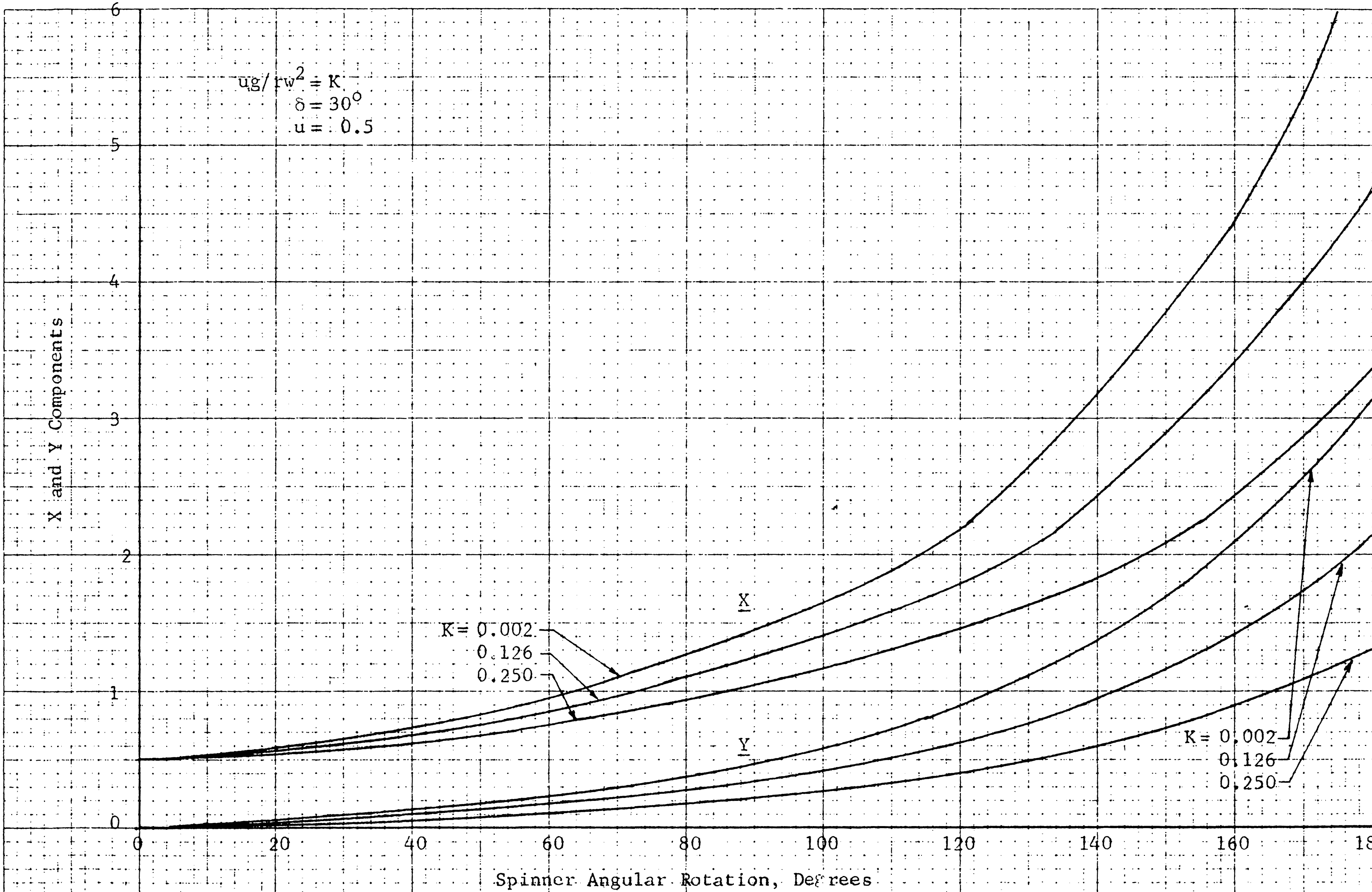

Figure 25 Dynamic Characteristics for Spinner With Forward-Pitched Blades
Components of Tangent of Departure Angle

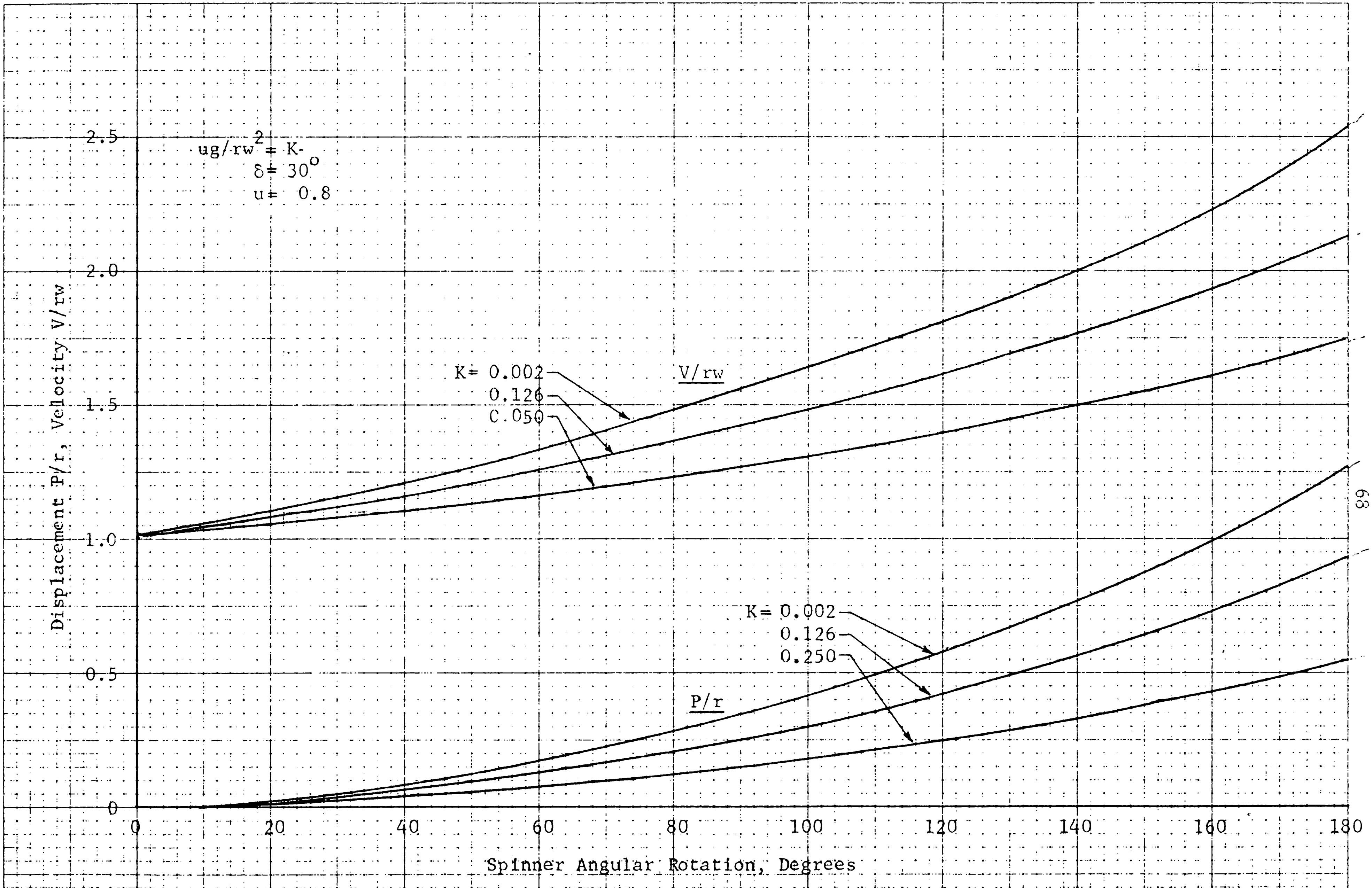

Figure 26 Dynamic Characteristics for Spinner With Forward-Pitched Blades

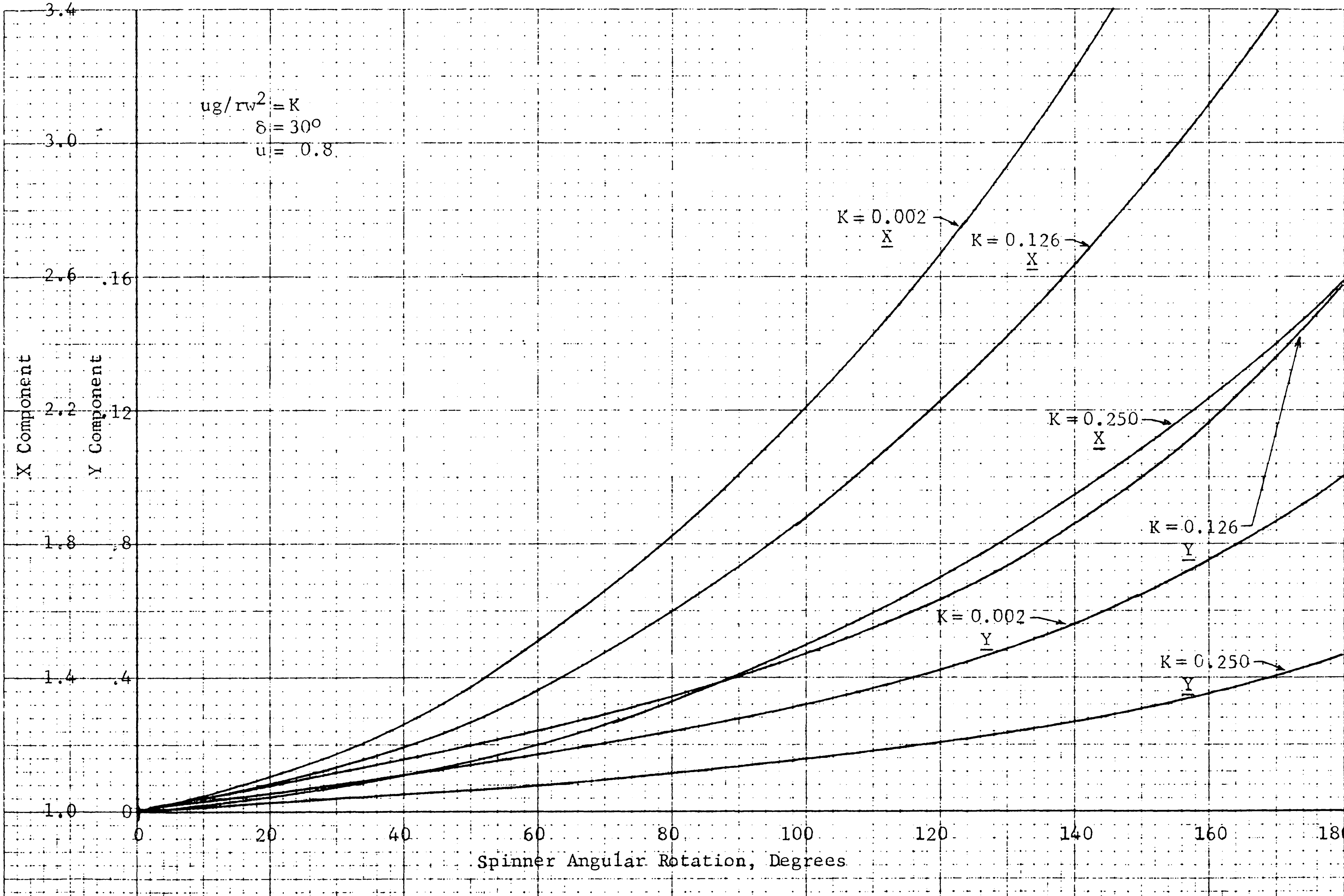

Figure 27 Dynamic Characteristics for Spinner With Forward-Pitched Blades. Components of Tangent of Departure Angle

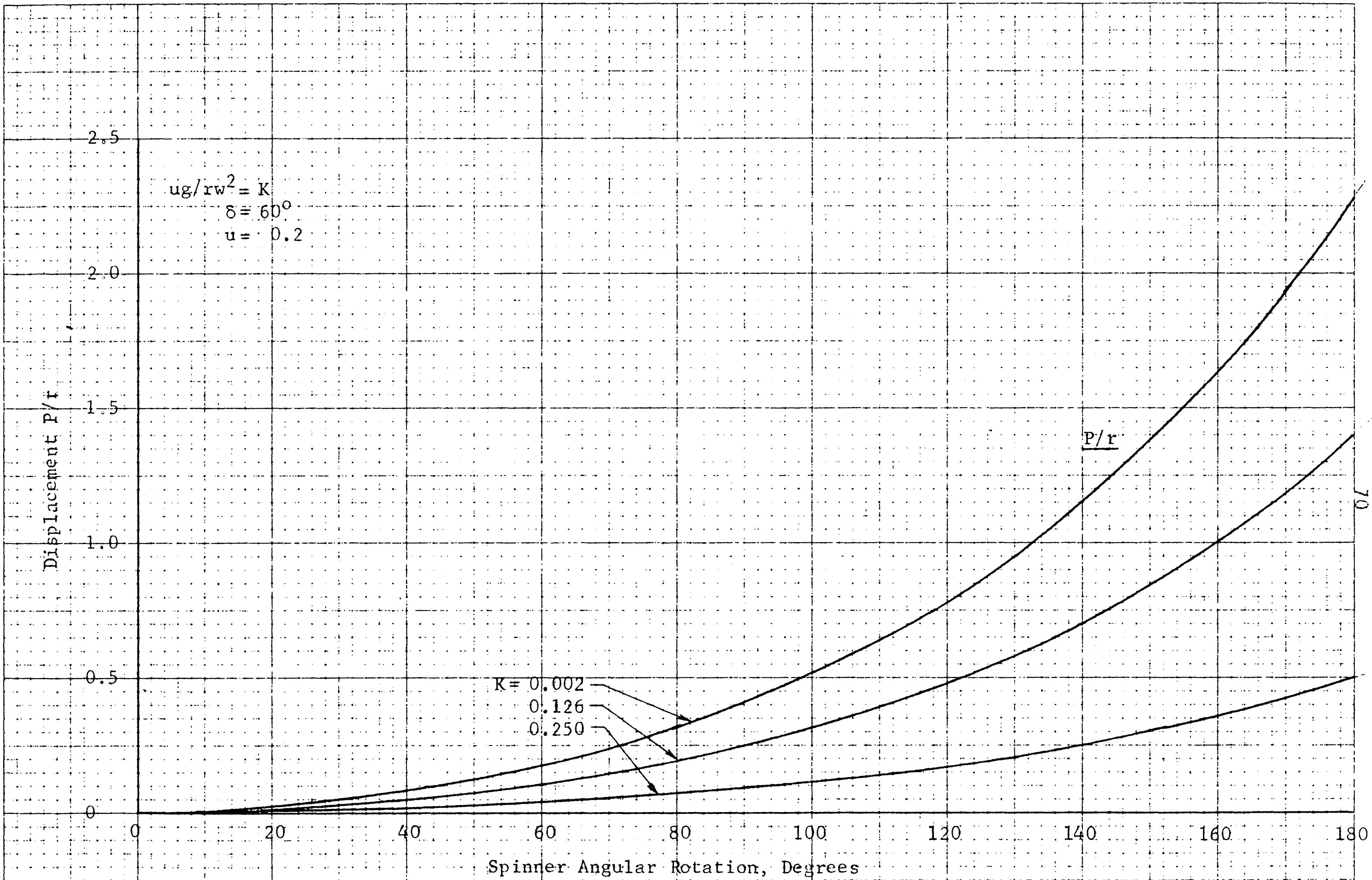

Figure 28 Dynamic Characteristics for Spinner With Forward-Pitched Blades

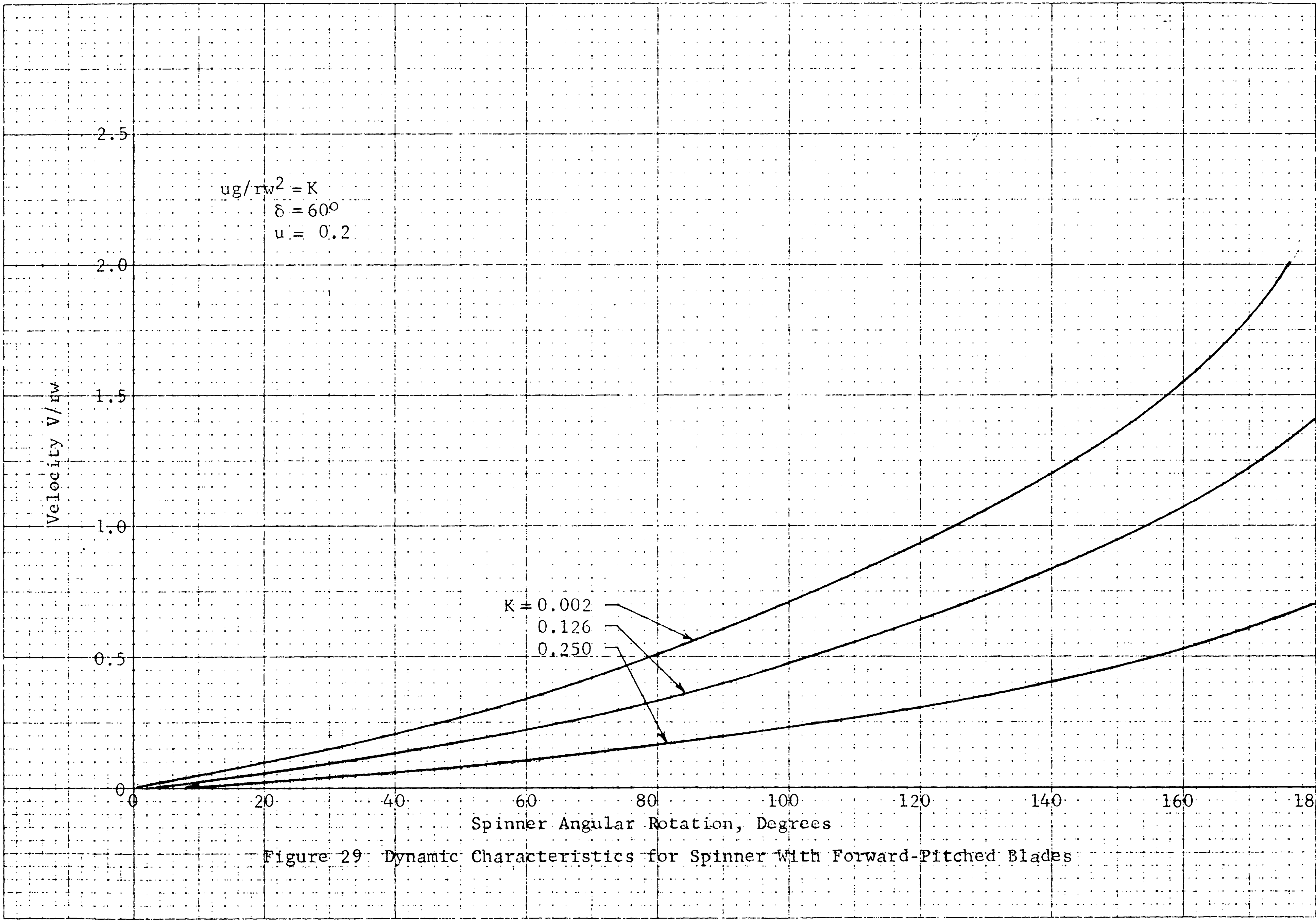

Figure 29 Dynamic Characteristics for Spinner With Forward-Pitched Blades

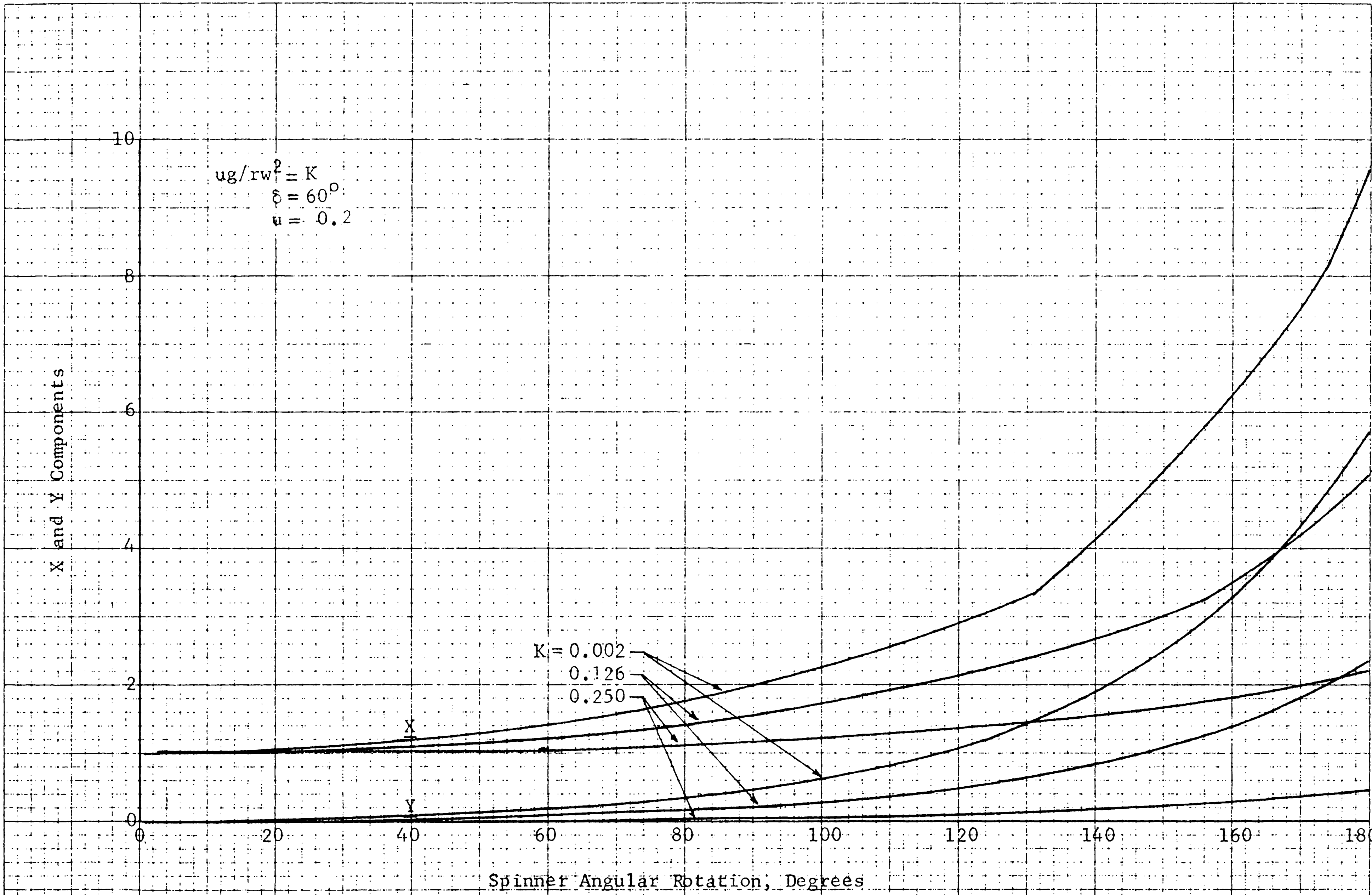

Figure 30 Dynamic Characteristics for Spinner With Forward-Pitched Blades. Components of Tangent of Departure Angle

72

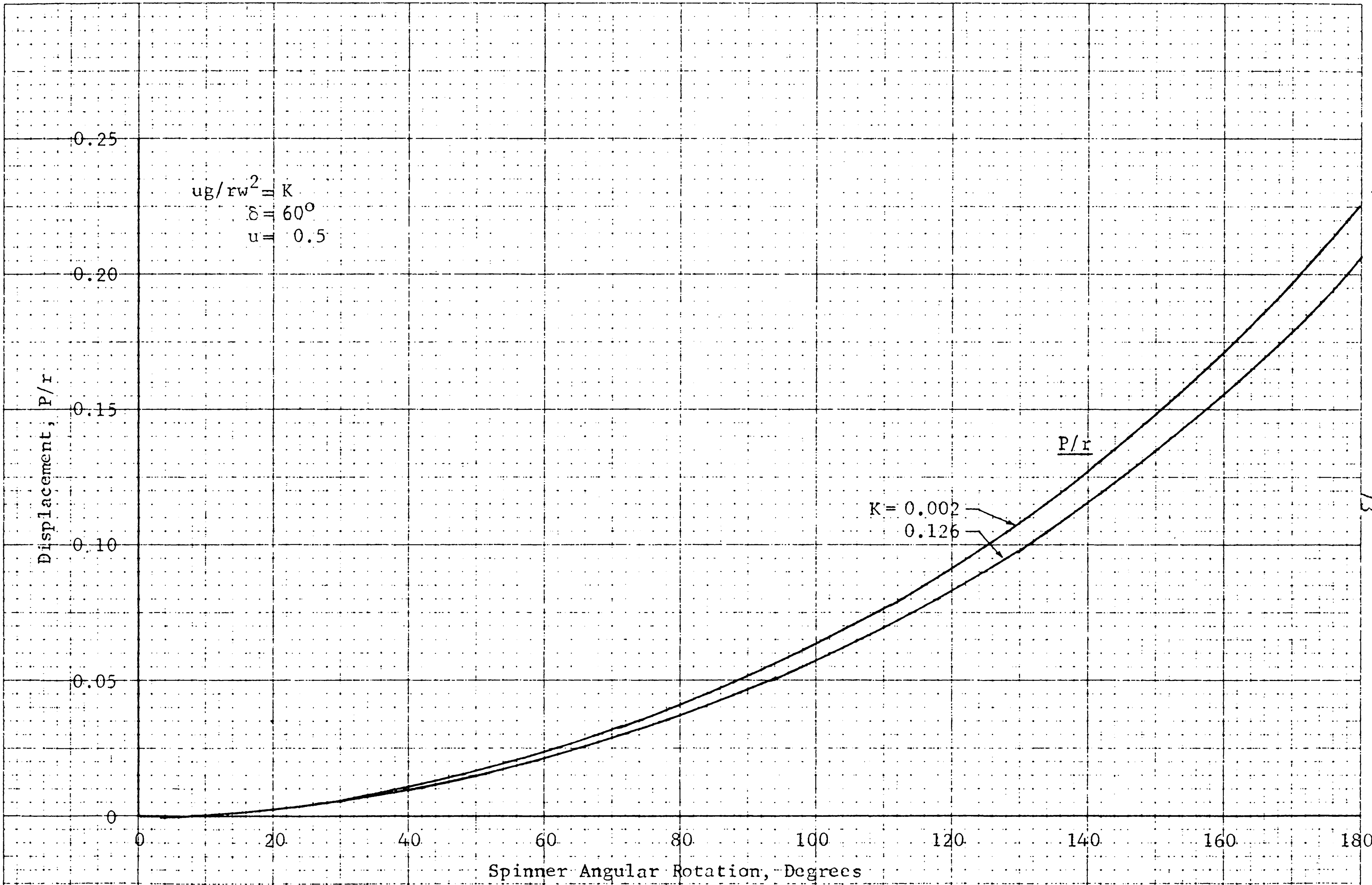

Figure 31 Dynamic Characteristics for Spinner With Forward-Pitched Blades

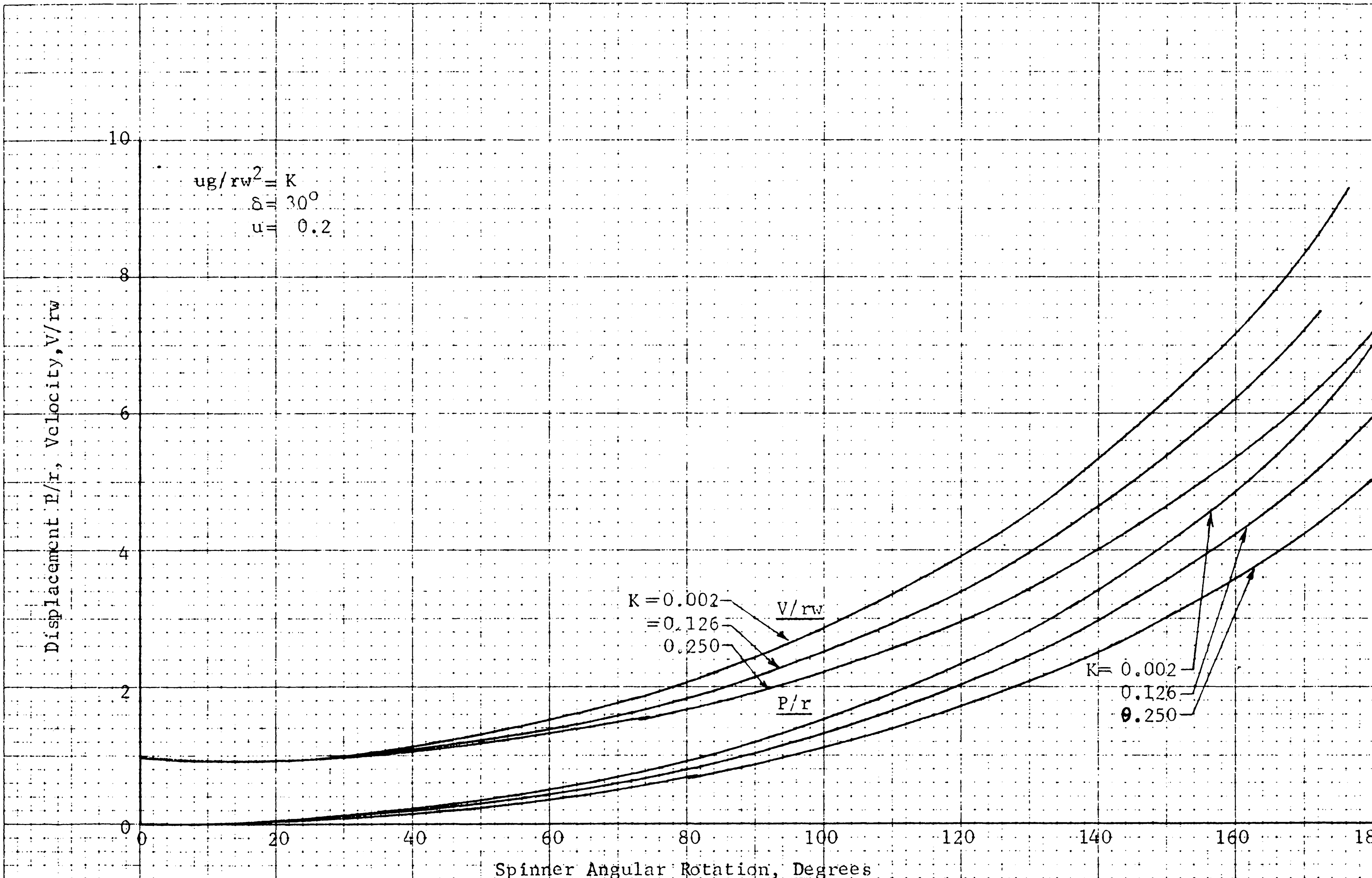

Figure 32 Dynamic Characteristics for Spinner With Backward-Pitched Blades

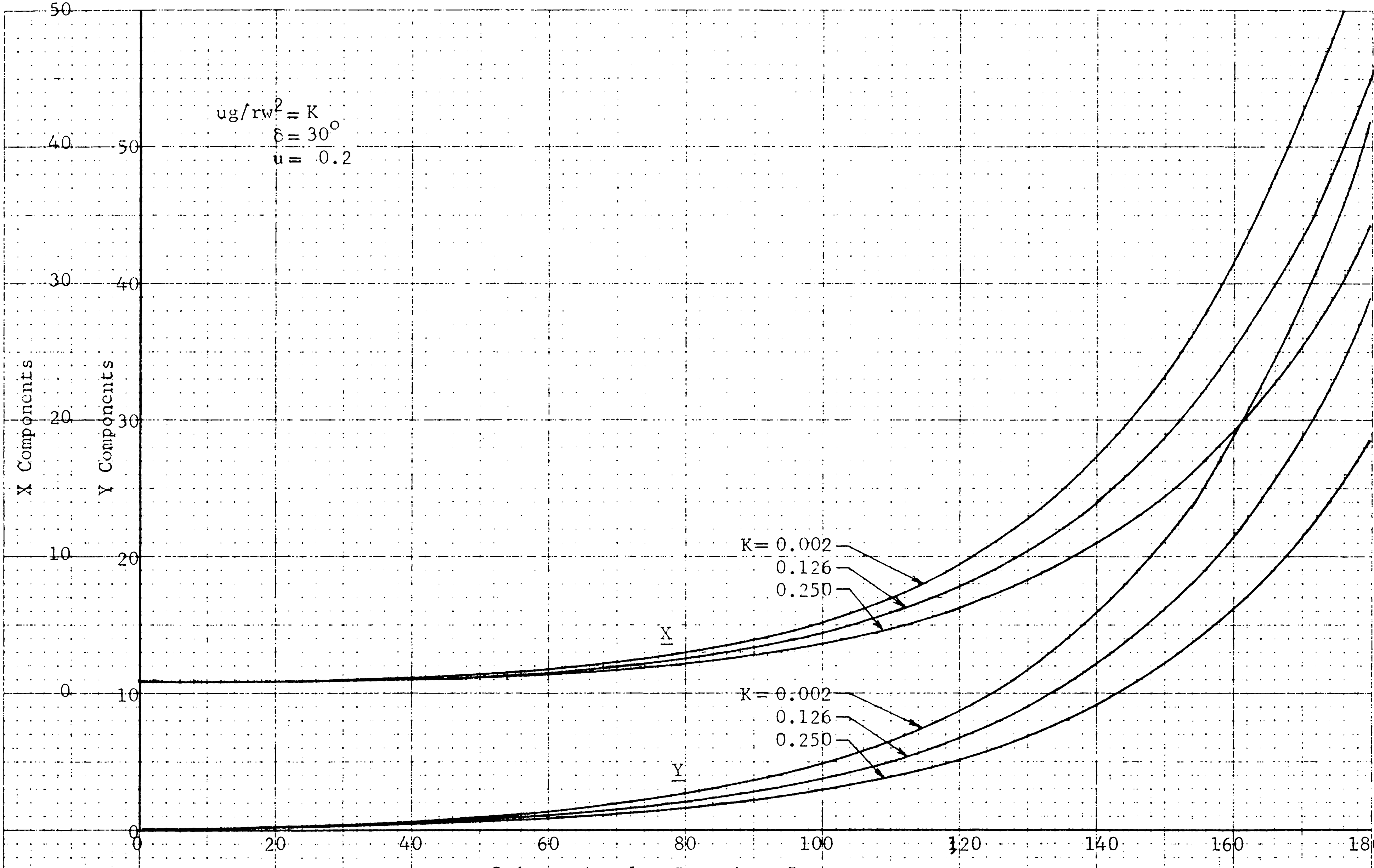

Figure 33 Dynamic Characteristics for Spinner With Backward-Pitched Blades.
Components of Tangent of Departure Angle

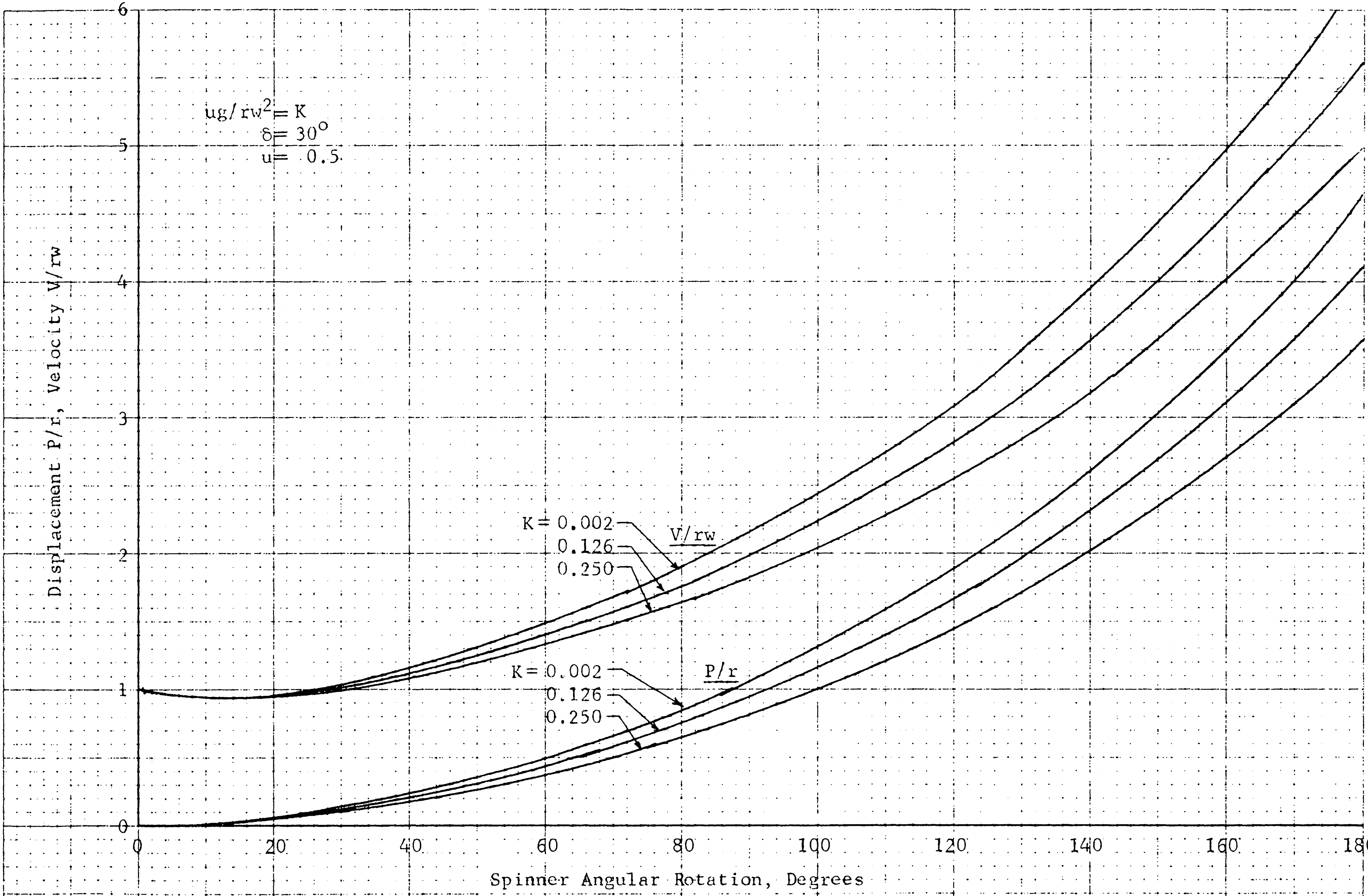

Figure 34 Dynamic Characteristics for Spinner With Backward-Pitched Blades

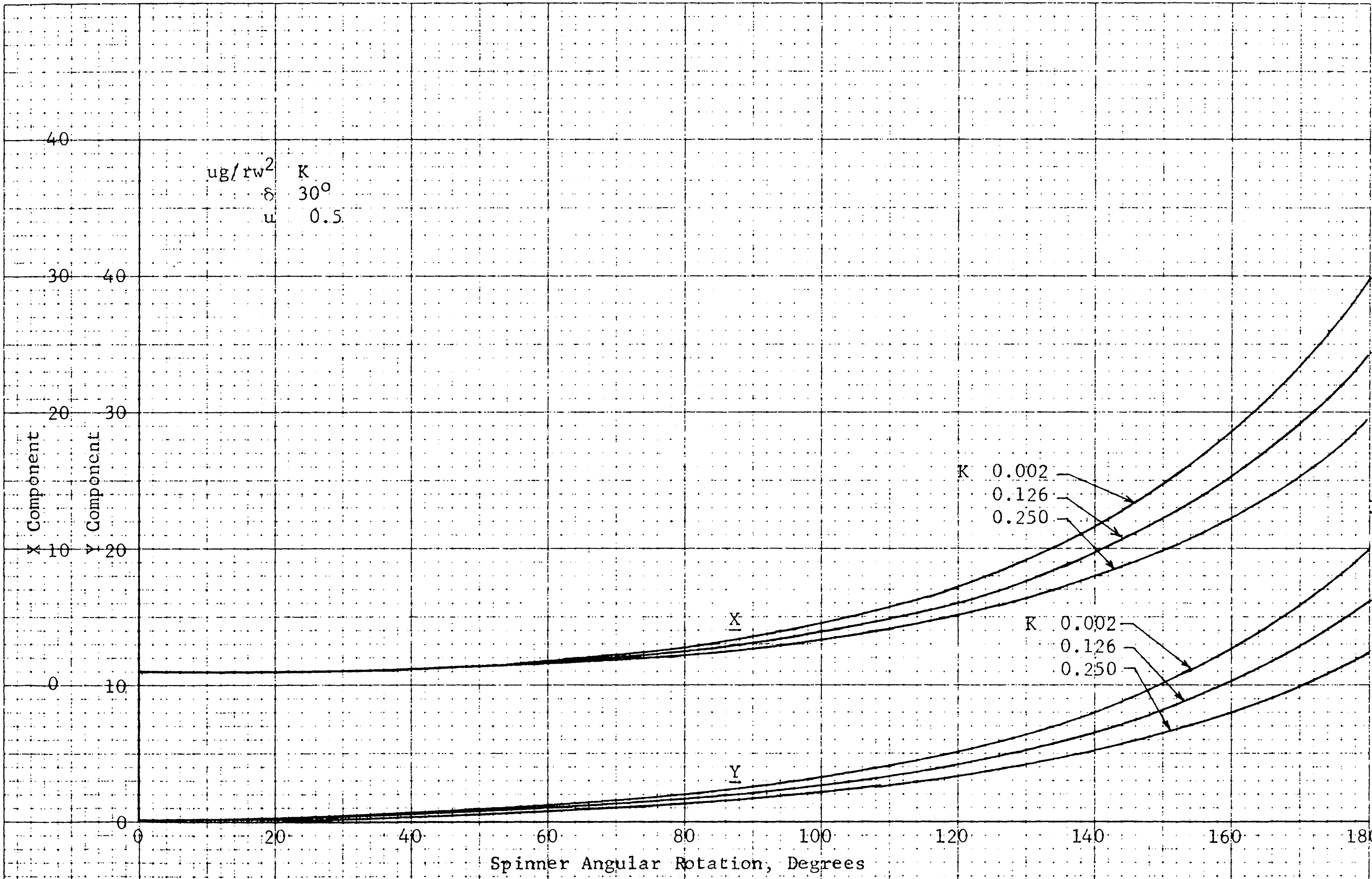

Figure 35 Dynamic Characteristics for Spinner With Backward-Pitched Blades.
Components of Tangent of Departure Angle

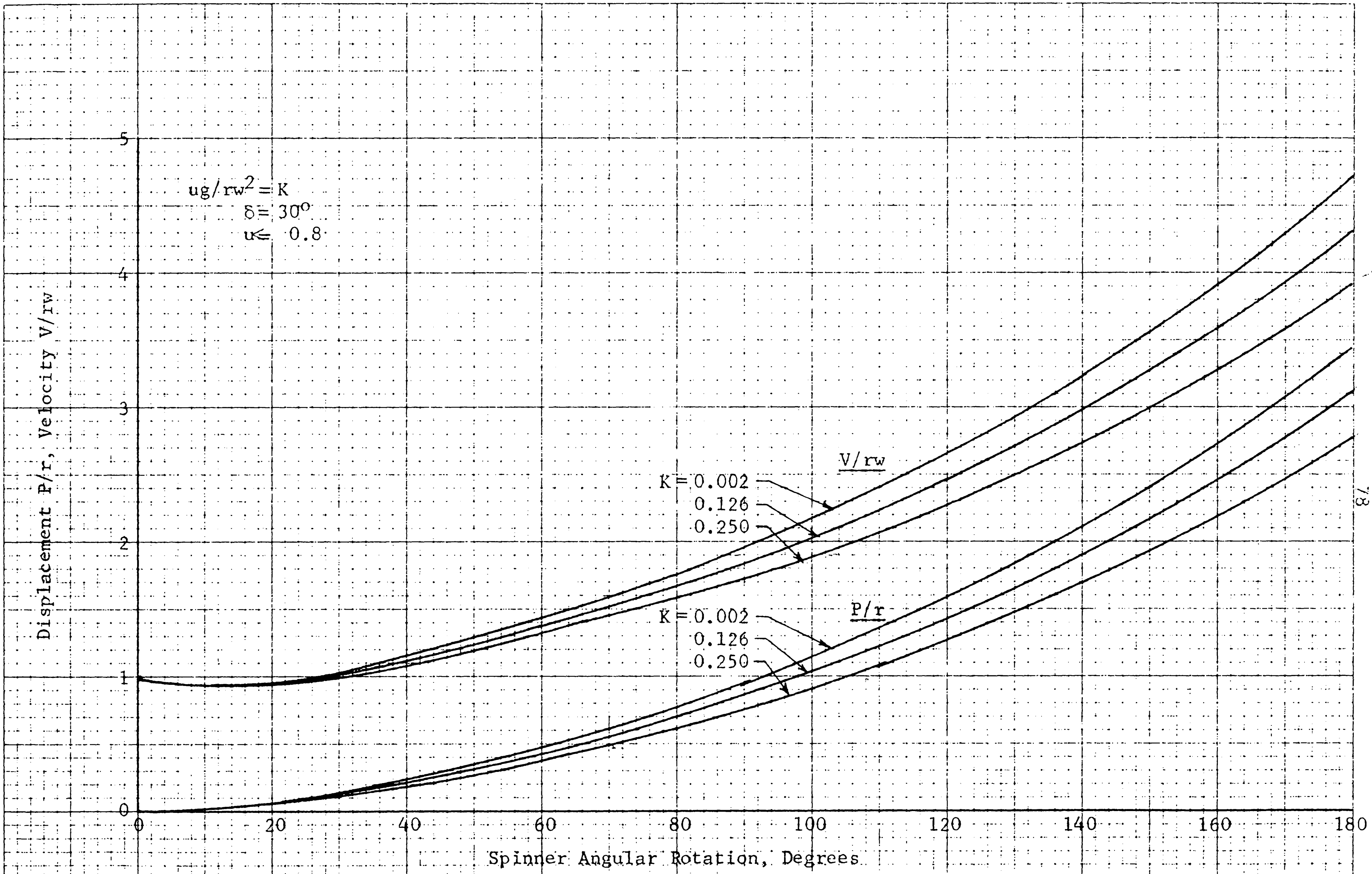

Figure 36 Dynamic Characteristics for Spinner With Backward-Pitched Blades

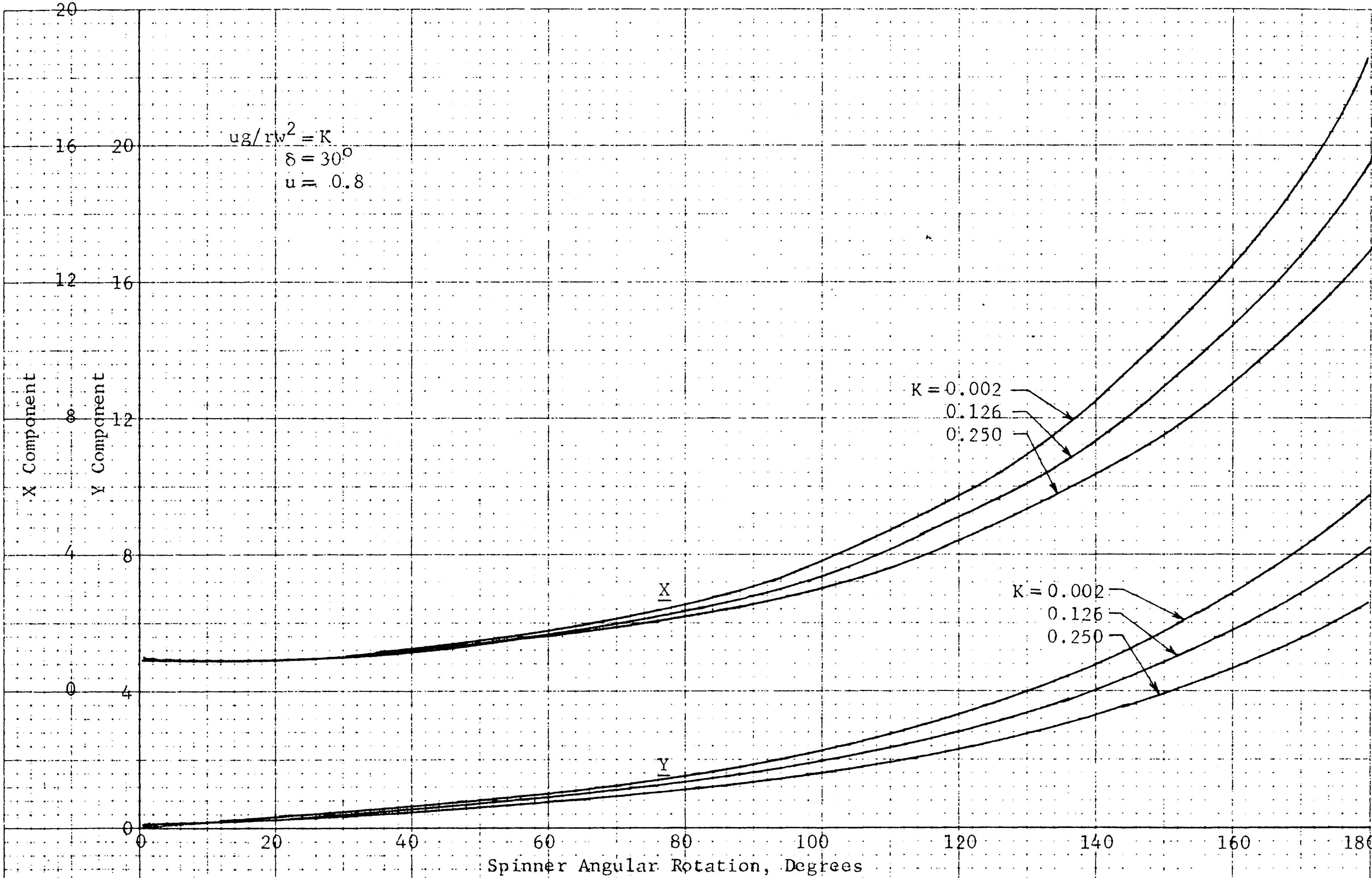

Figure 37 Dynamic Characteristics for Spinner With Backward-Pitched Blades, Components of Tangent of Departure Angle

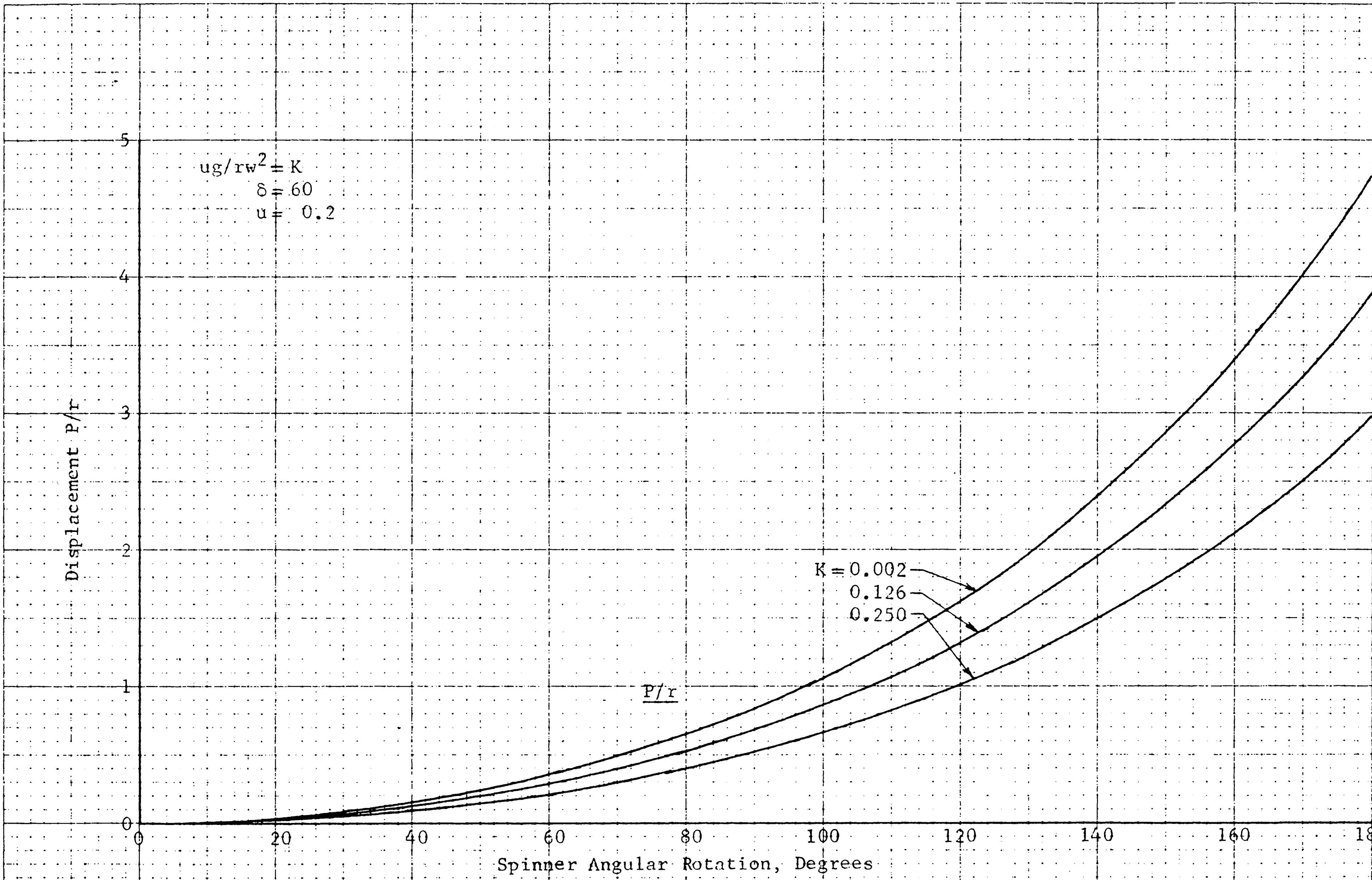

Figure 38 Dynamic Characteristics for Spinner With Backward-Pitched Blades

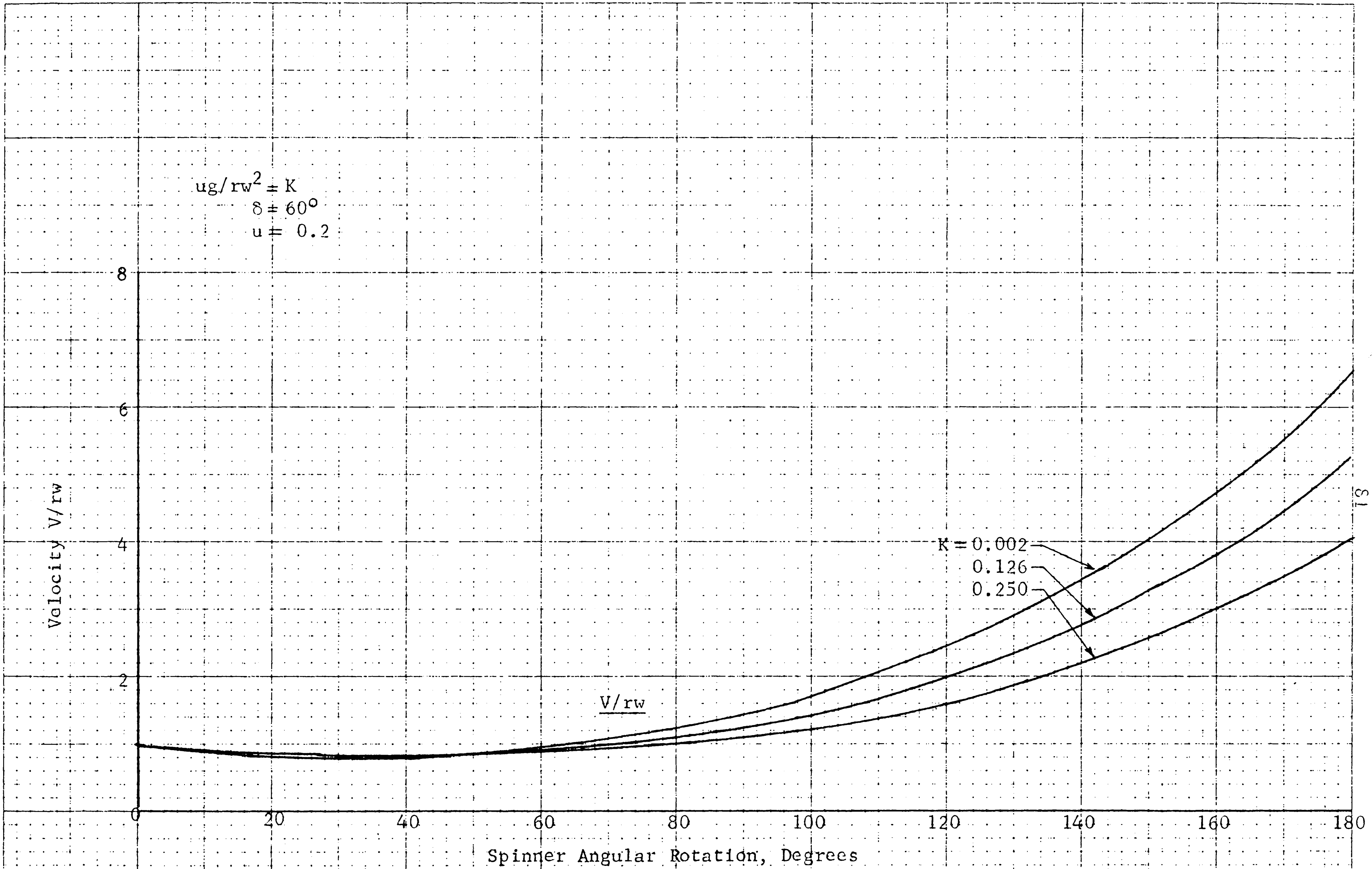

Figure 39 Dynamic Characteristics for Spinner With Backward-Pitched Blades

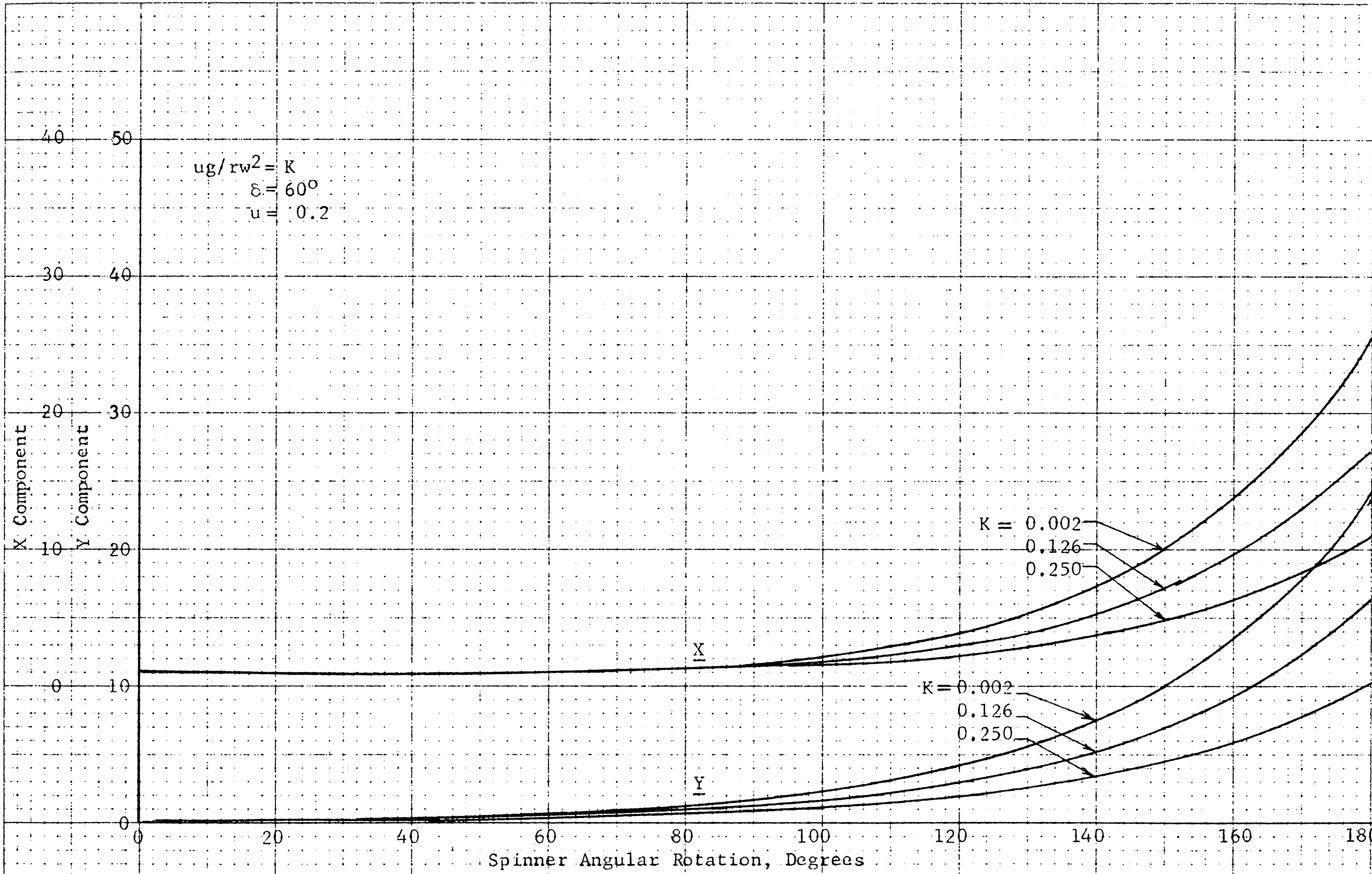

Figure 40 Dynamic Characteristics for Spinner With Backward-Pitched Blades. Components of Tangent of Departure Angle

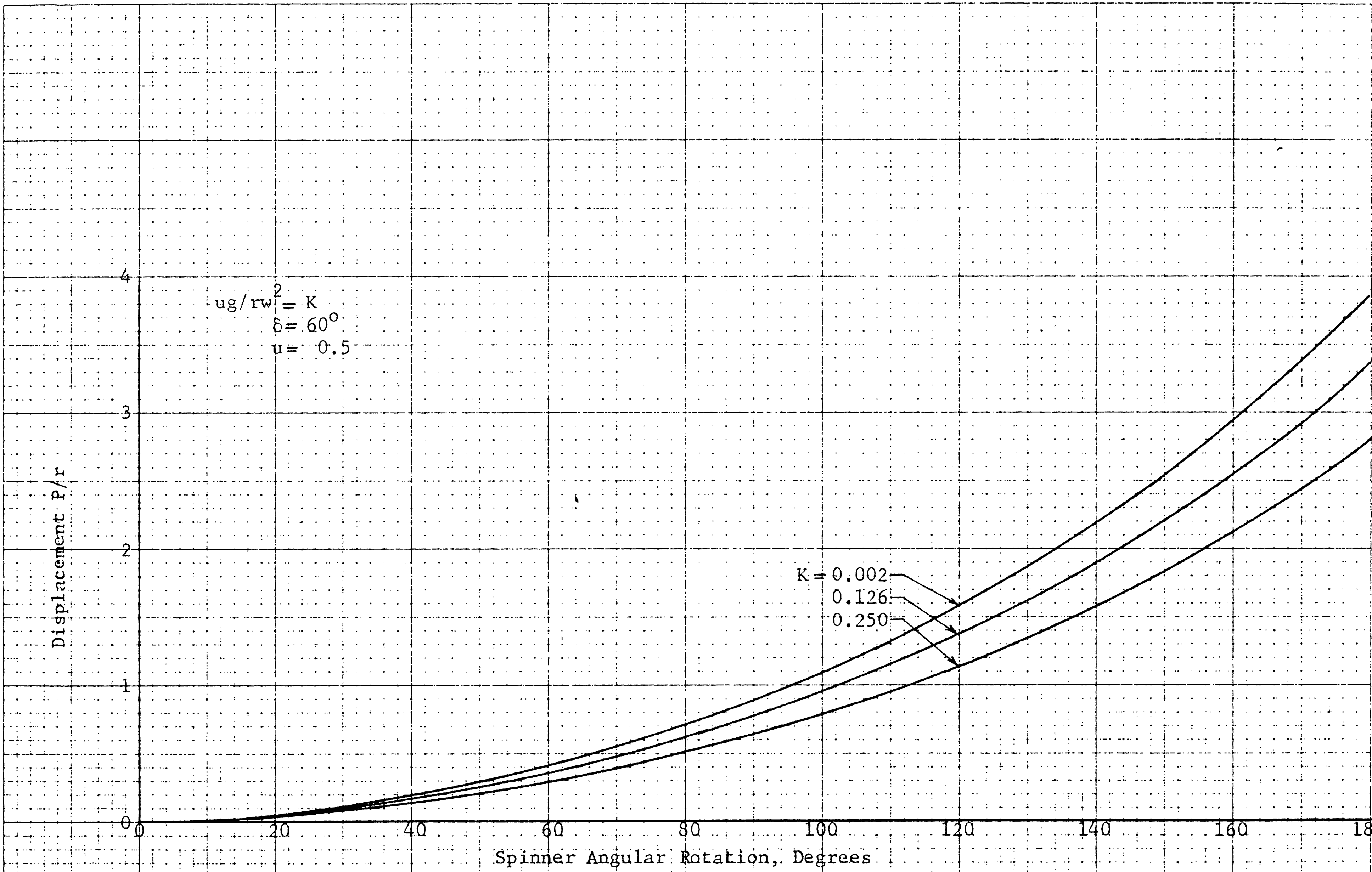

Figure 41 Dynamic Characteristics For Spinner With Backward-Pitched Blades

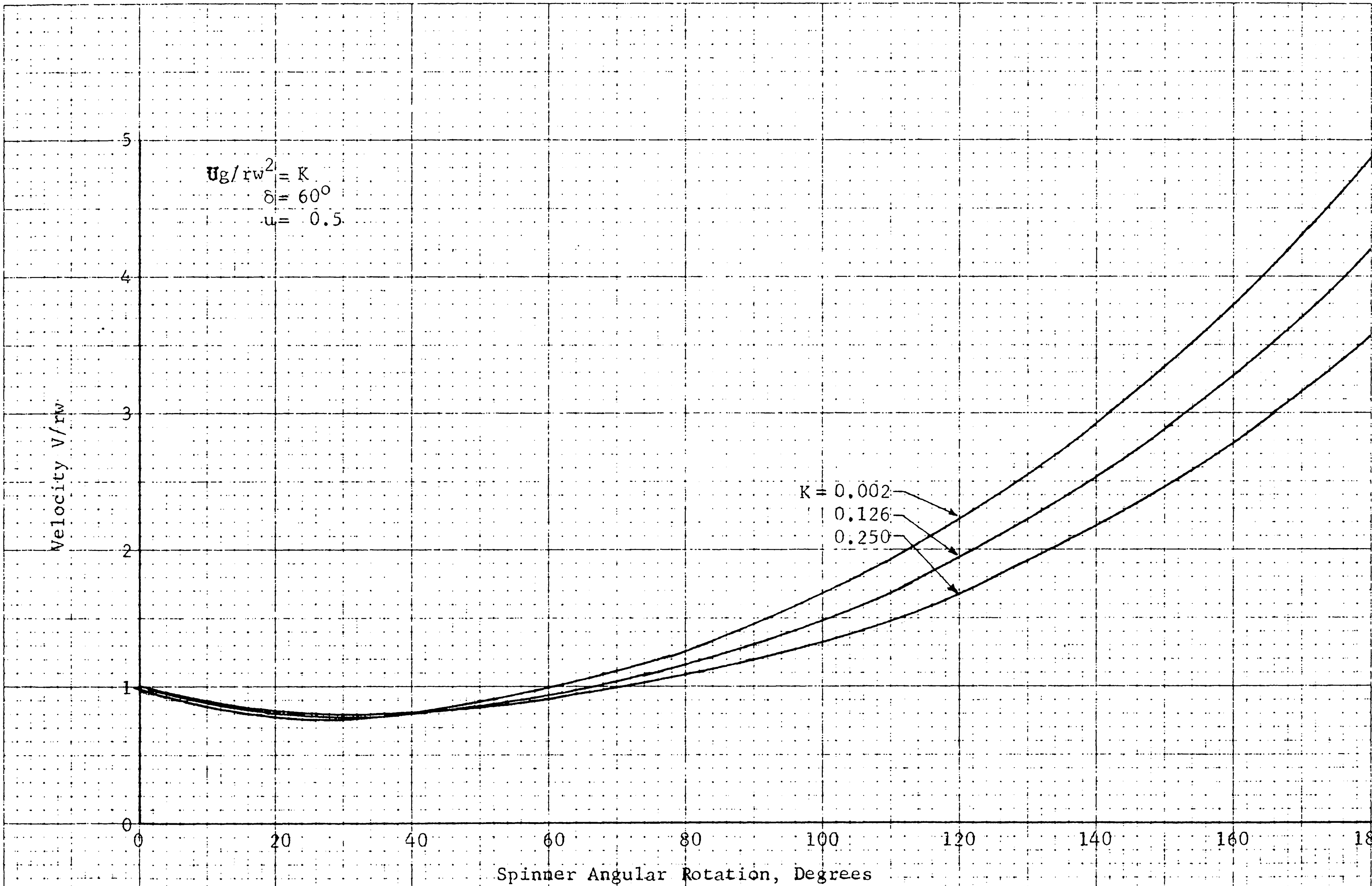

Figure 42 Dynamic Characteristics For Spinner With Backward-Pitched Blades

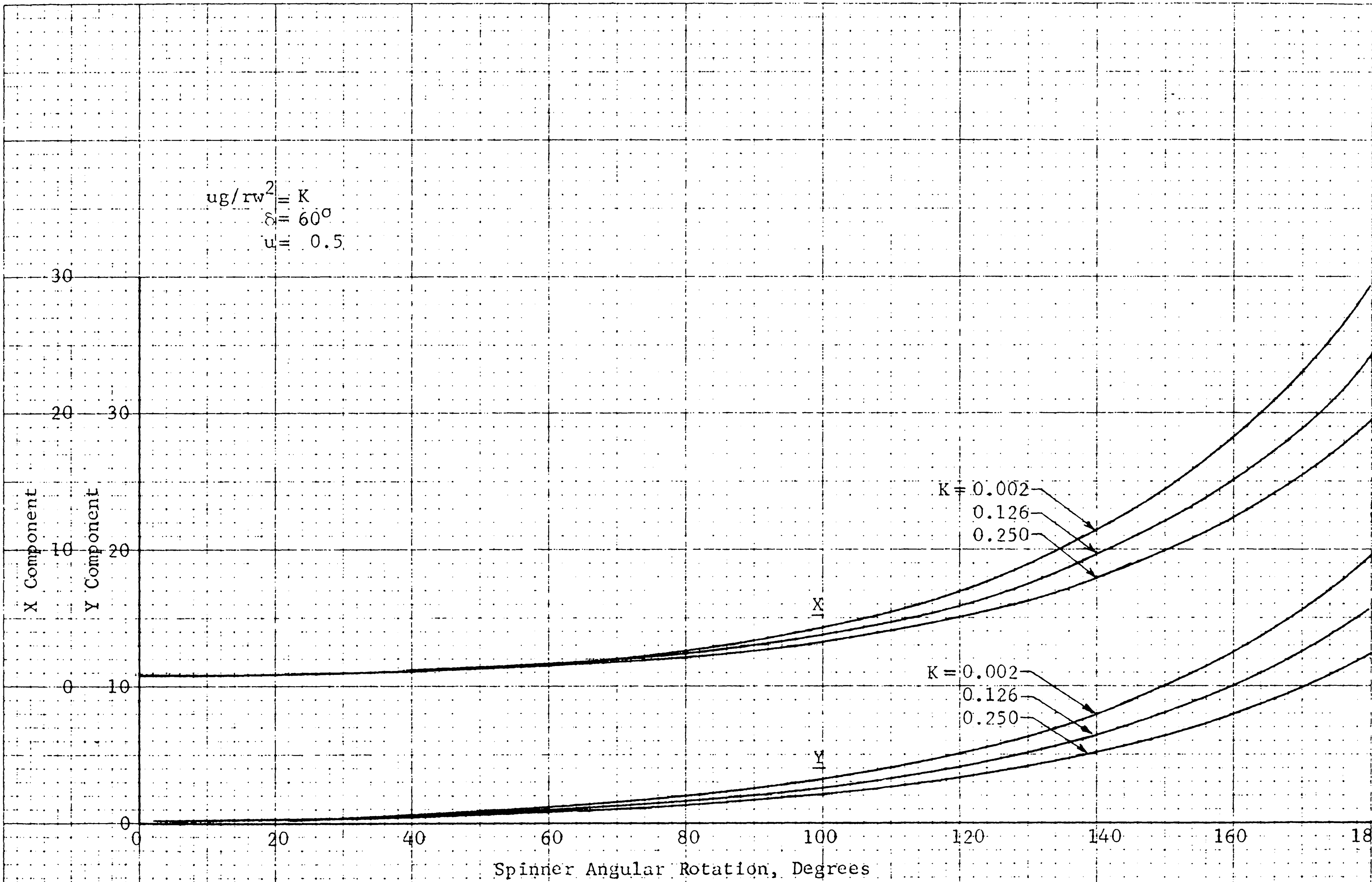

Figure 43 Dynamic Characteristics For Spinner With Backward-Pitched Blades
Components of Tangent of Departure Angle

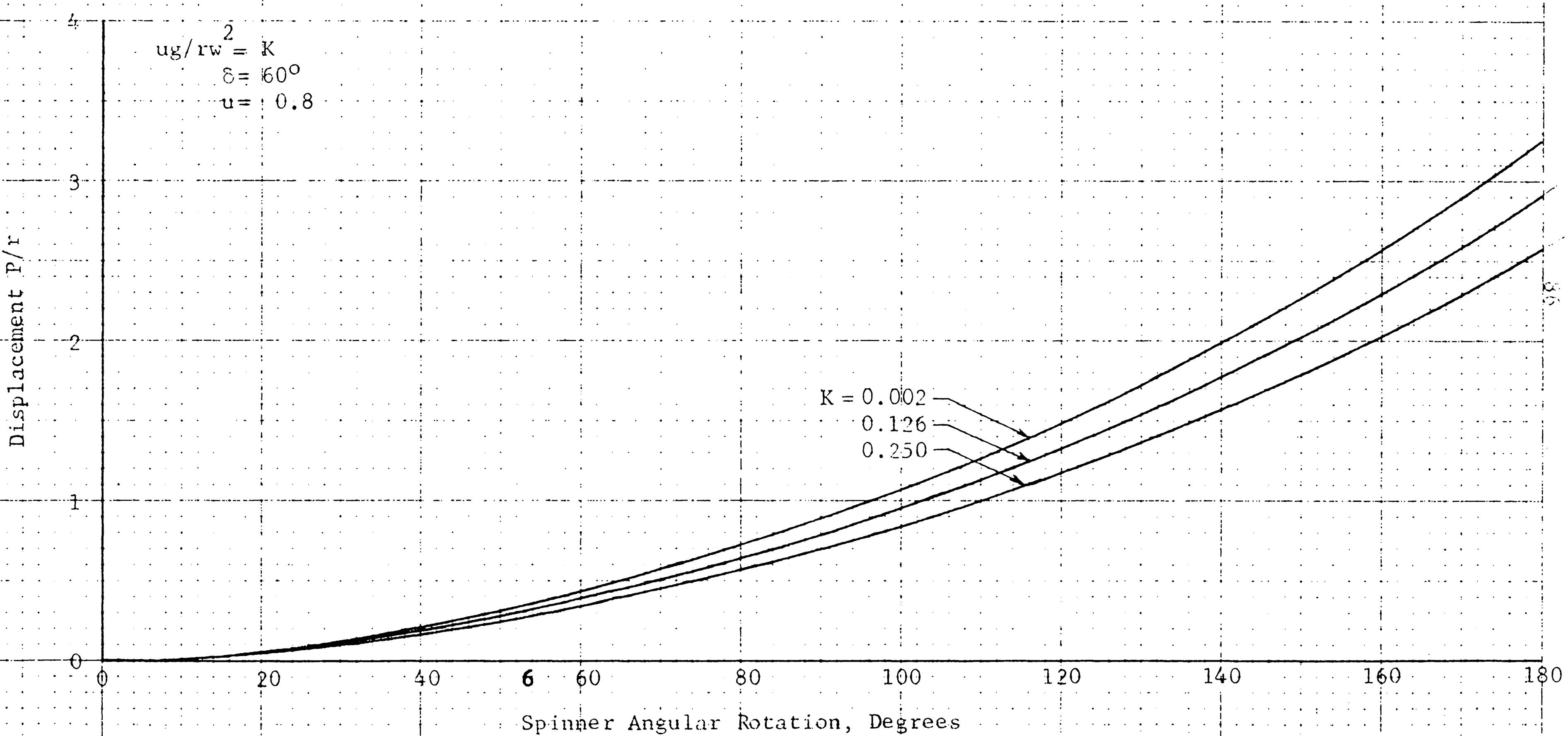

Figure 44 Dynamic Characteristics For Spinner With Backward-Pitched Blades

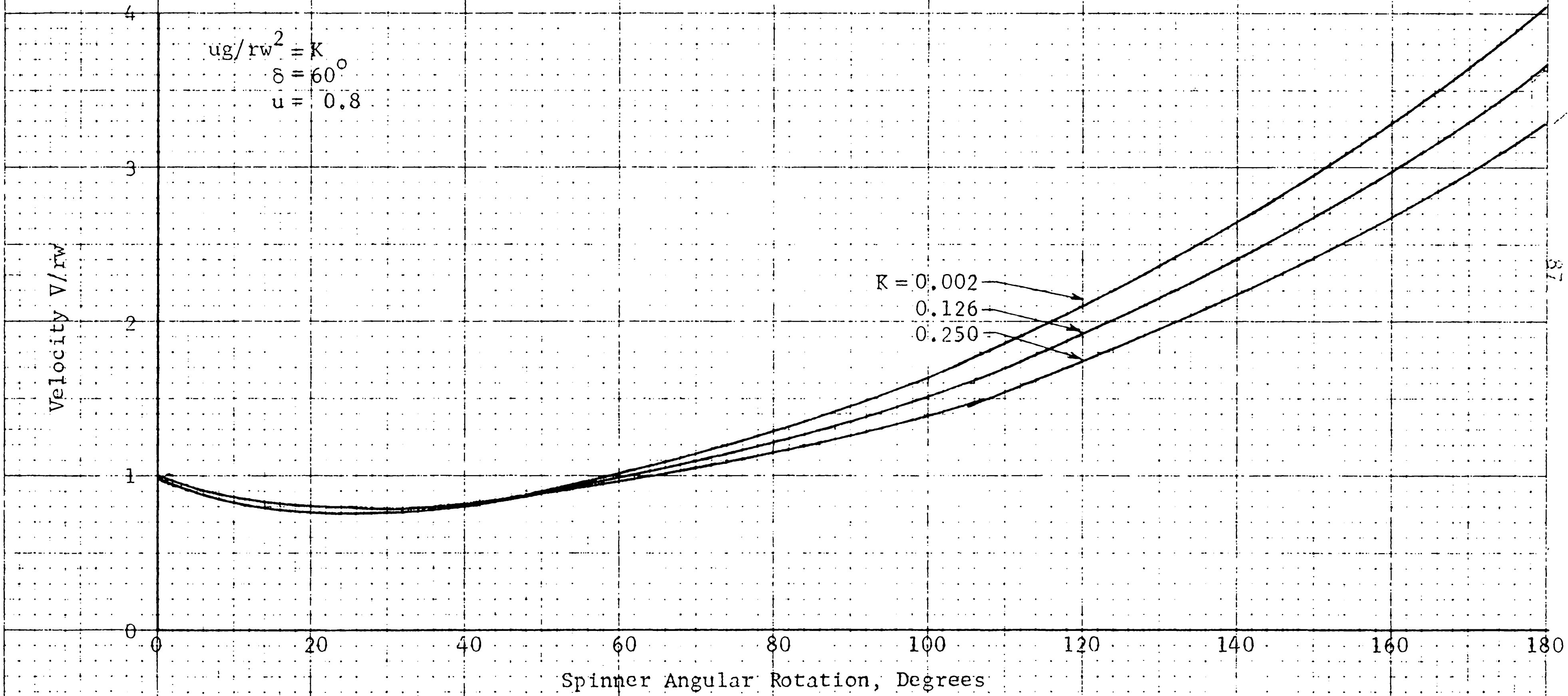

Figure 45 Dynamic Characteristics for Spinner With Backward-Pitched Blades

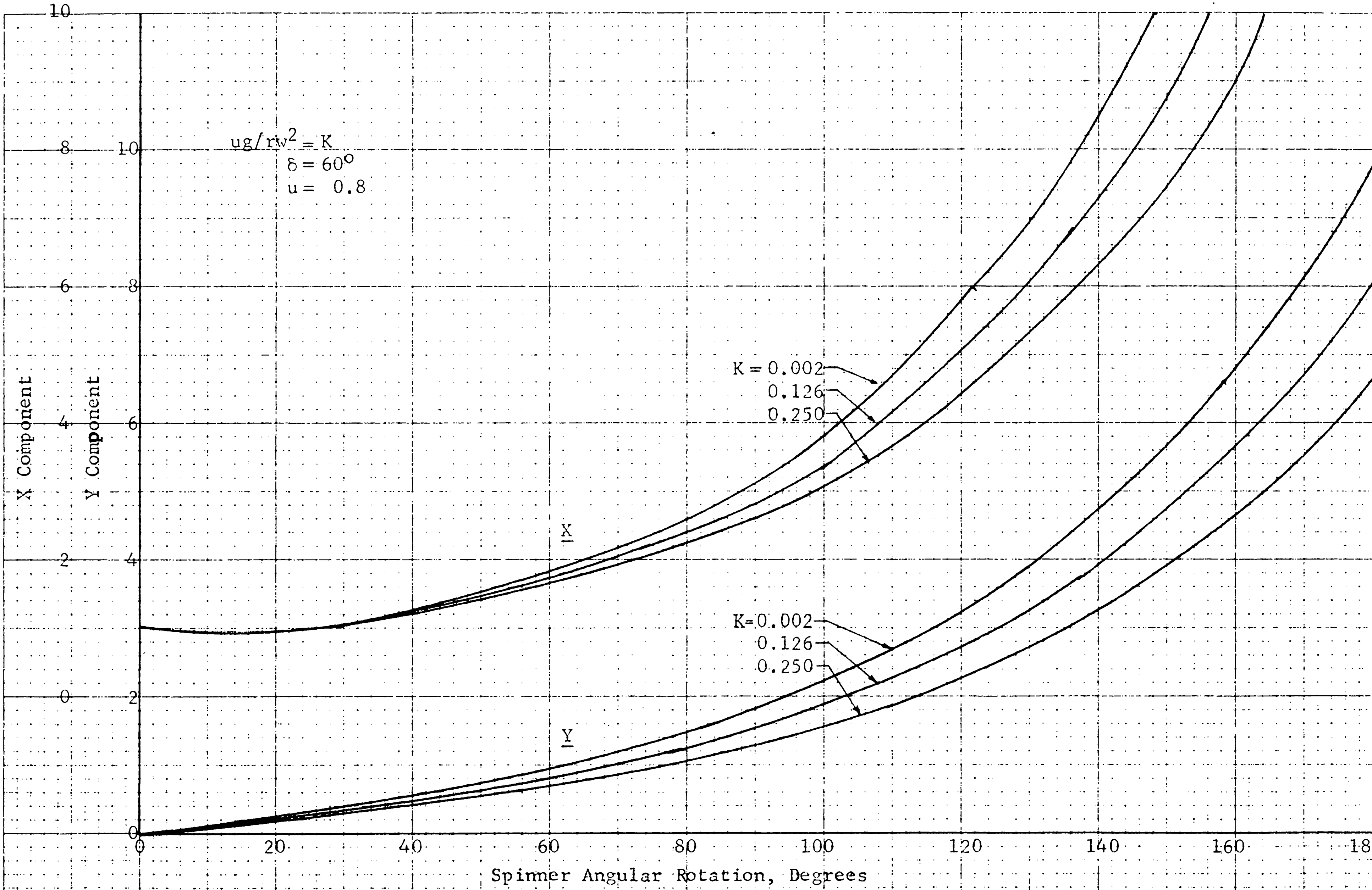

Figure 46 Dynamic Characteristics for Spinner With Backward-Pitched Blades.
Components of Tangent of Departure Angle

Appendix III

Dynamic Characteristics for Spinner With Forward and Backward-Curved Blades

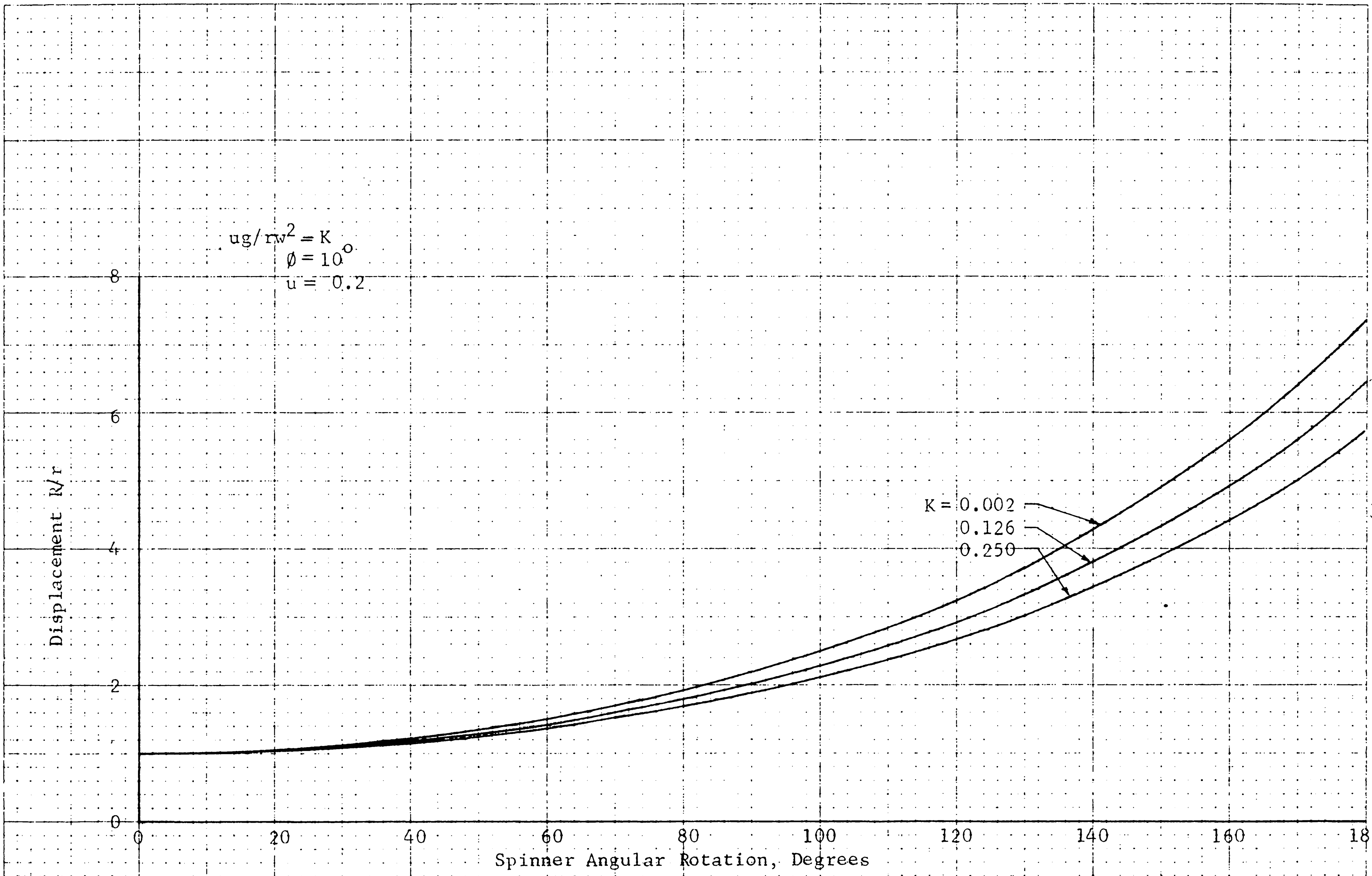

Figure 47 Dynamic Characteristics for Spinner With Forward Curved Blades

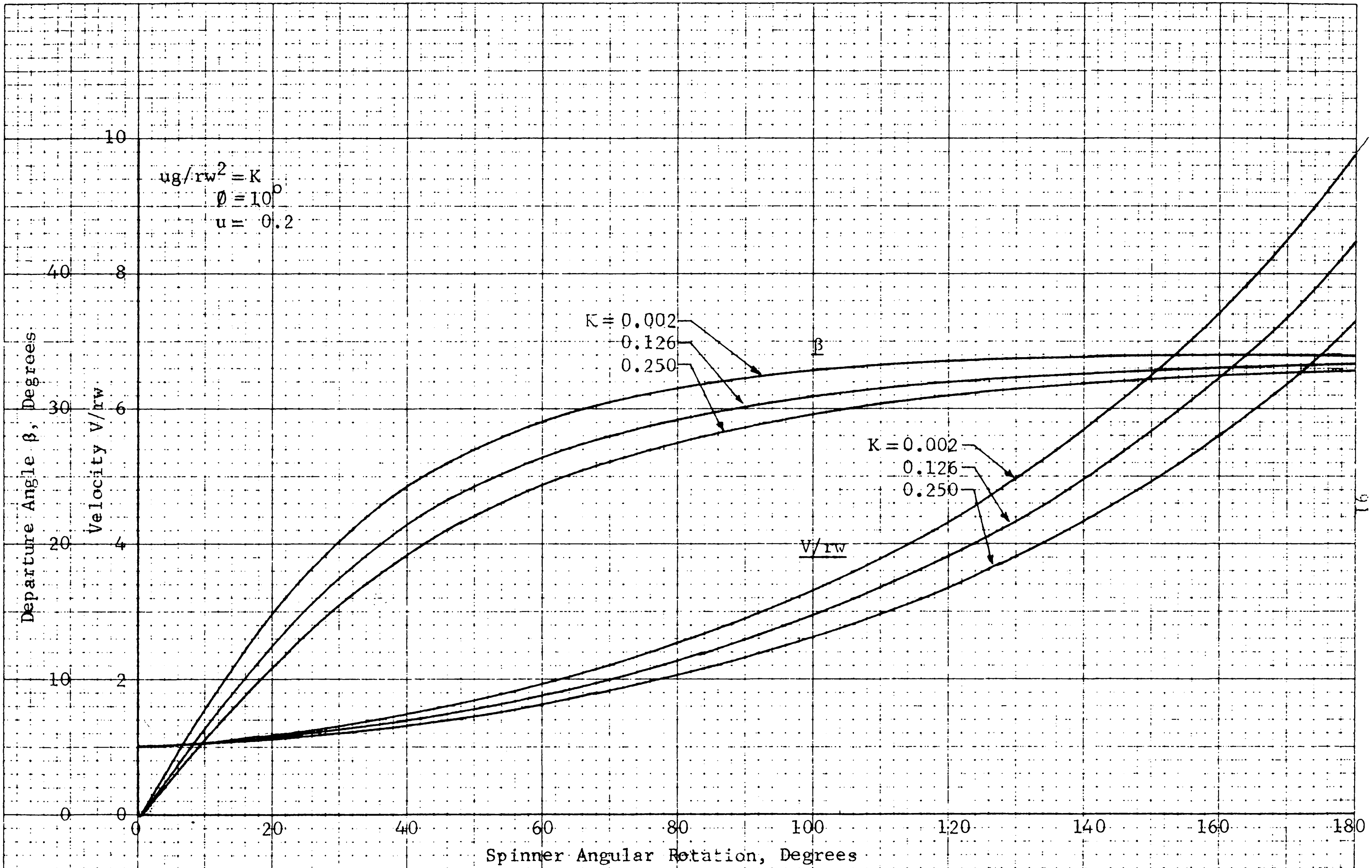

Figure 48 Dynamic Characteristics for Spinner With Forward Curved Blades

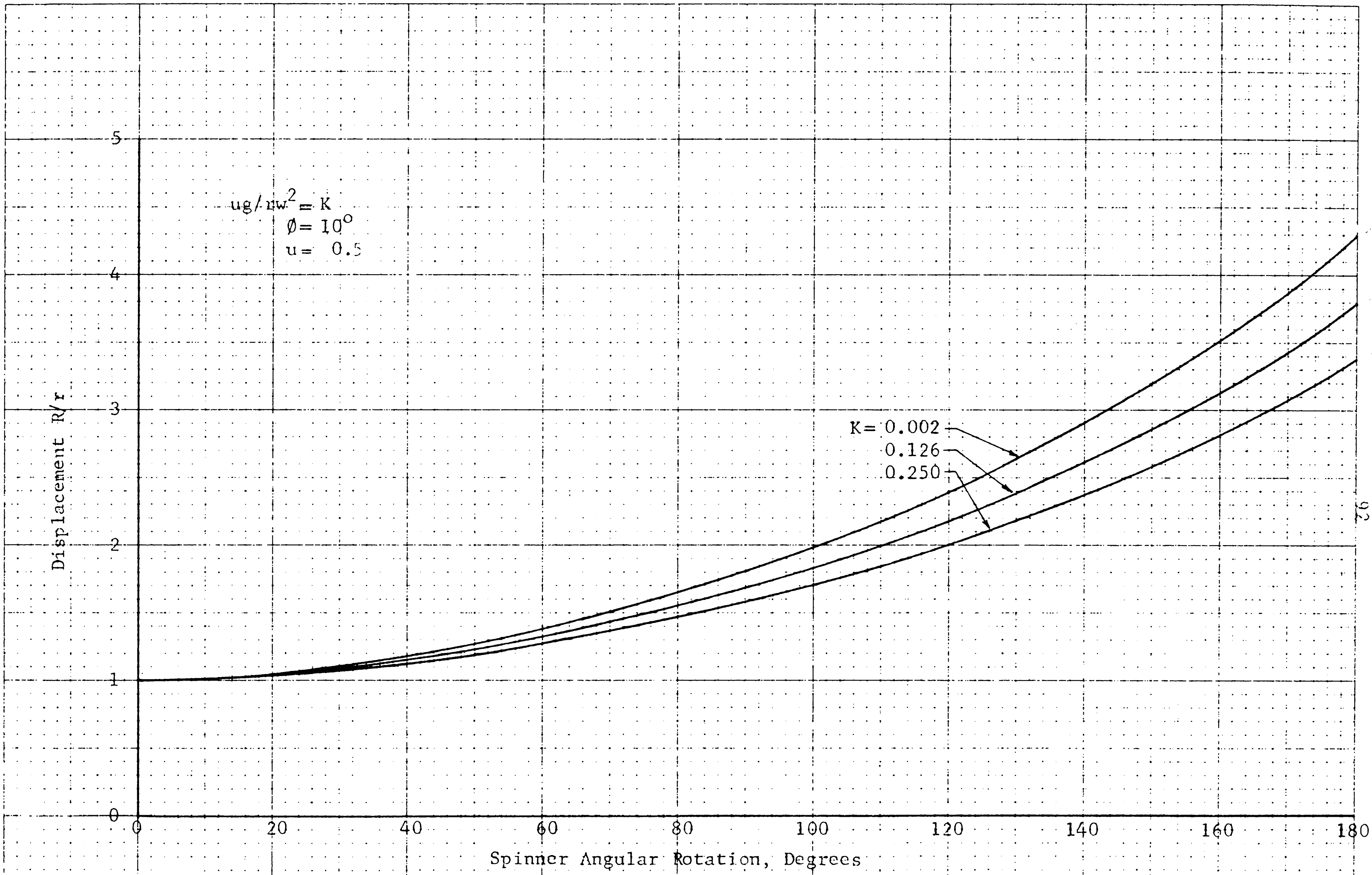

Figure 49 Dynamic Characteristics for Spinner With Forward-Curved Blades

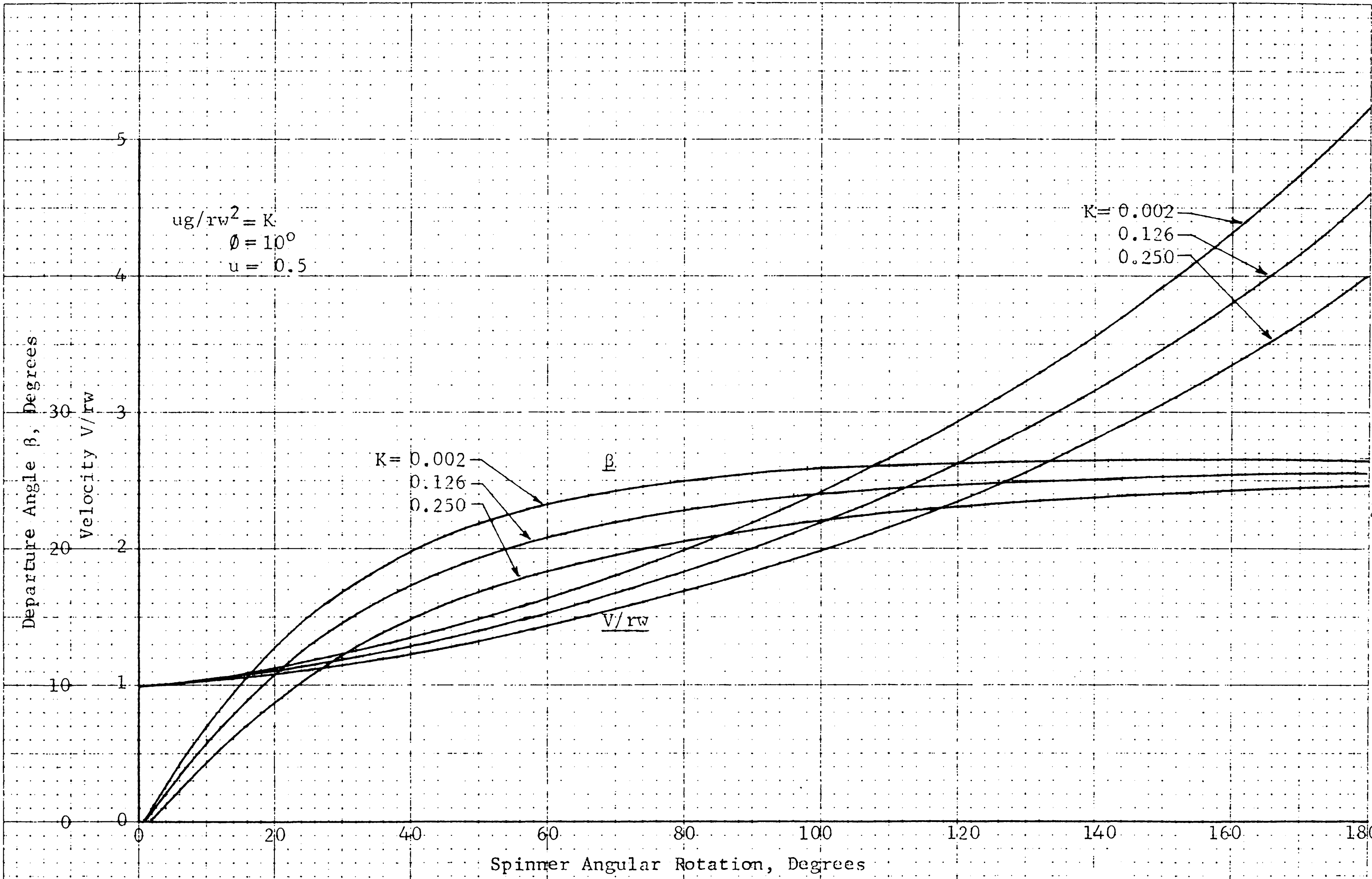

Figure 50 Dynamic Characteristics for Spinner With Forward-Curved Blades

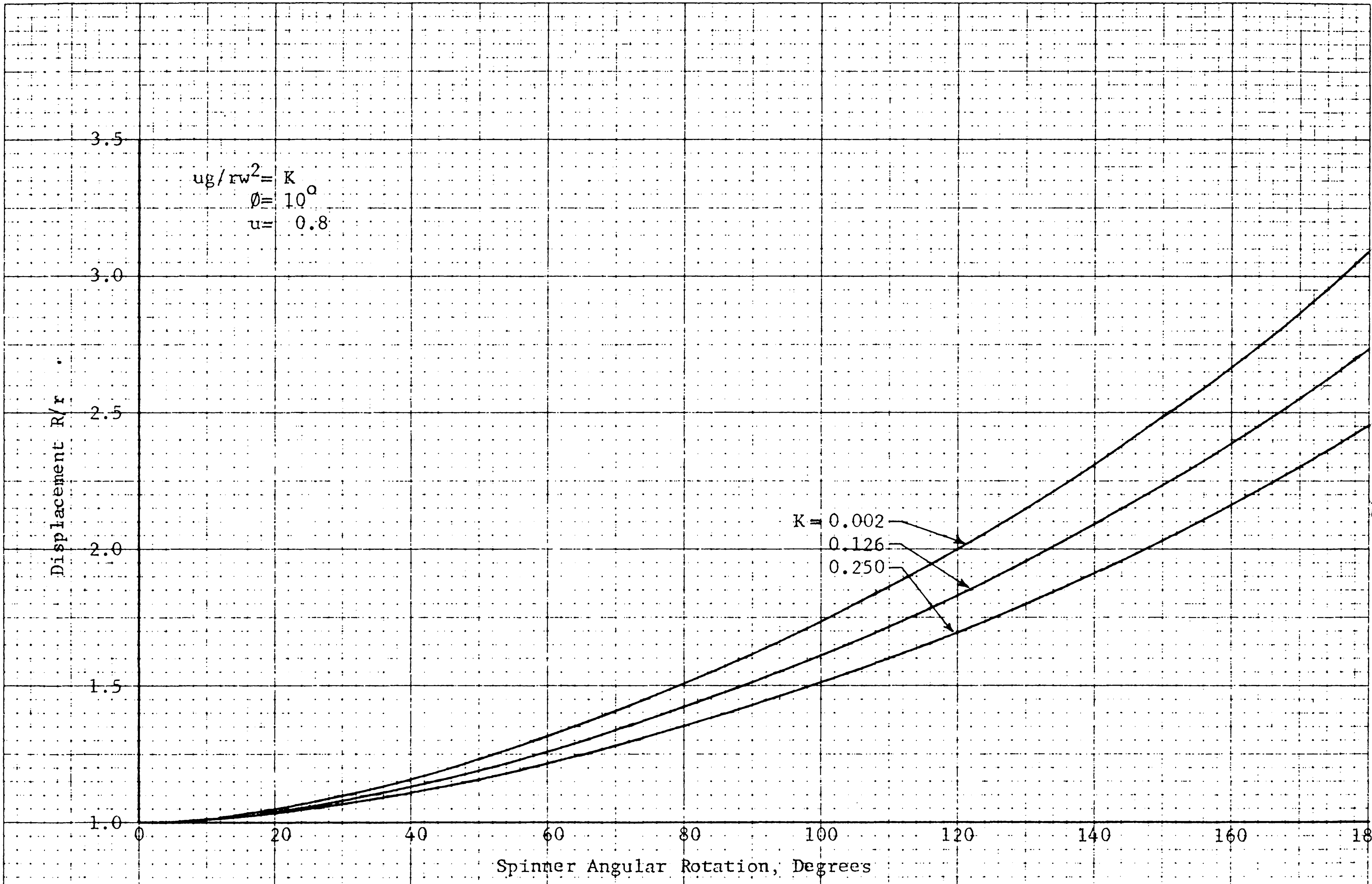

Figure 51 Dynamic Characteristics for Spinner With Forward-Curved Blades

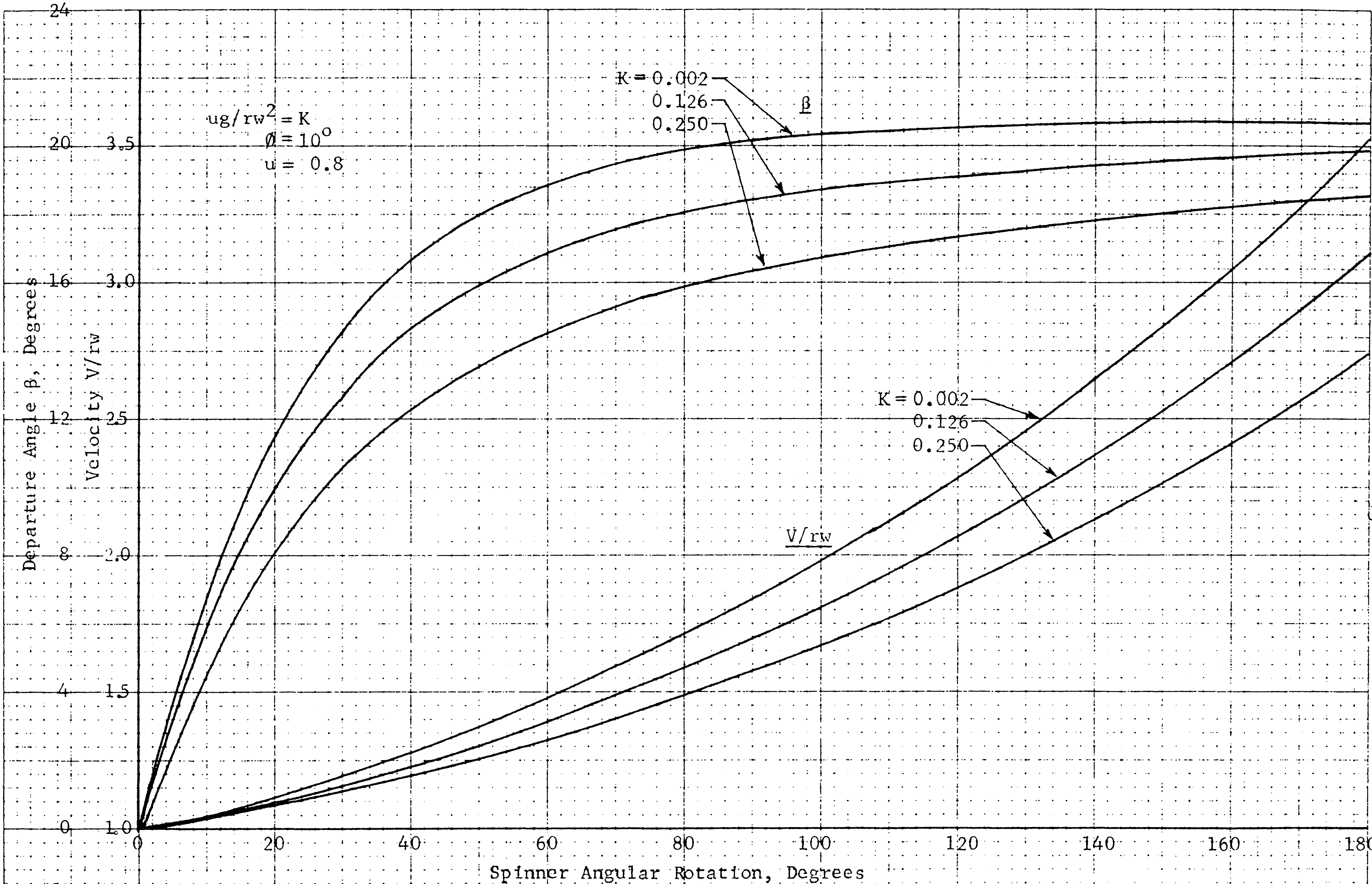

Figure 52 Dynamic Characteristics for Spinner With Forward-Curved Blades

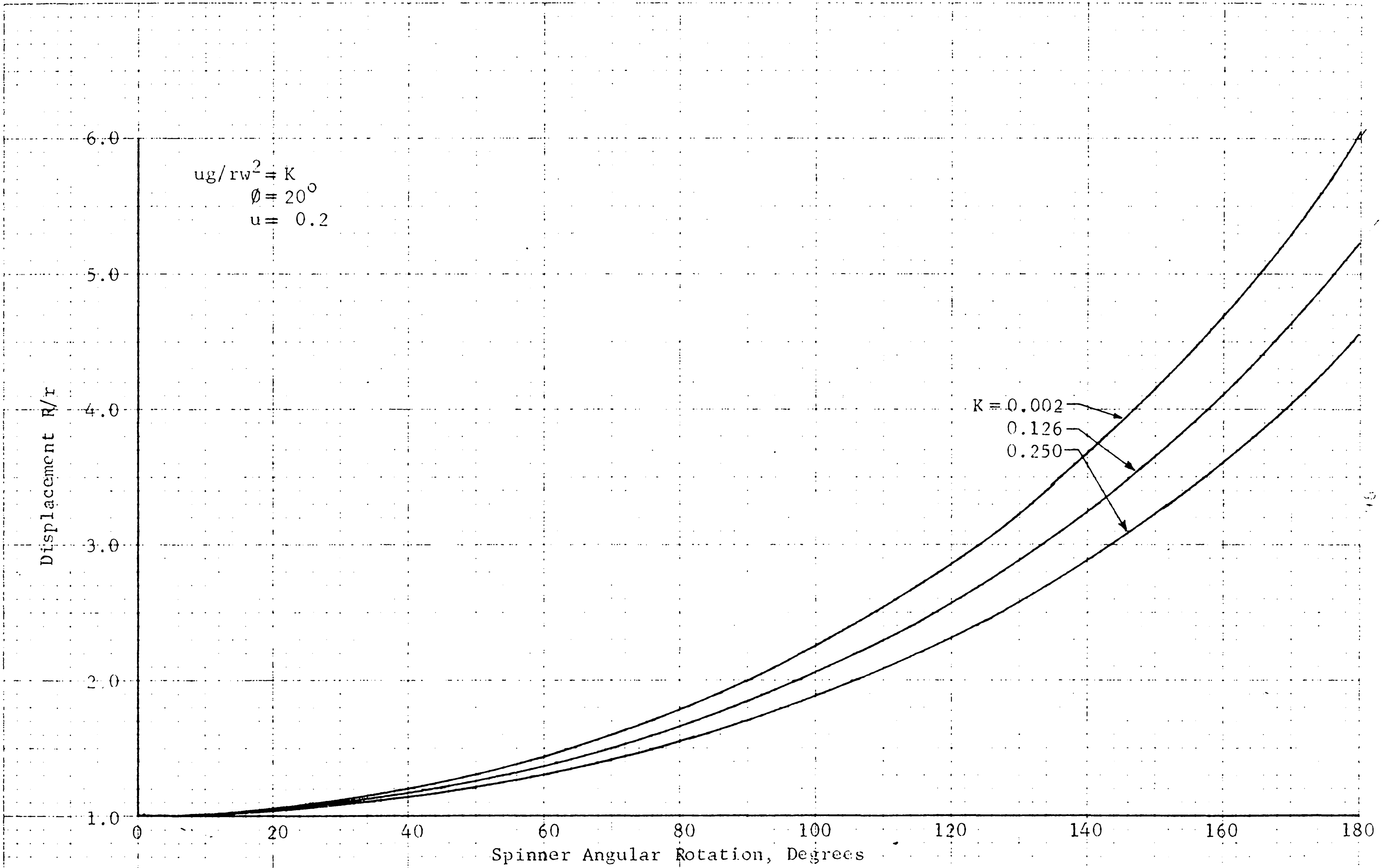

Figure 53 Dynamic Characteristics for Spinner With Forward-Curved Blades

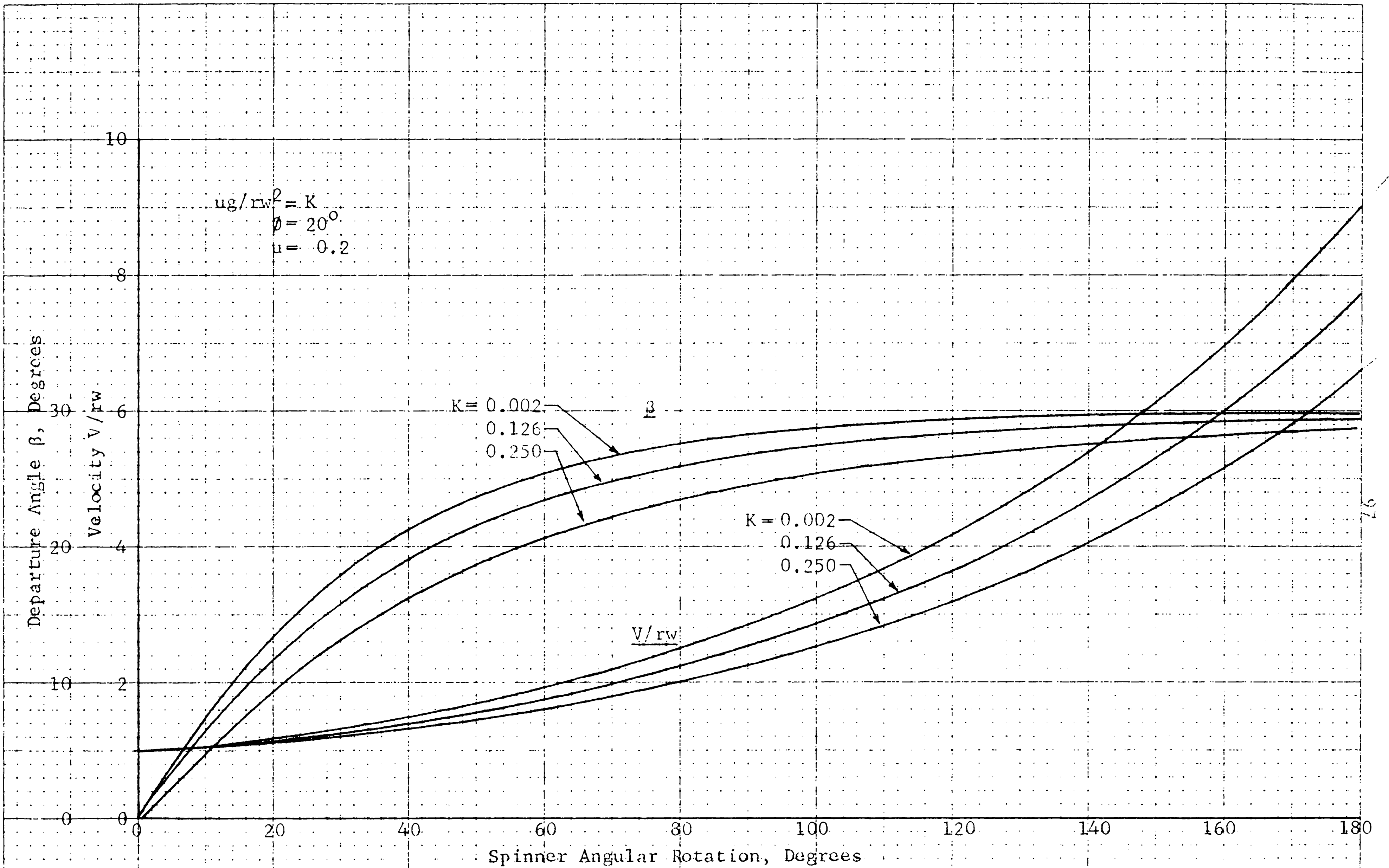

Figure 54 Dynamic Characteristics for Spinner With Forward-Curved Blades

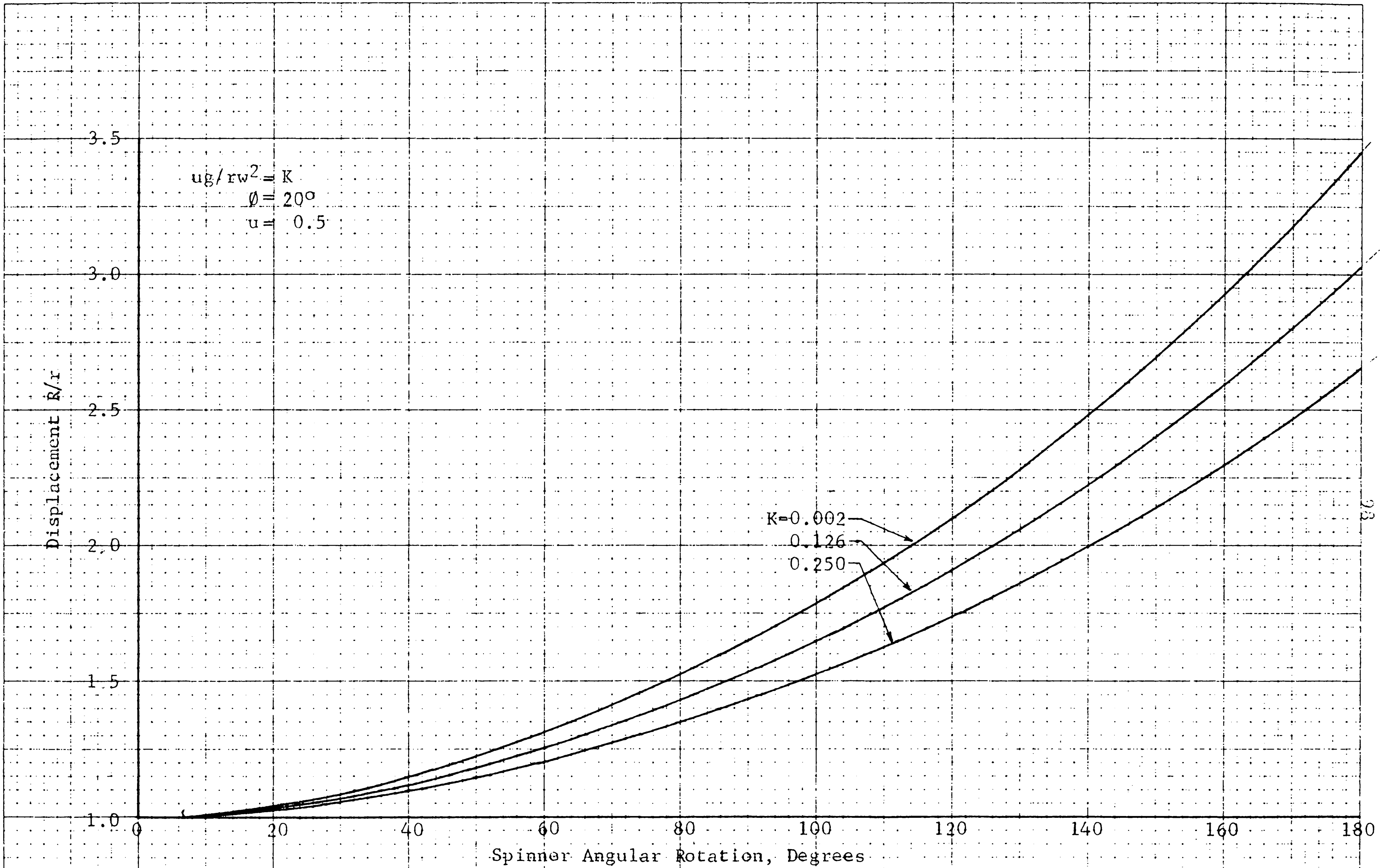

Figure 55 Dynamic Characteristics for Spinner With Forward-Curved Blades

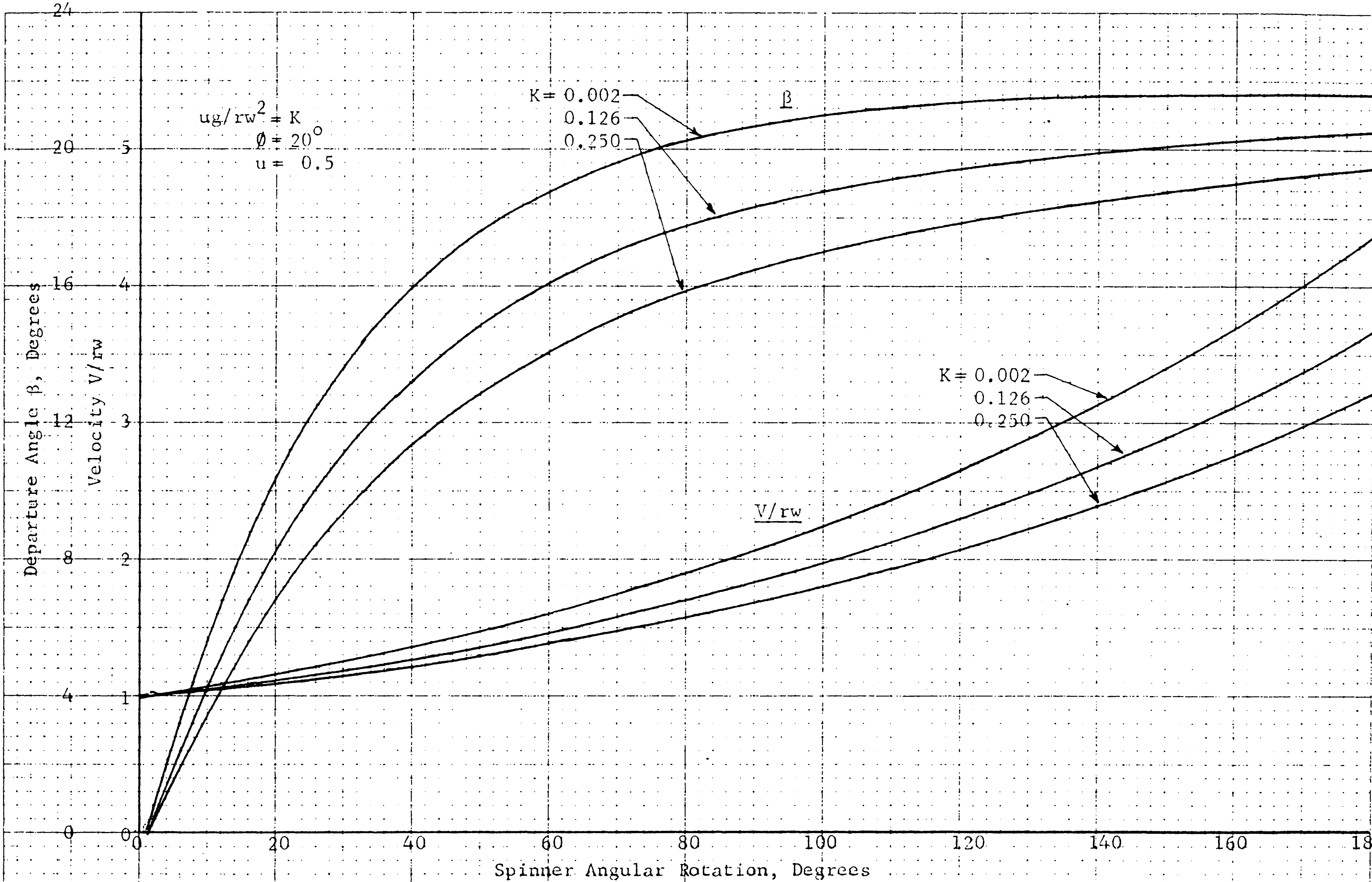

Figure 56 Dynamic Characteristics for Spinner With Forward-Curved Blades

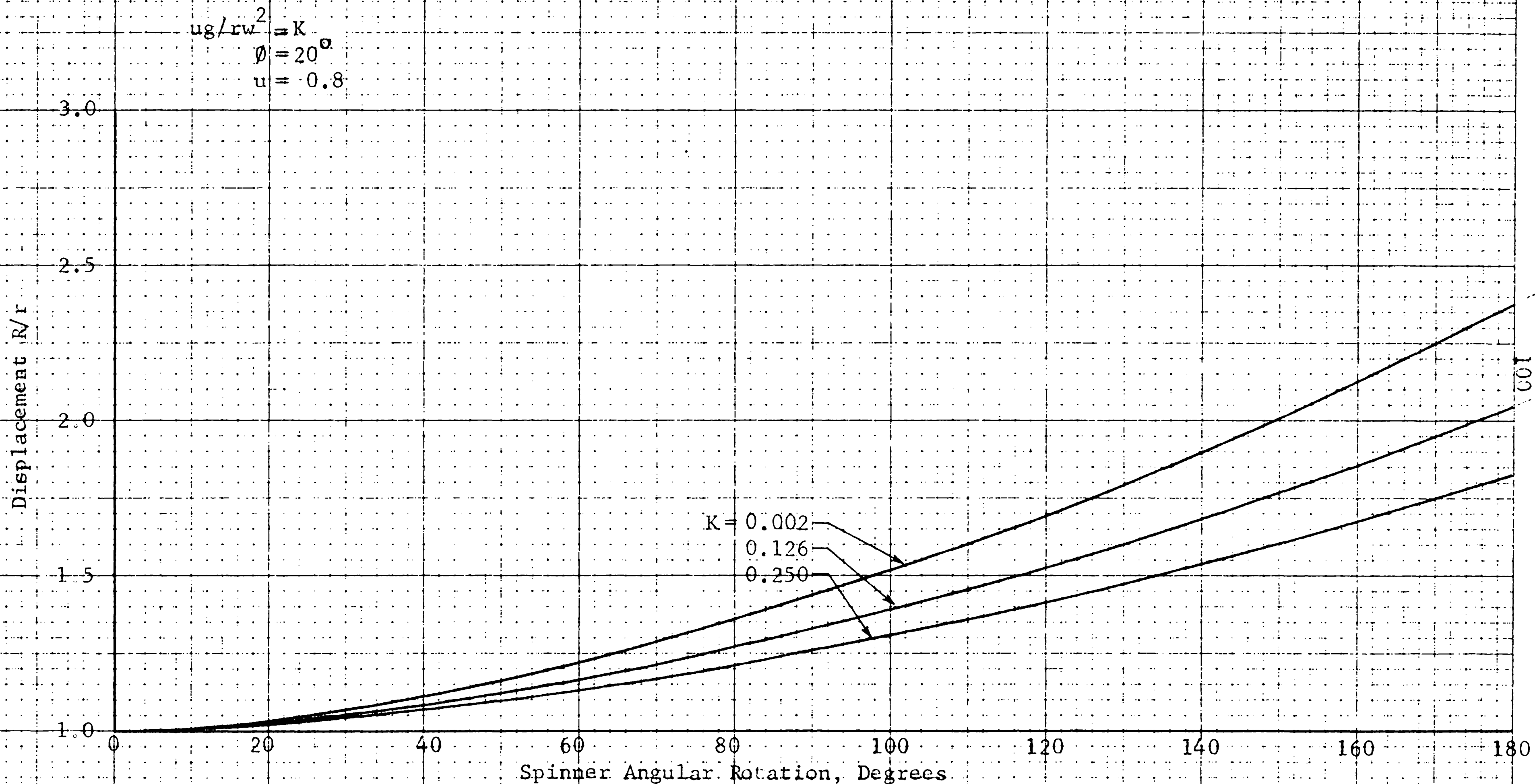

Figure 57 - Dynamic Characteristics for Spinner With Forward-Curved Blades

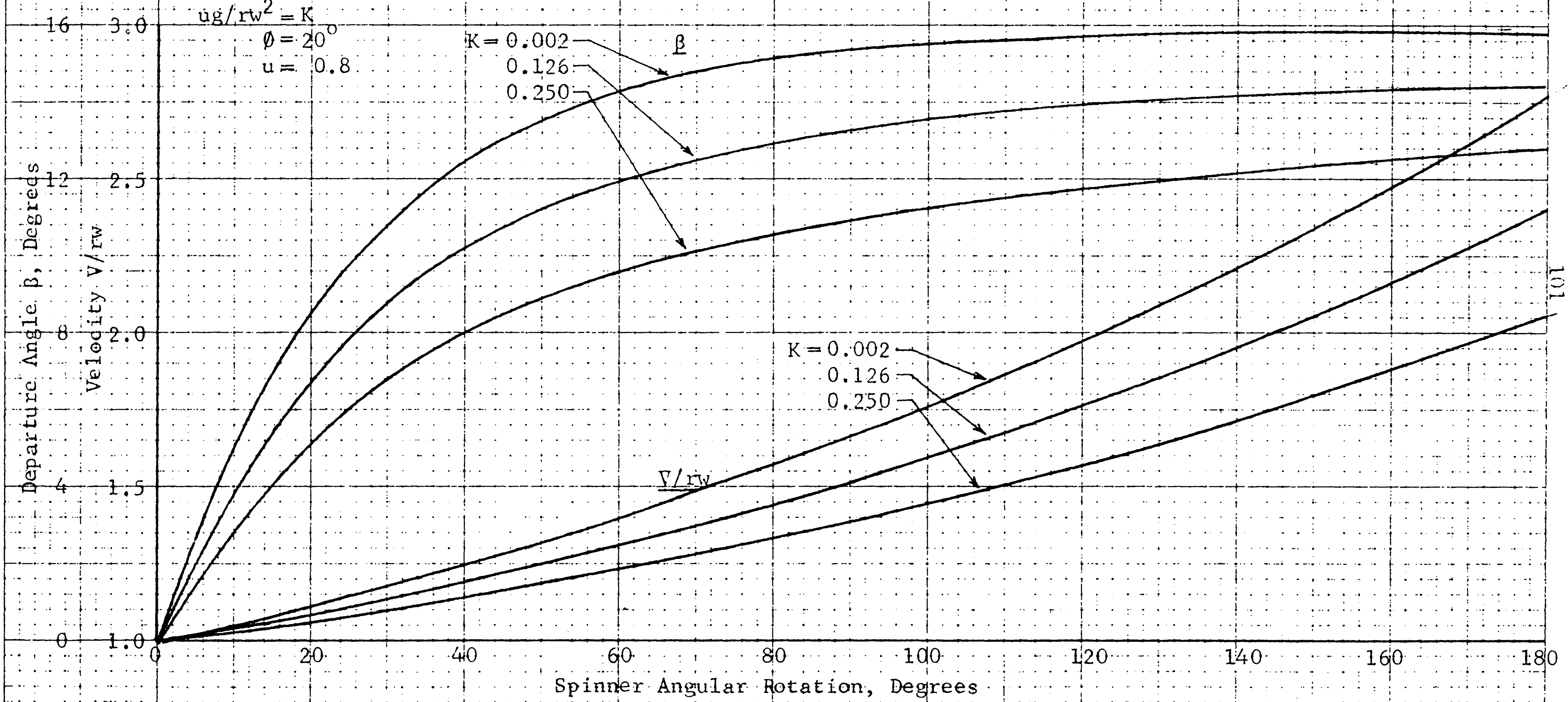

Figure 58 Dynamic Characteristics for Spinner With Forward-Curved Blades

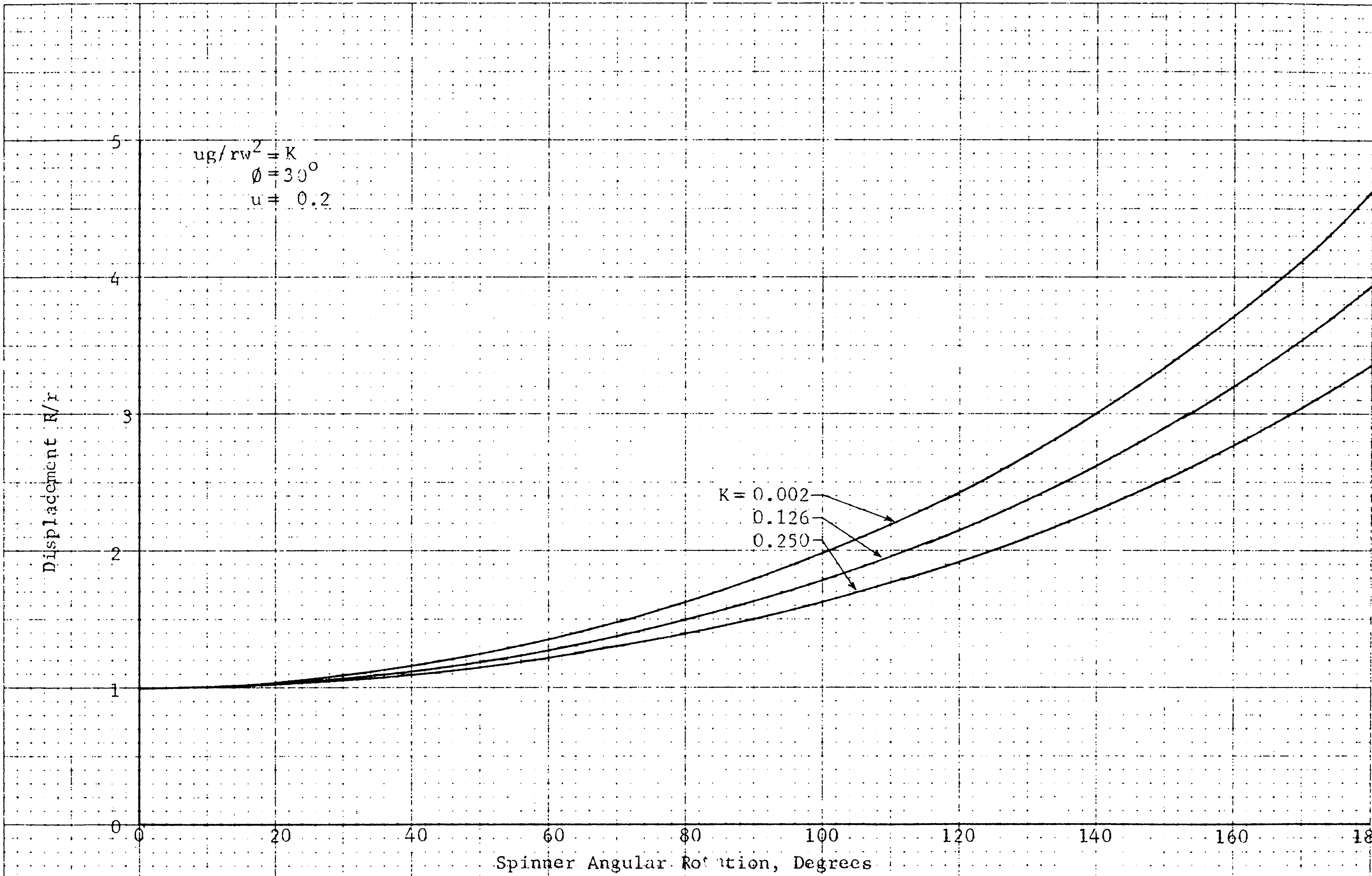

Figure 59 Dynamic Characteristics for Spinner With Forward-Curved Blades

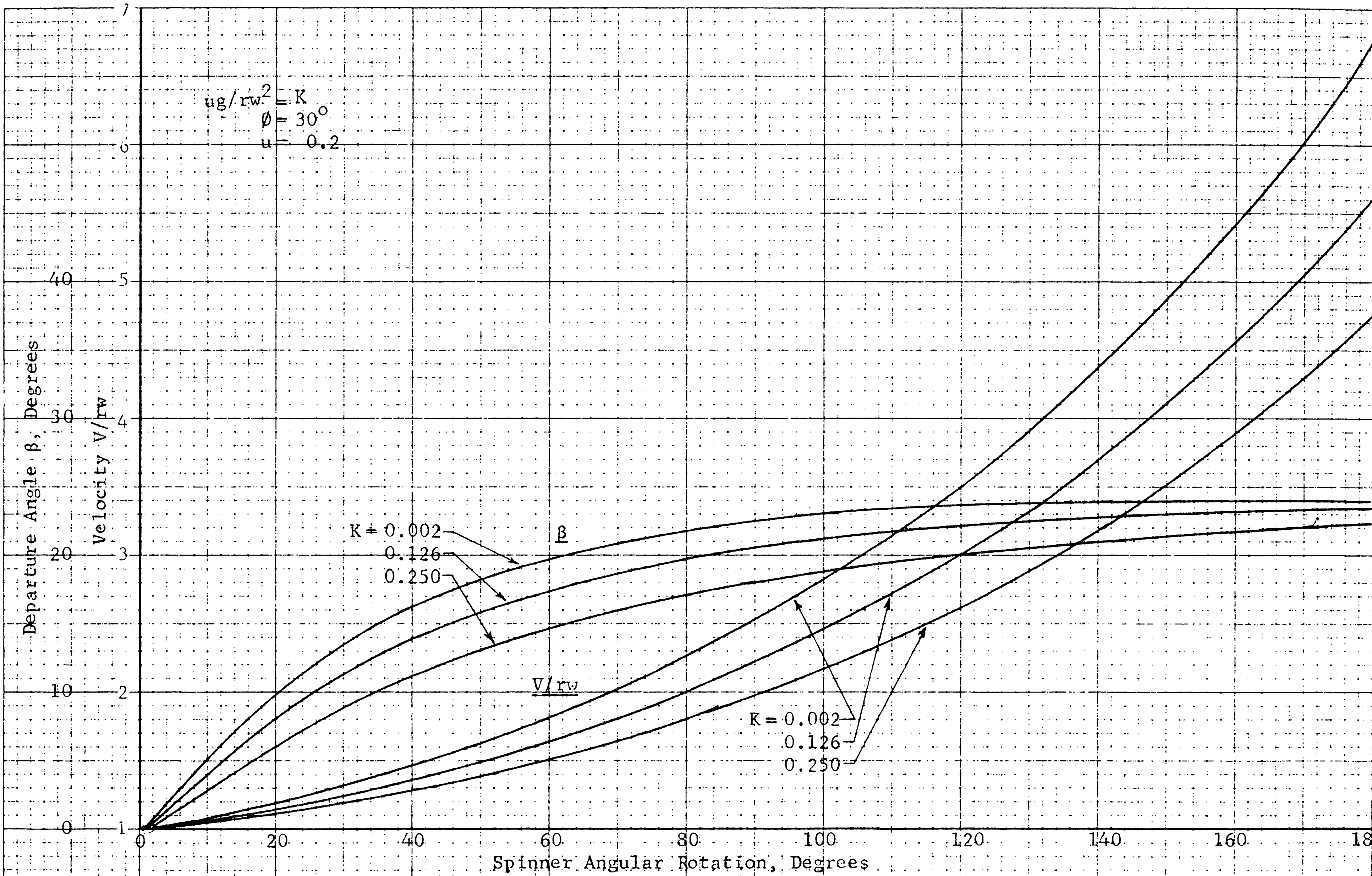

Figure 60 Dynamic Characteristics for Spinner With Forward-Curved Blades

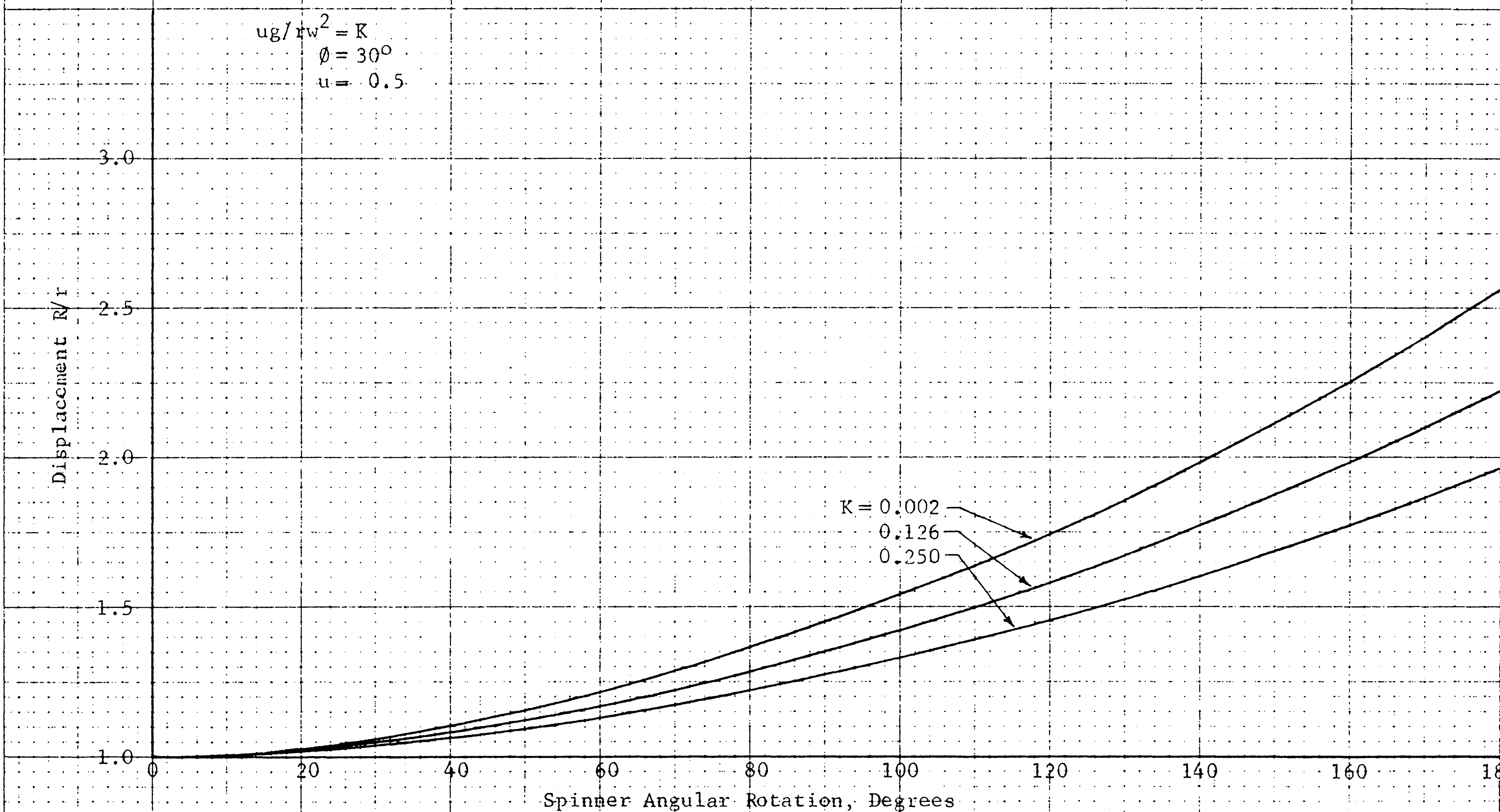

Figure 61 Dynamic Characteristics for Spinner With Forward-Curved Blades

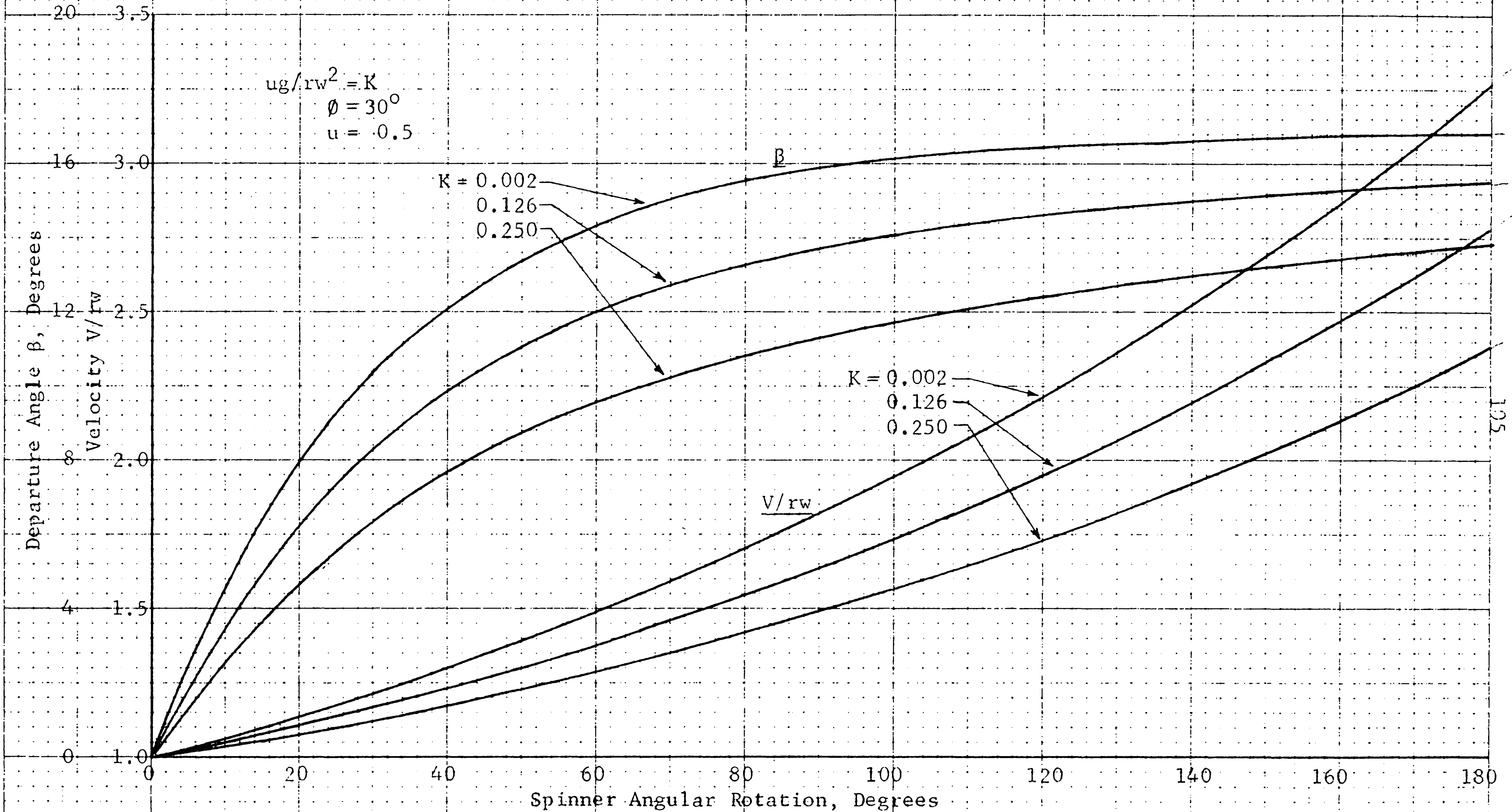

Figure 62 Dynamic Characteristics for Spinner With Forward-Curved Blades

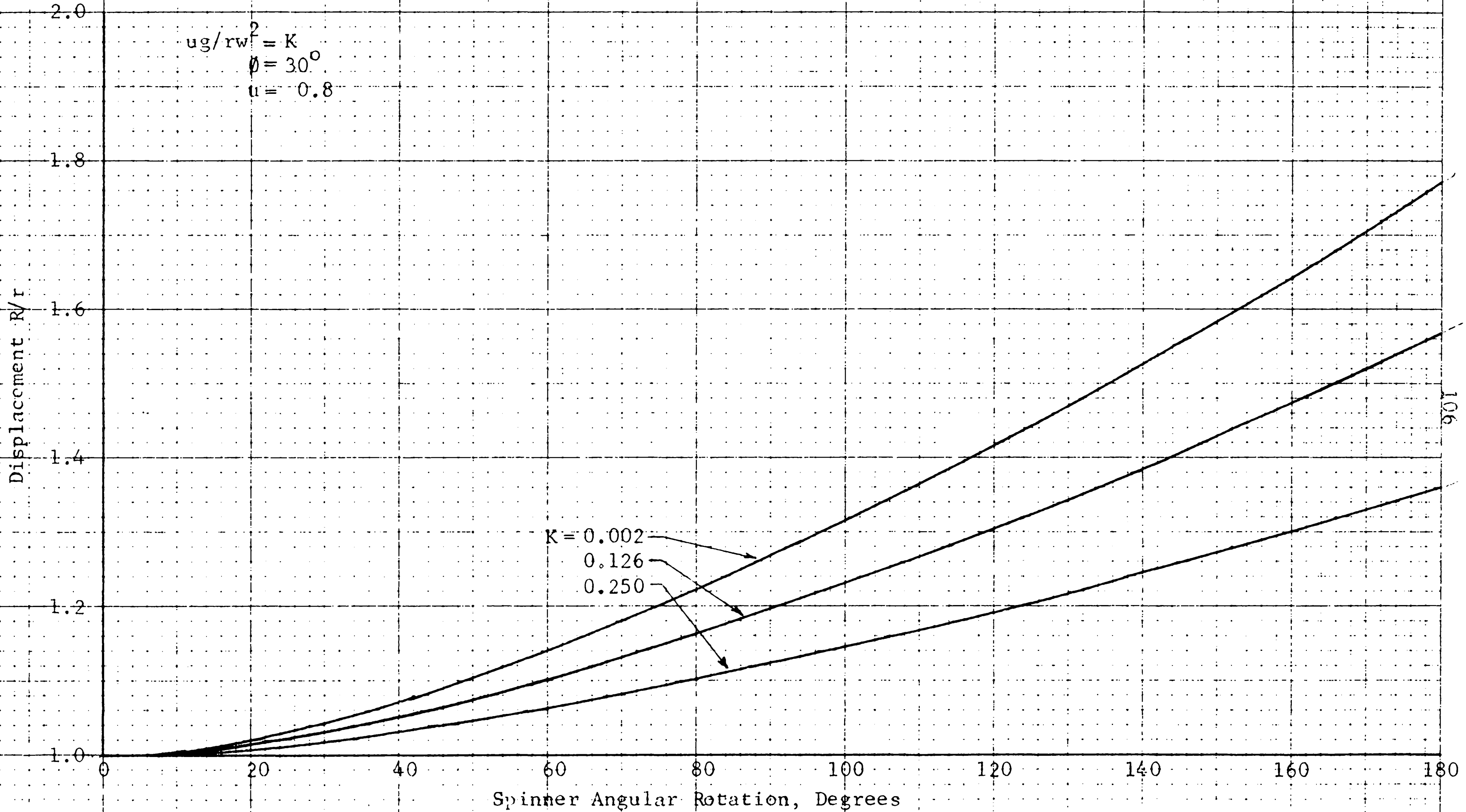

Figure 63 Dynamic Characteristics for Spinner With Forward-Curved Blades

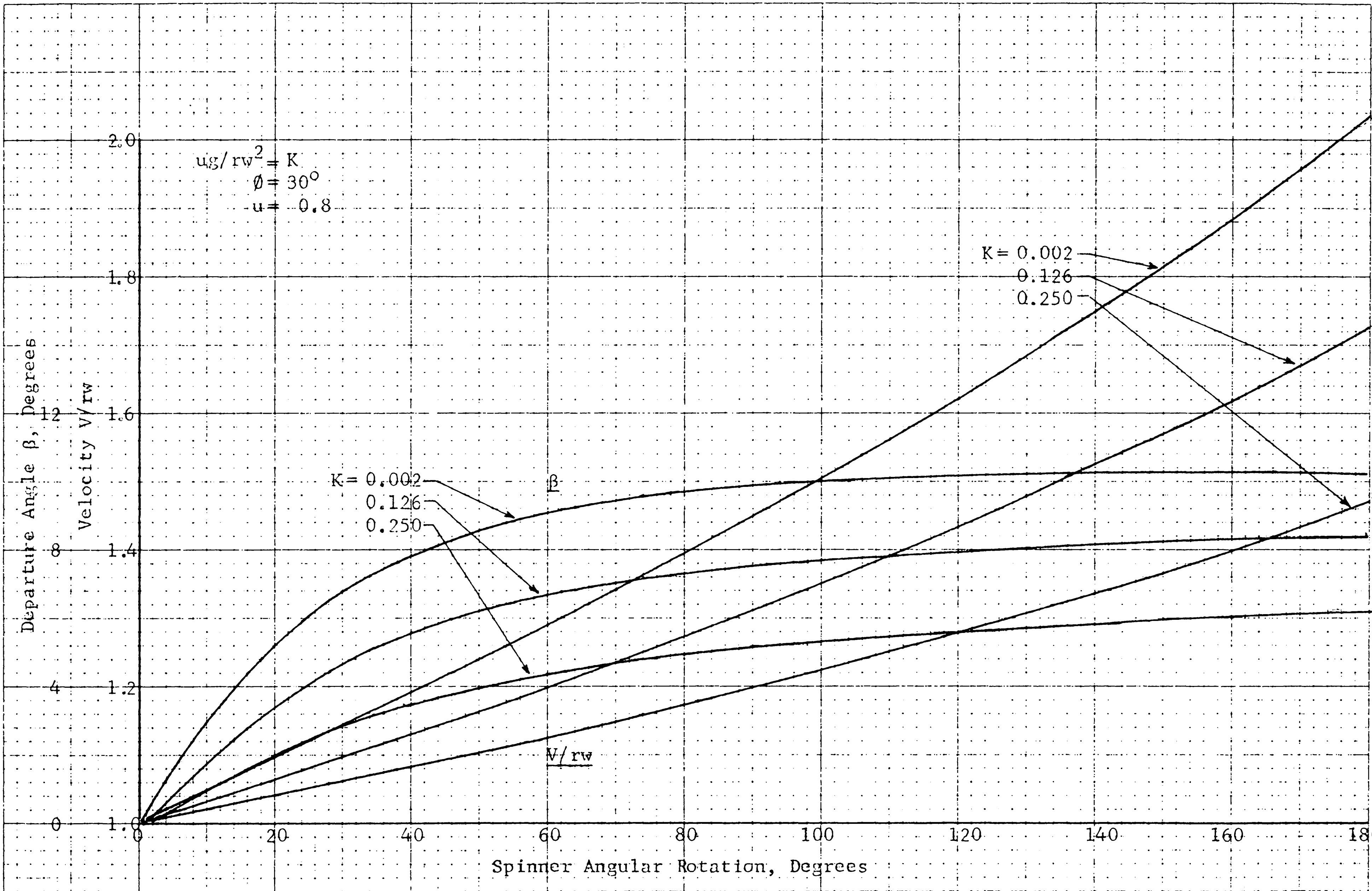

Figure 64 Dynamic Characteristics for Spinner With Forward-Curved Blades

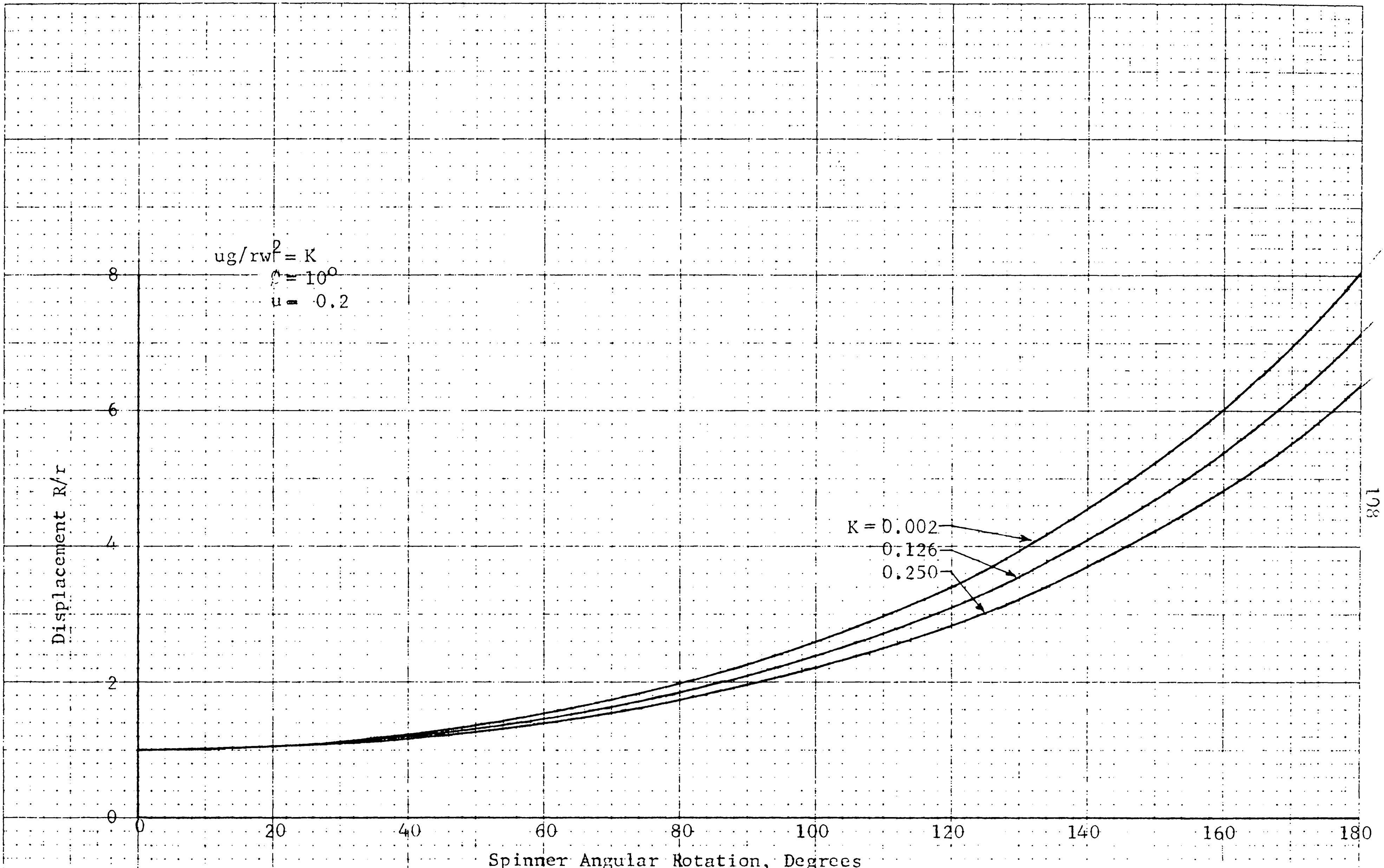

Figure 65 Dynamic Characteristics for Spinner With Backward-Curved Blades

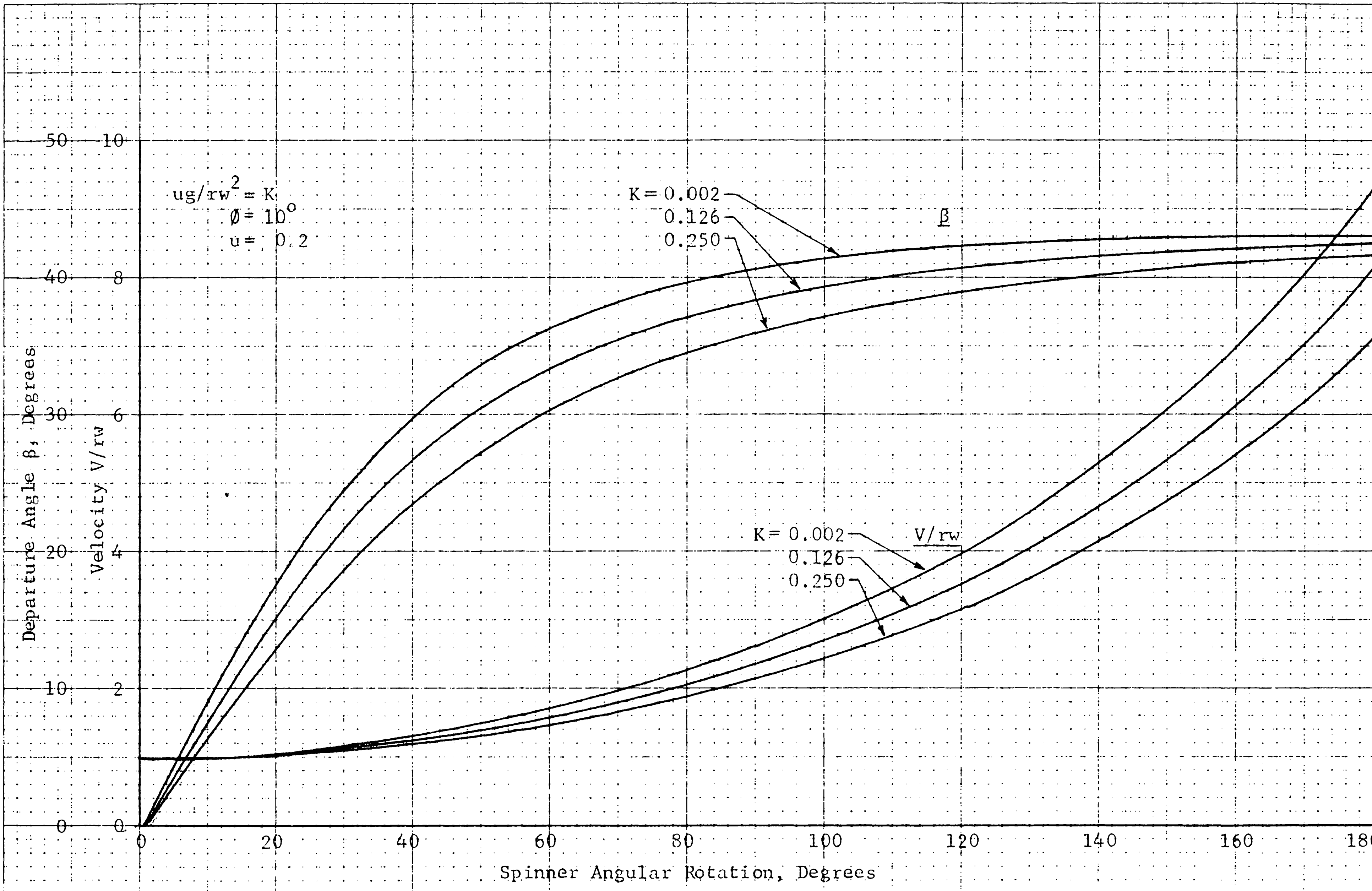

Figure 66 Dynamic Characteristics for Spinner With Backward-Curved Blades

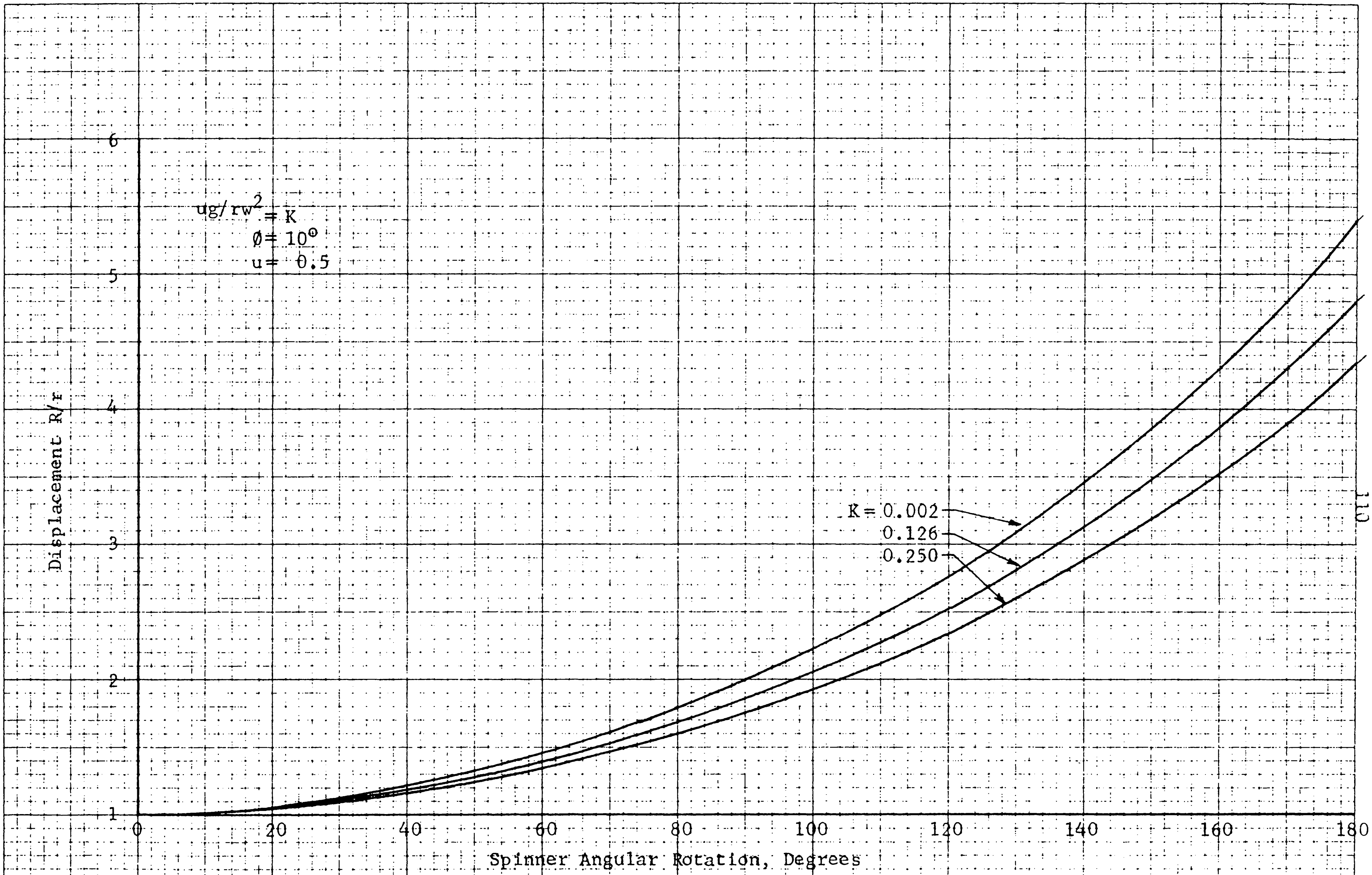

Figure 67 Dynamic Characteristics for Spinner With Backward-Curved Blades

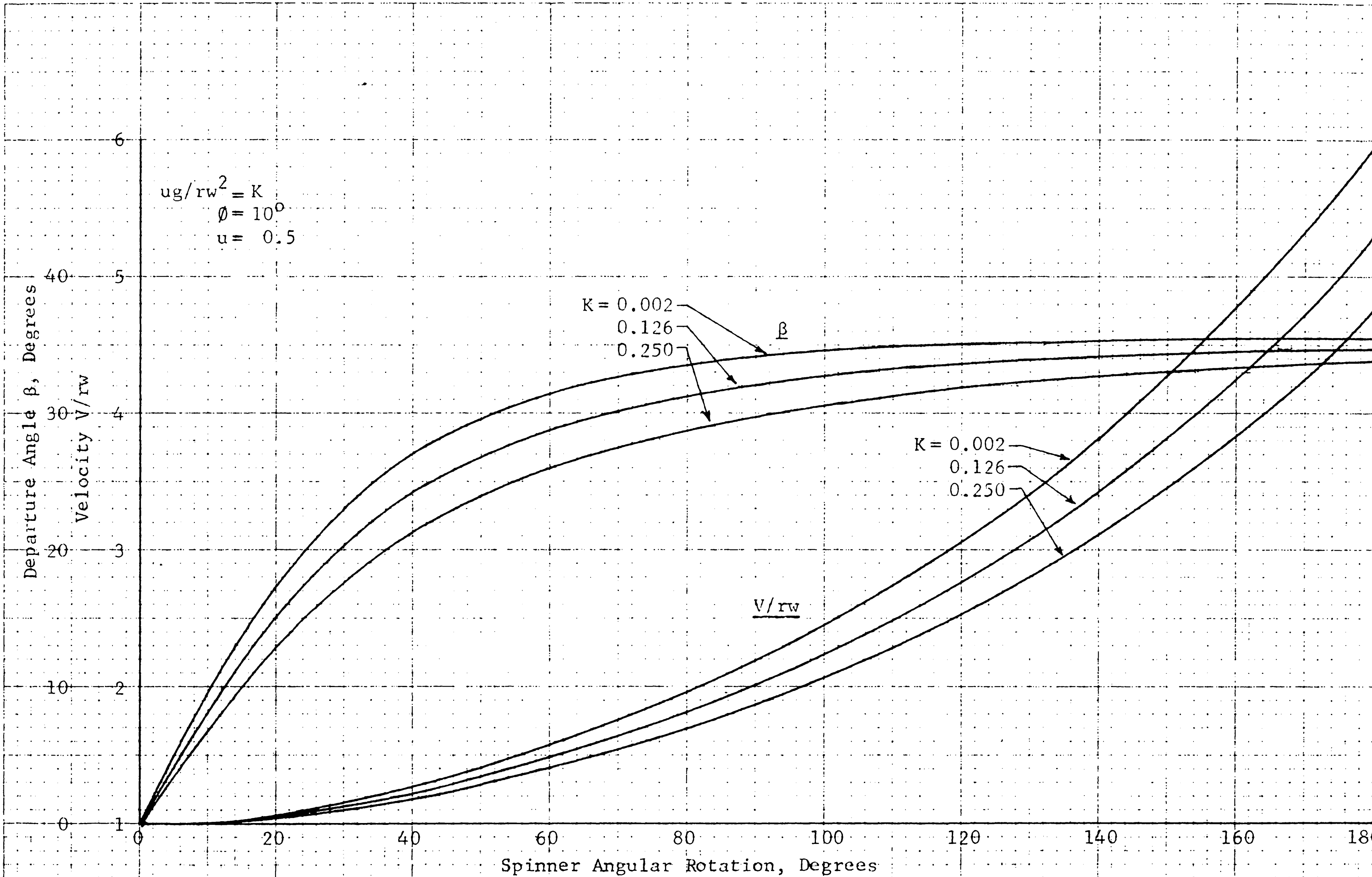

Figure 68 Dynamic Characteristics for Spinner With Backward-Curved Blades

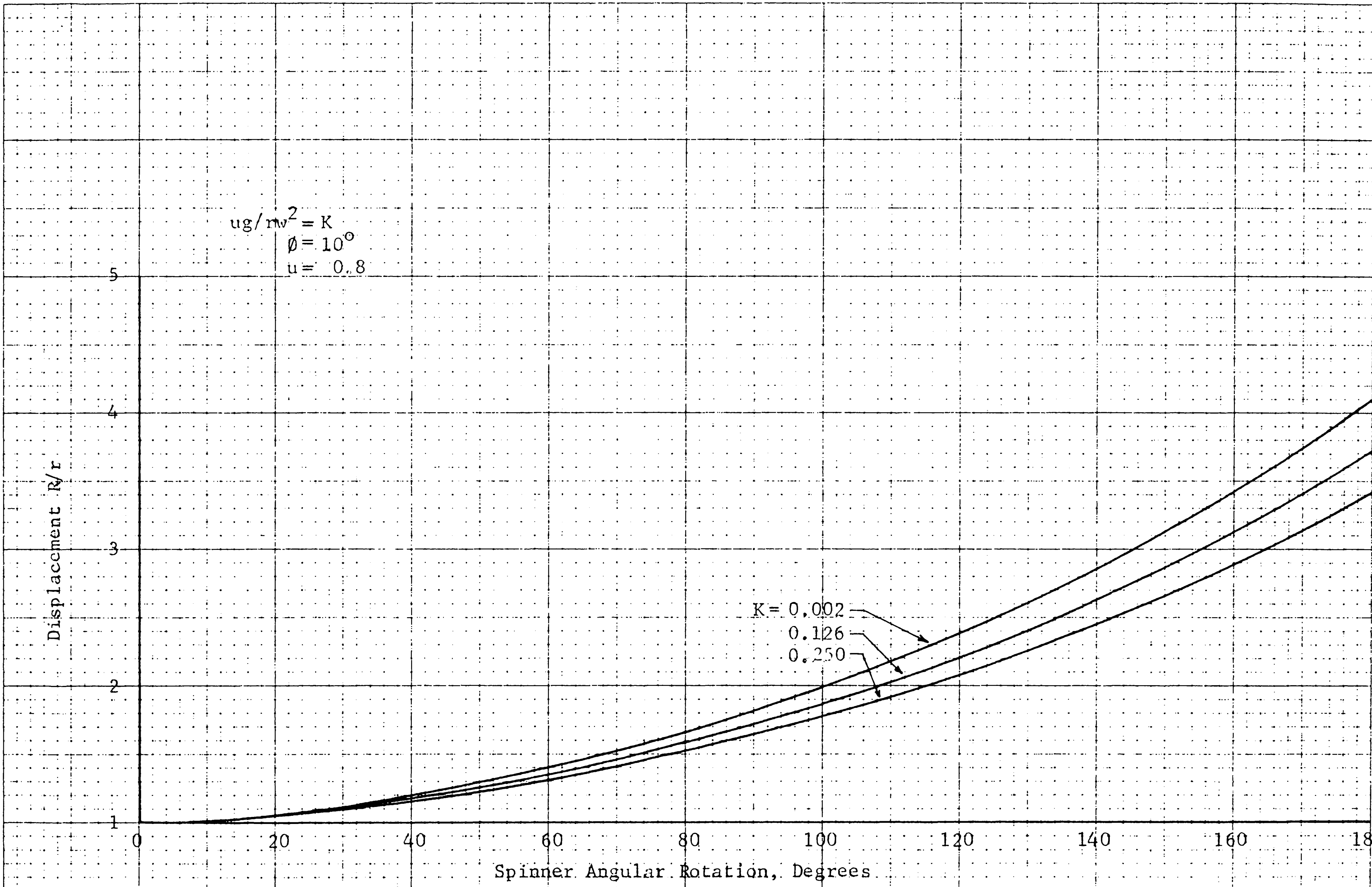

Figure 69 Dynamic Characteristics for Spinner With Backward-Curved Blades

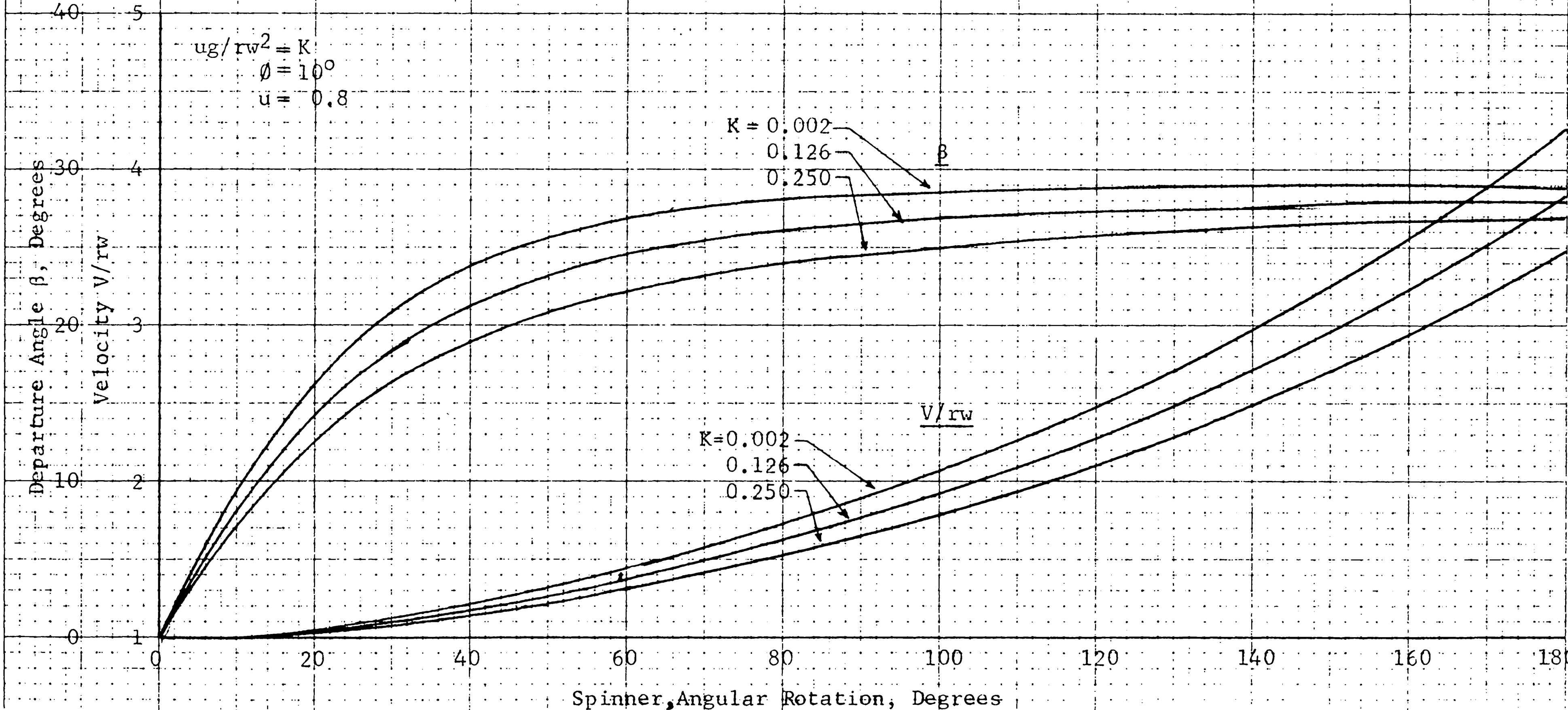

Figure 70 Dynamic Characteristics for Spinner With Backward-Curved Blades

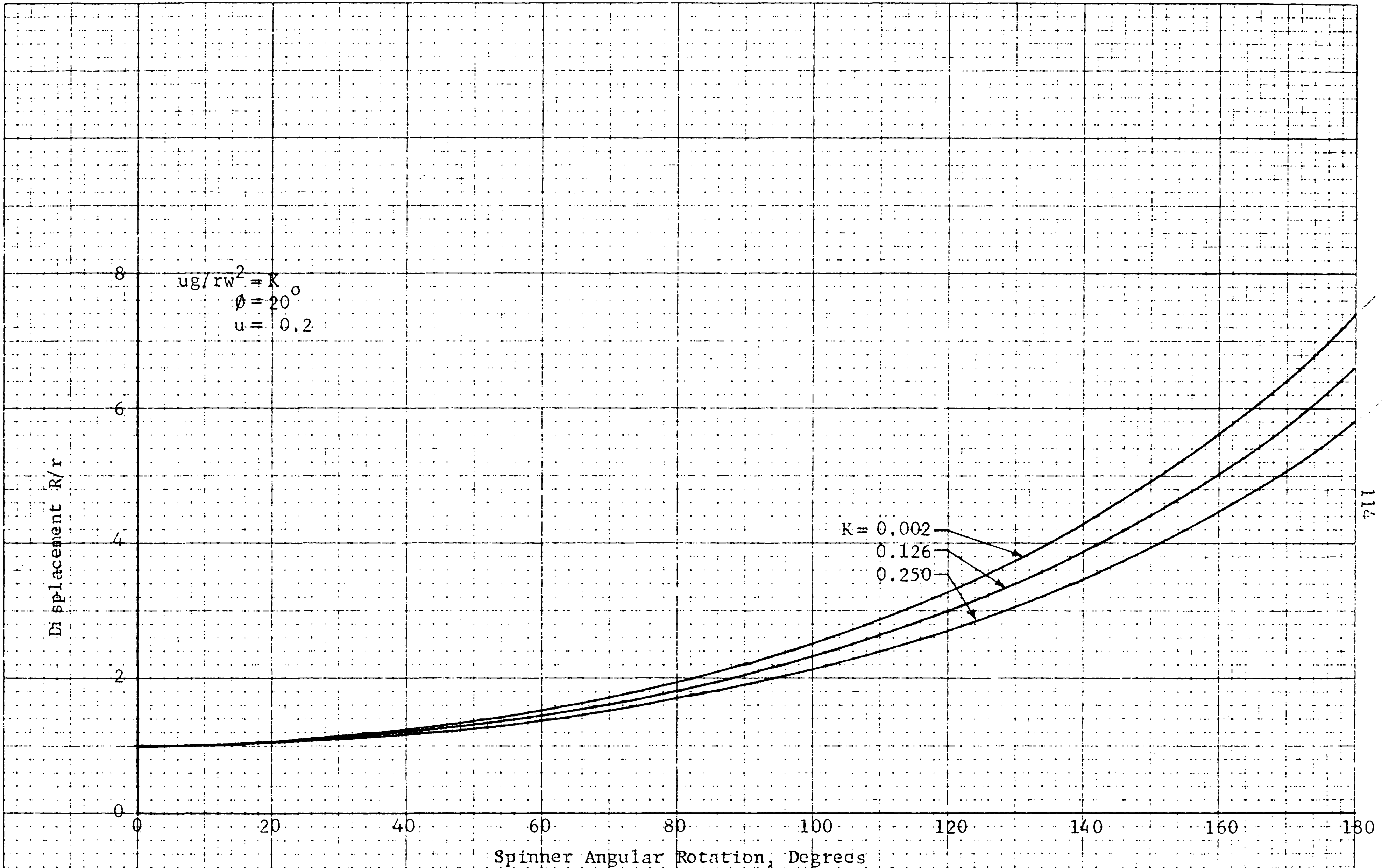

Figure 71 Dynamic Characteristics for Spinner With Backward-Curved Blades

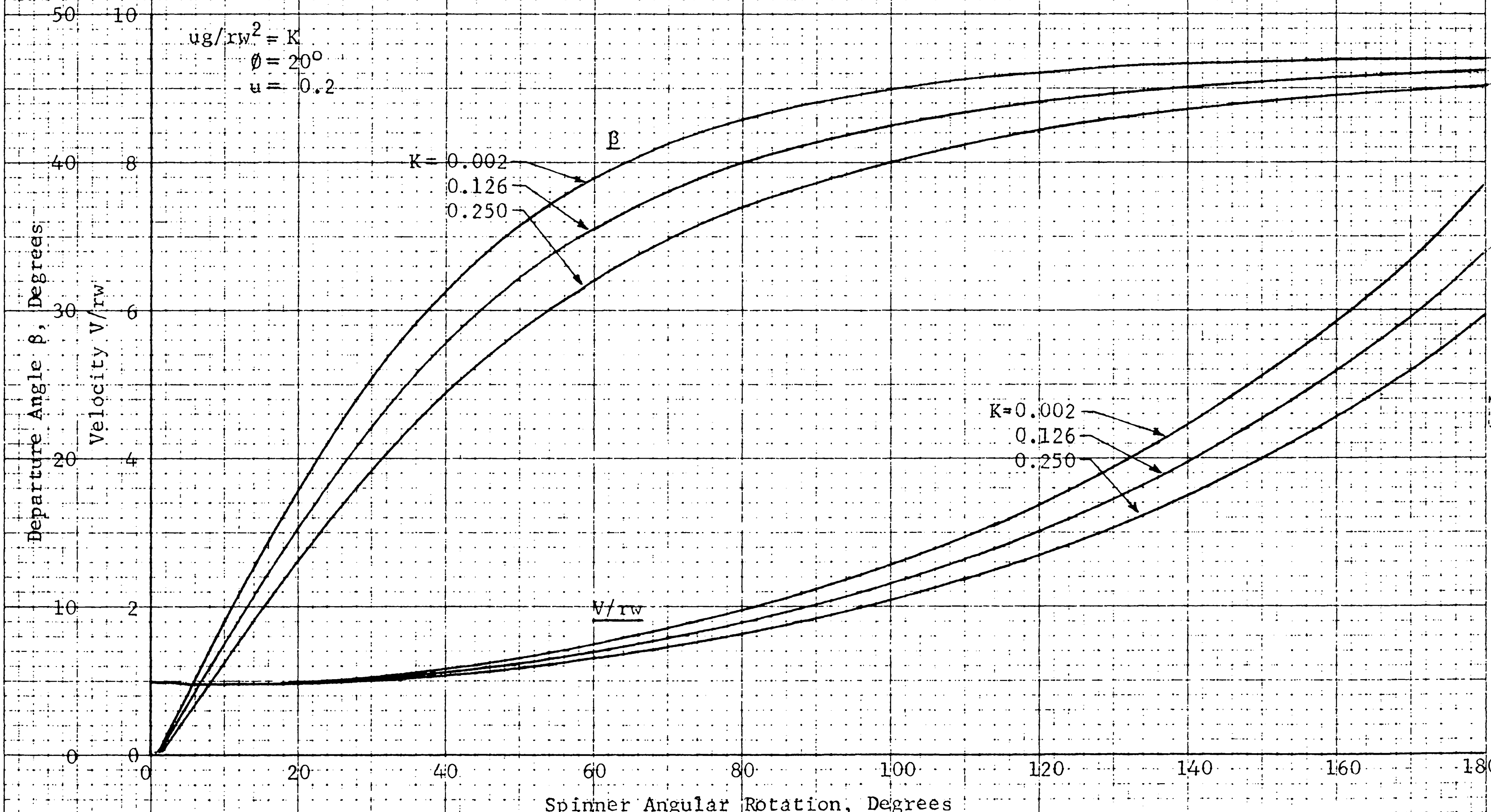

Figure 7.2 Dynamic Characteristics for Spinner With Backward-Curved Blades

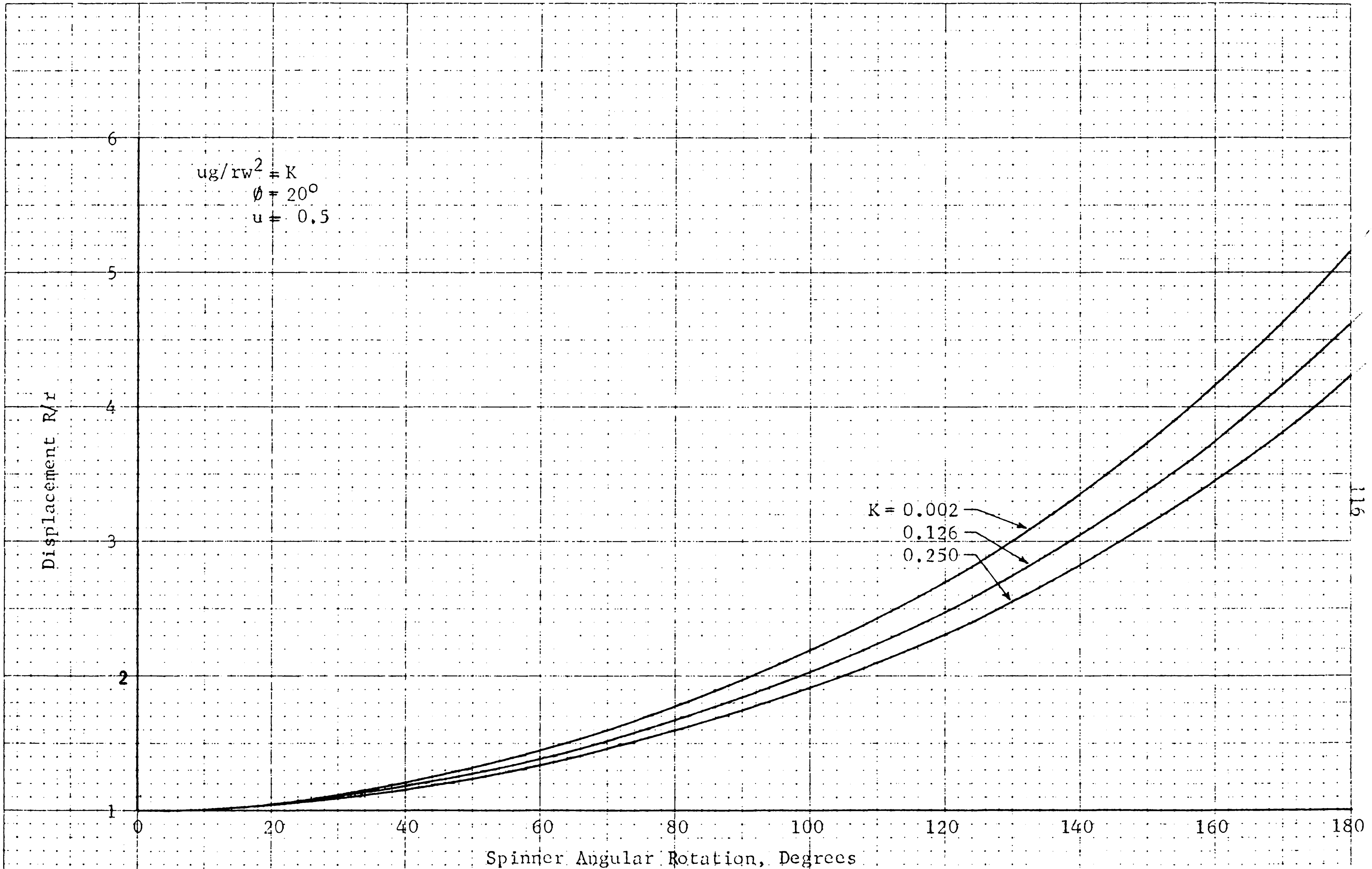

Figure 73   Dynamic Characteristics for Spinner With Backward-Curved Blades

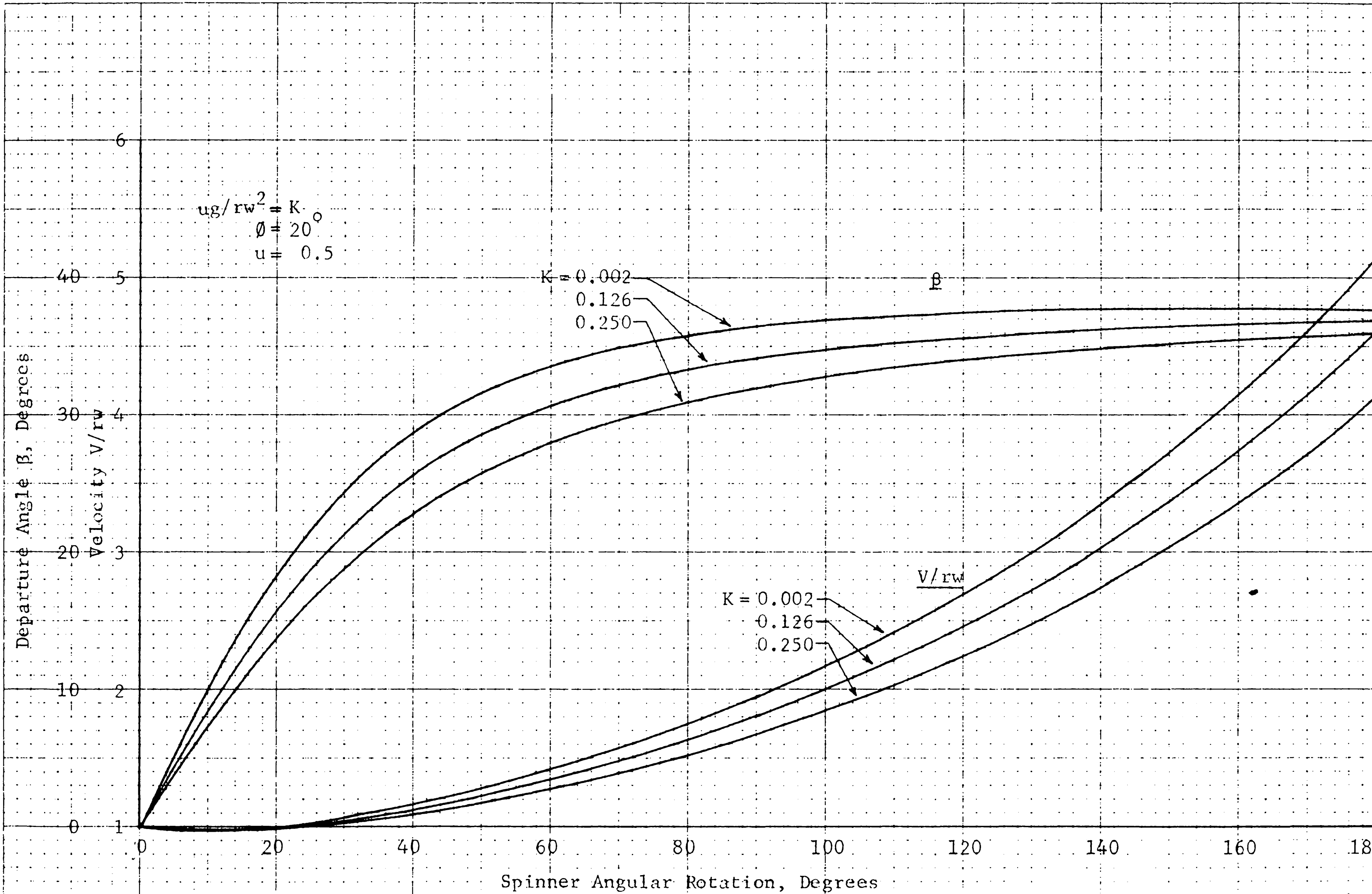

Figure 74 Dynamic Characteristics for Spinner With Backward-Curved Blades

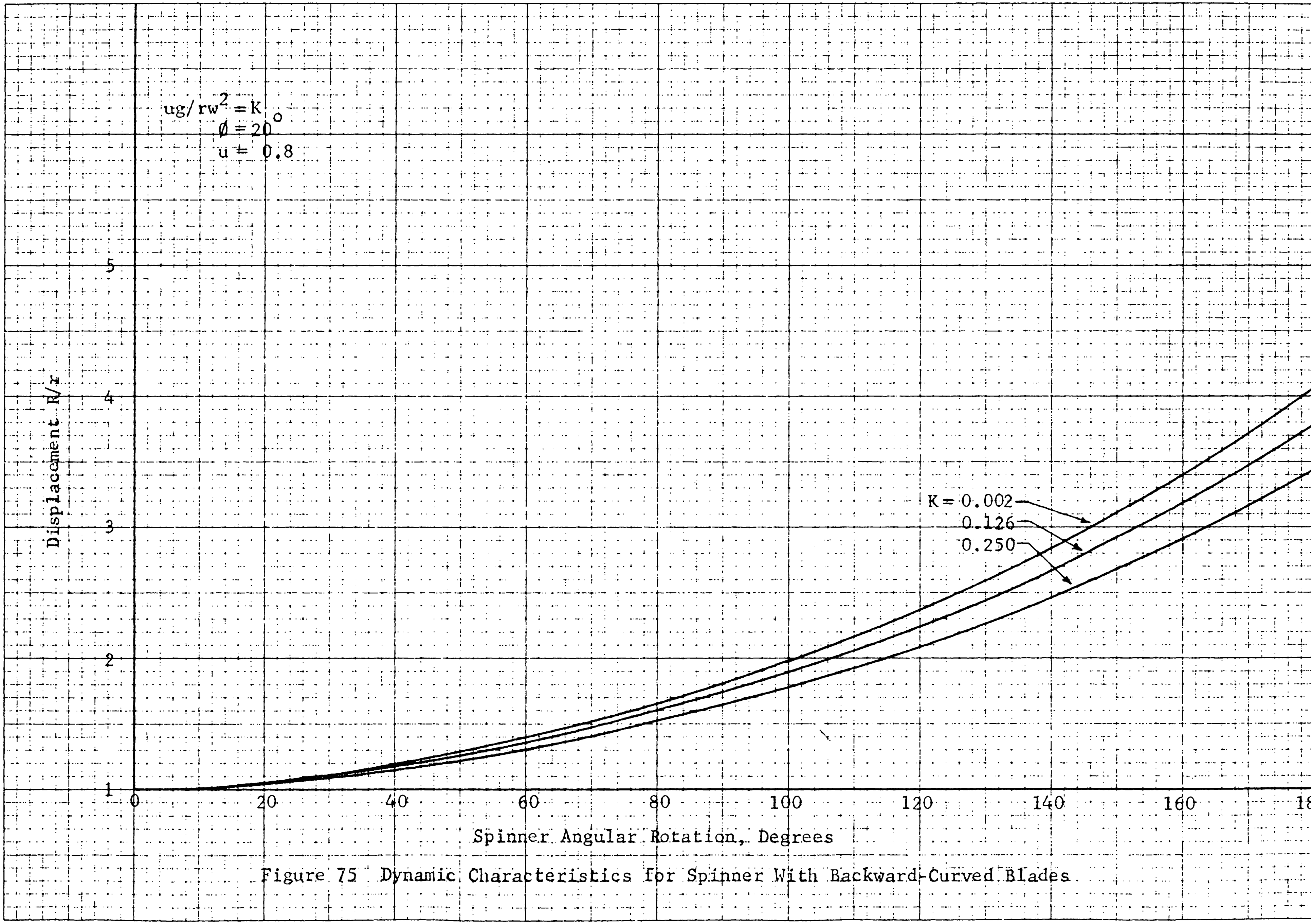

Figure 75 Dynamic Characteristics for Spinner With Backward-Curved Blades

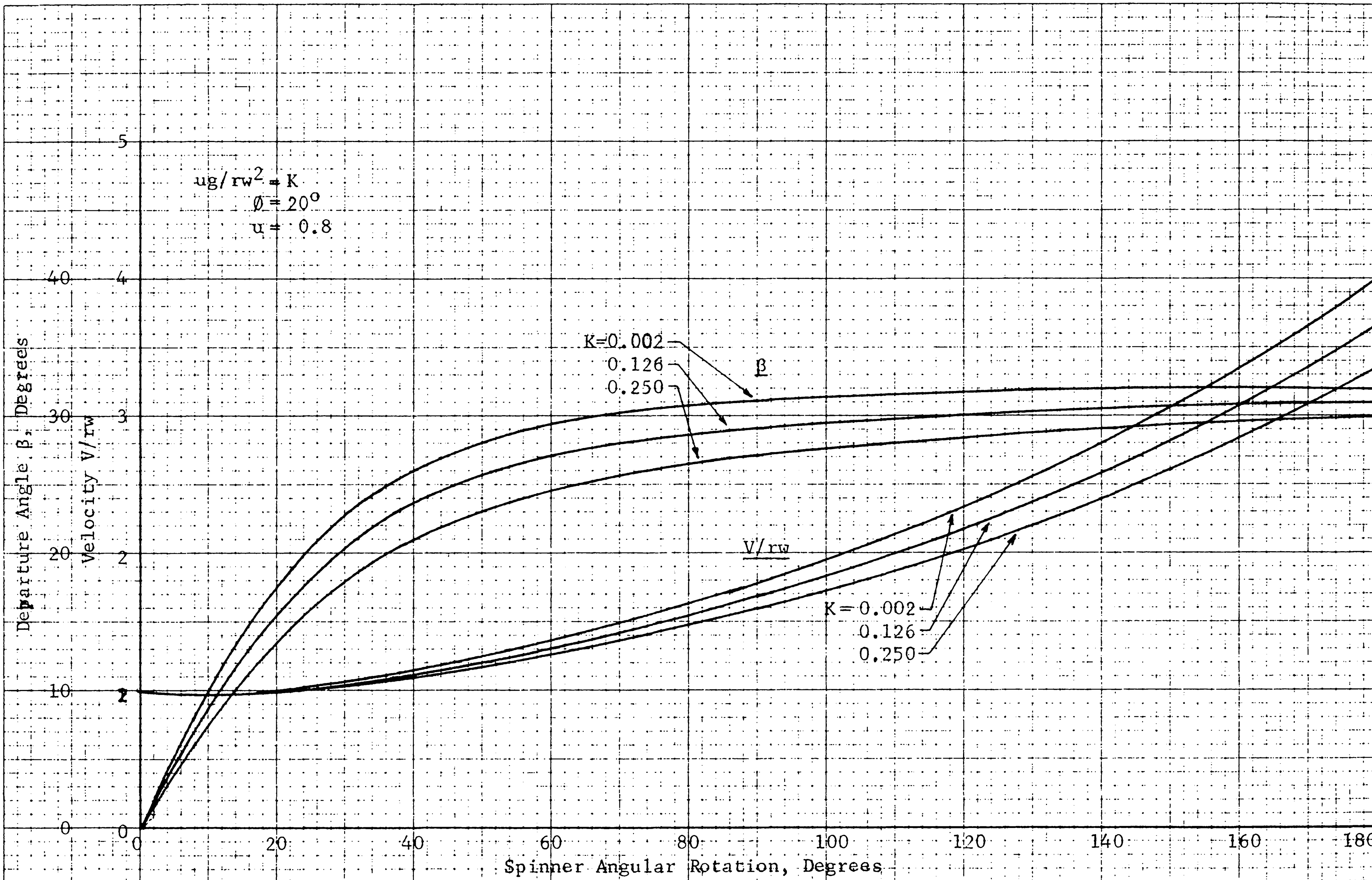

Figure 76 – Dynamic Characteristics for Spinner With Backward-Curved Blades

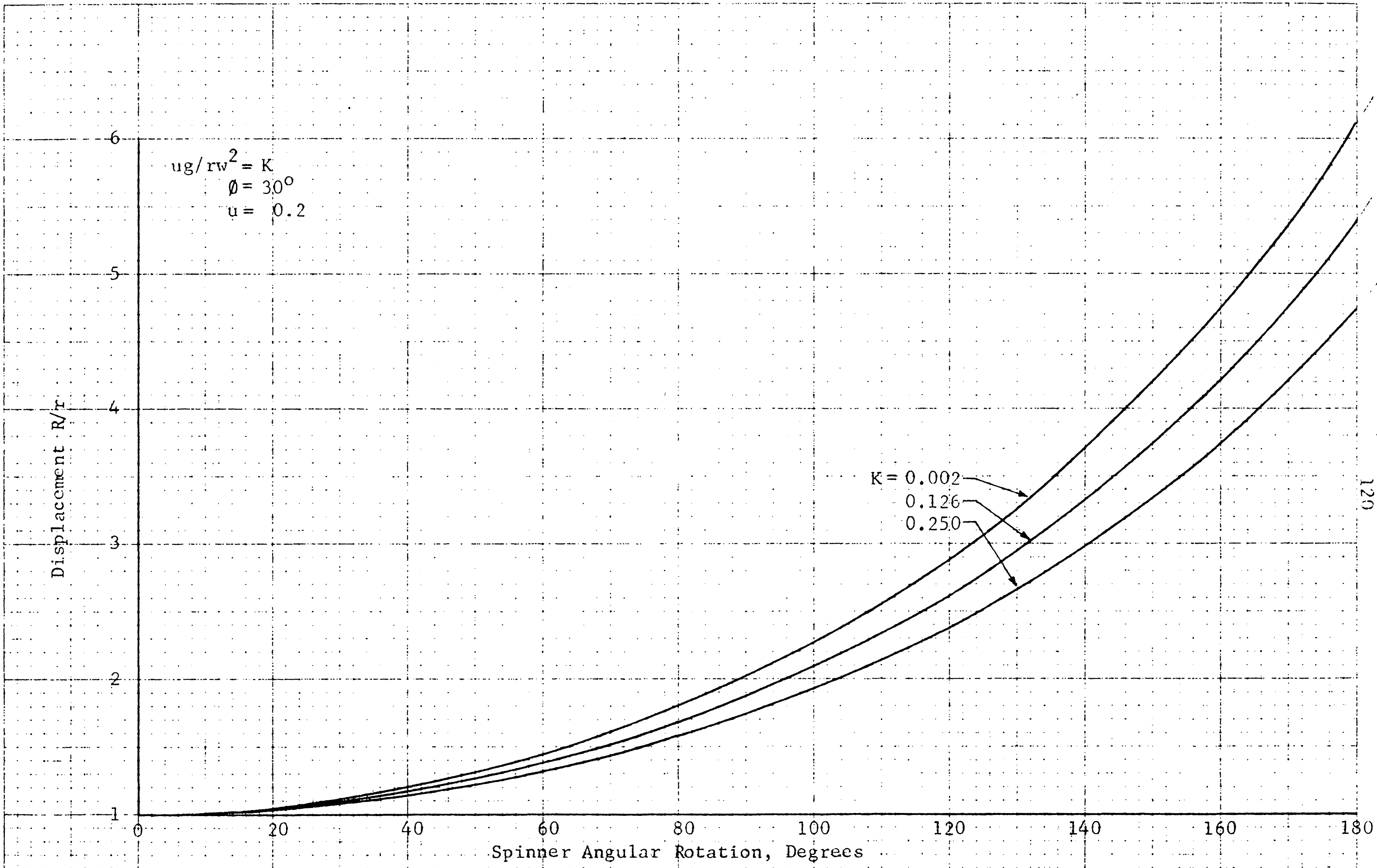

Figure 77 Dynamic Characteristics for Spinner With Backward-Curved Blades

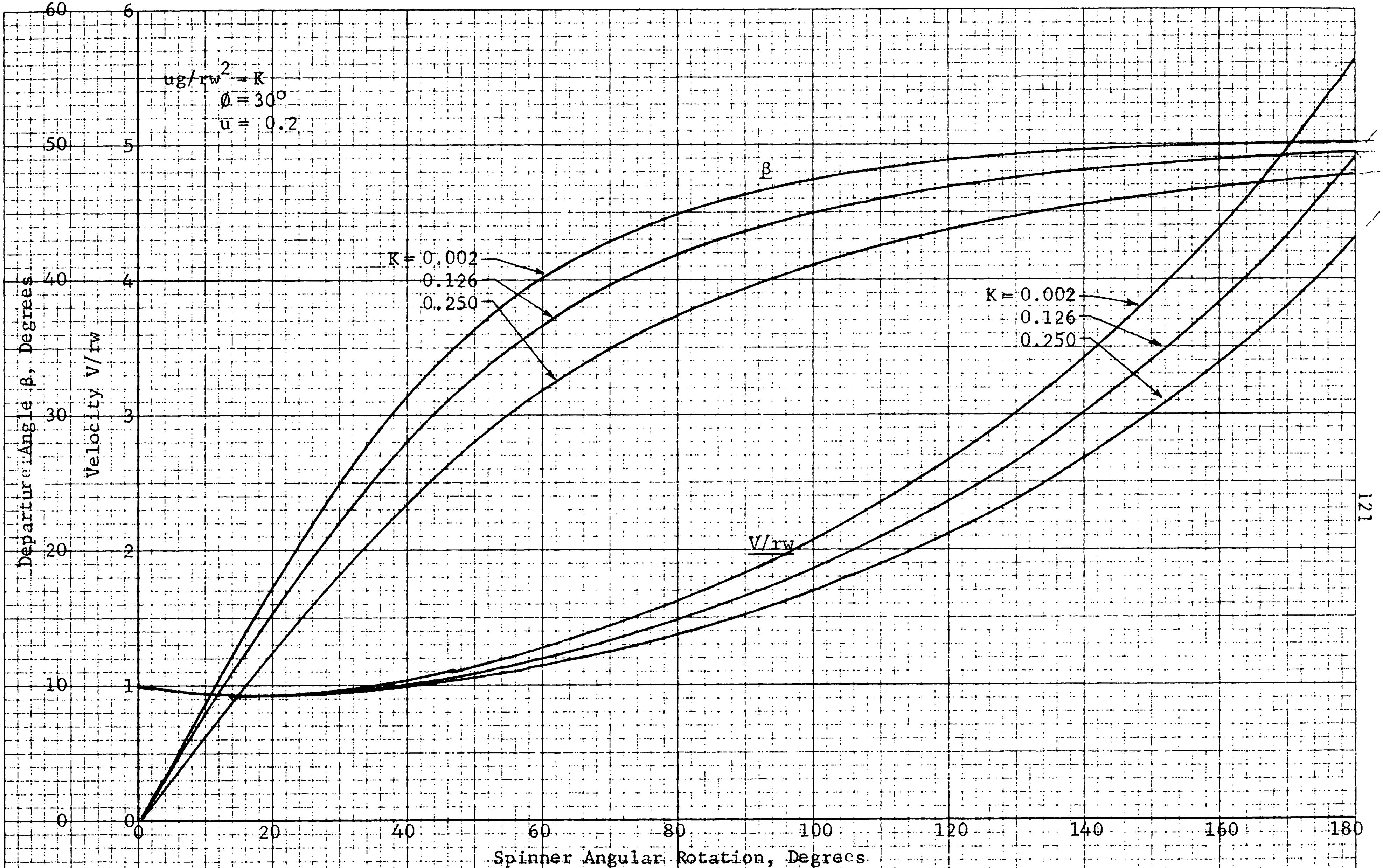

Figure 78 Dynamic Characteristics for Spinner With Backward-Curved Blades

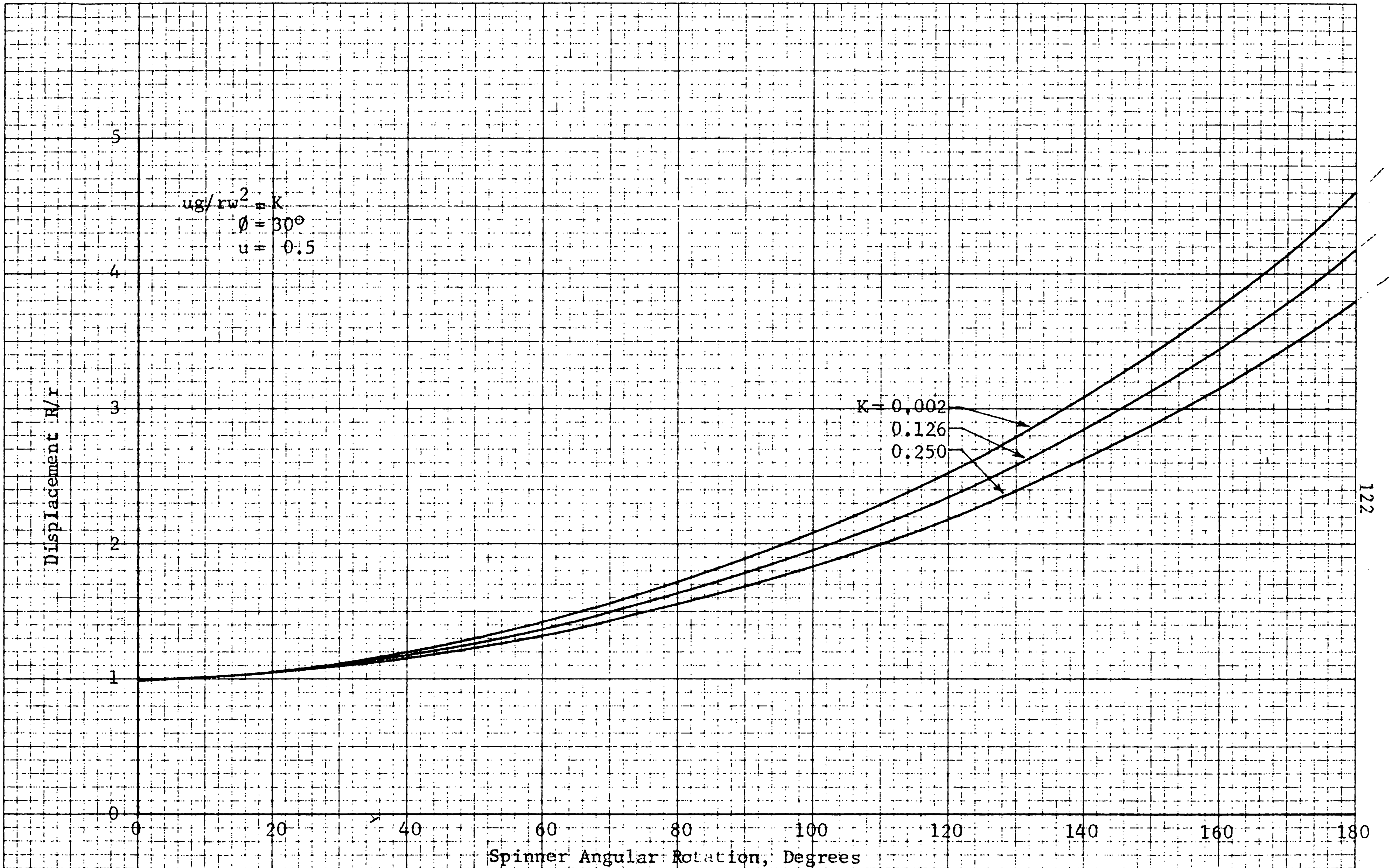

Figure 79 Dynamic Characteristics for Spinner With Backward-Curved Blades

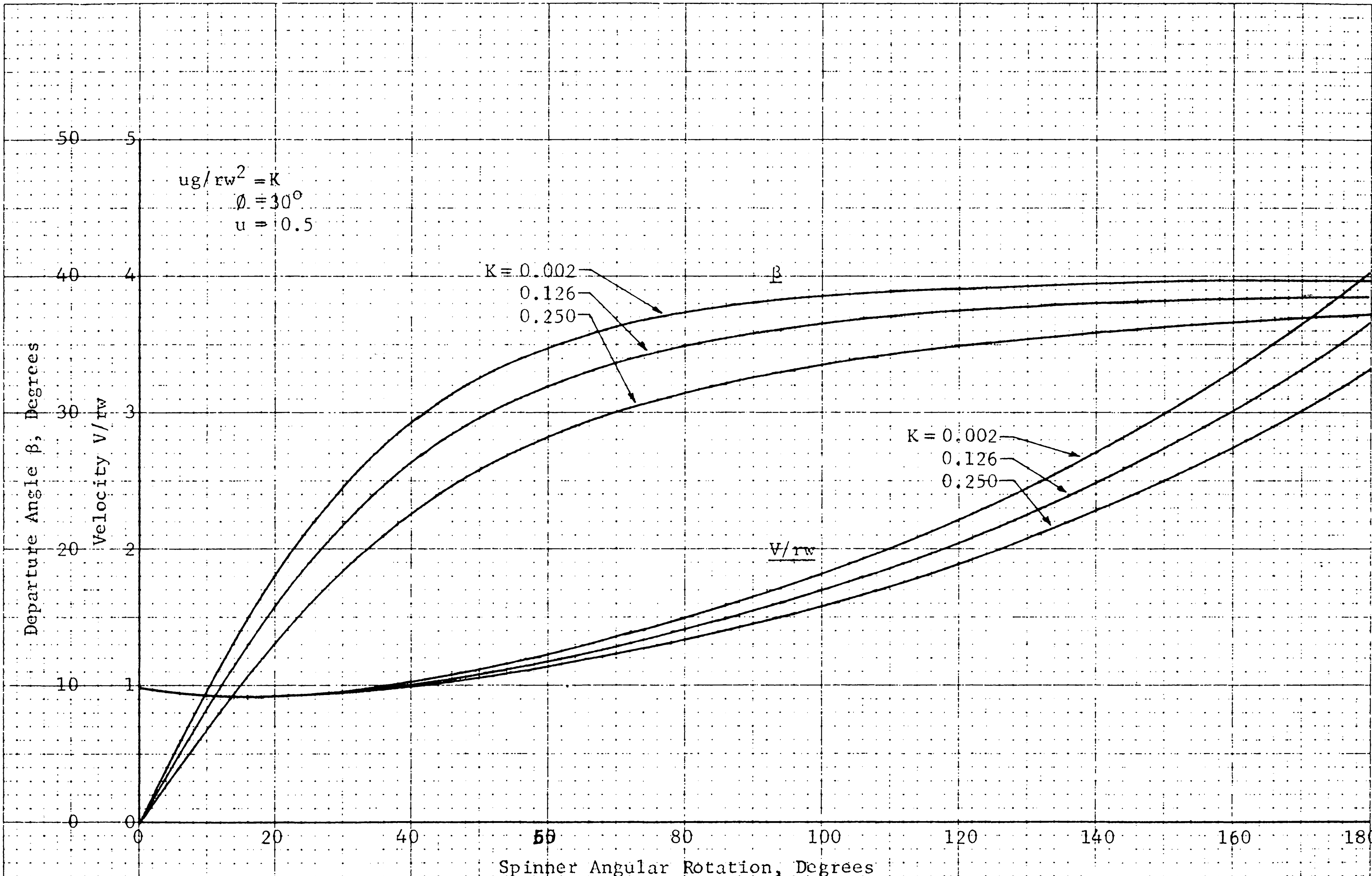

Figure 80 Dynamic Characteristics for Spinner With Backward-Curved Blades

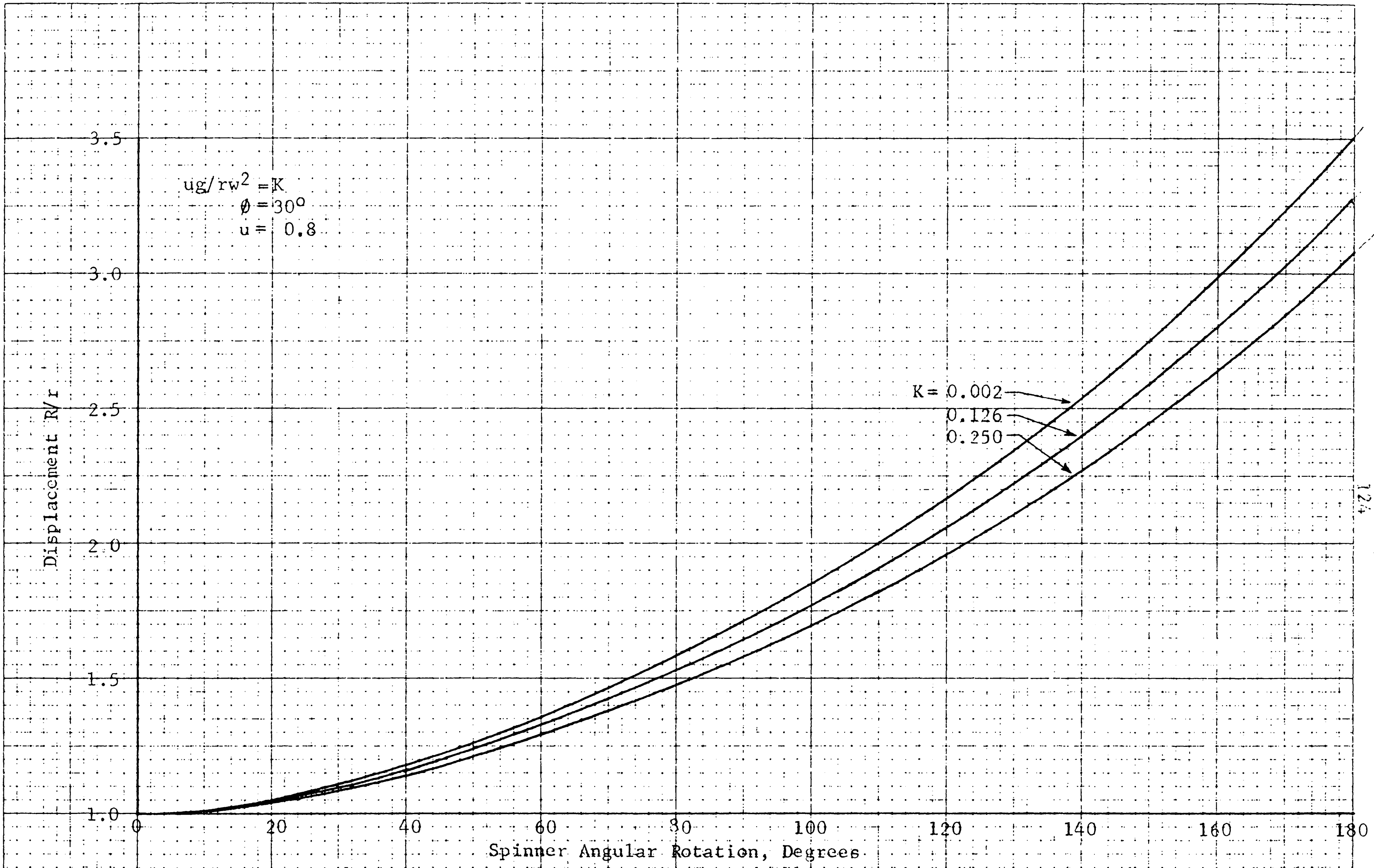

Figure 81 Dynamic Characteristics for Spinner With Backward-Curved Blades

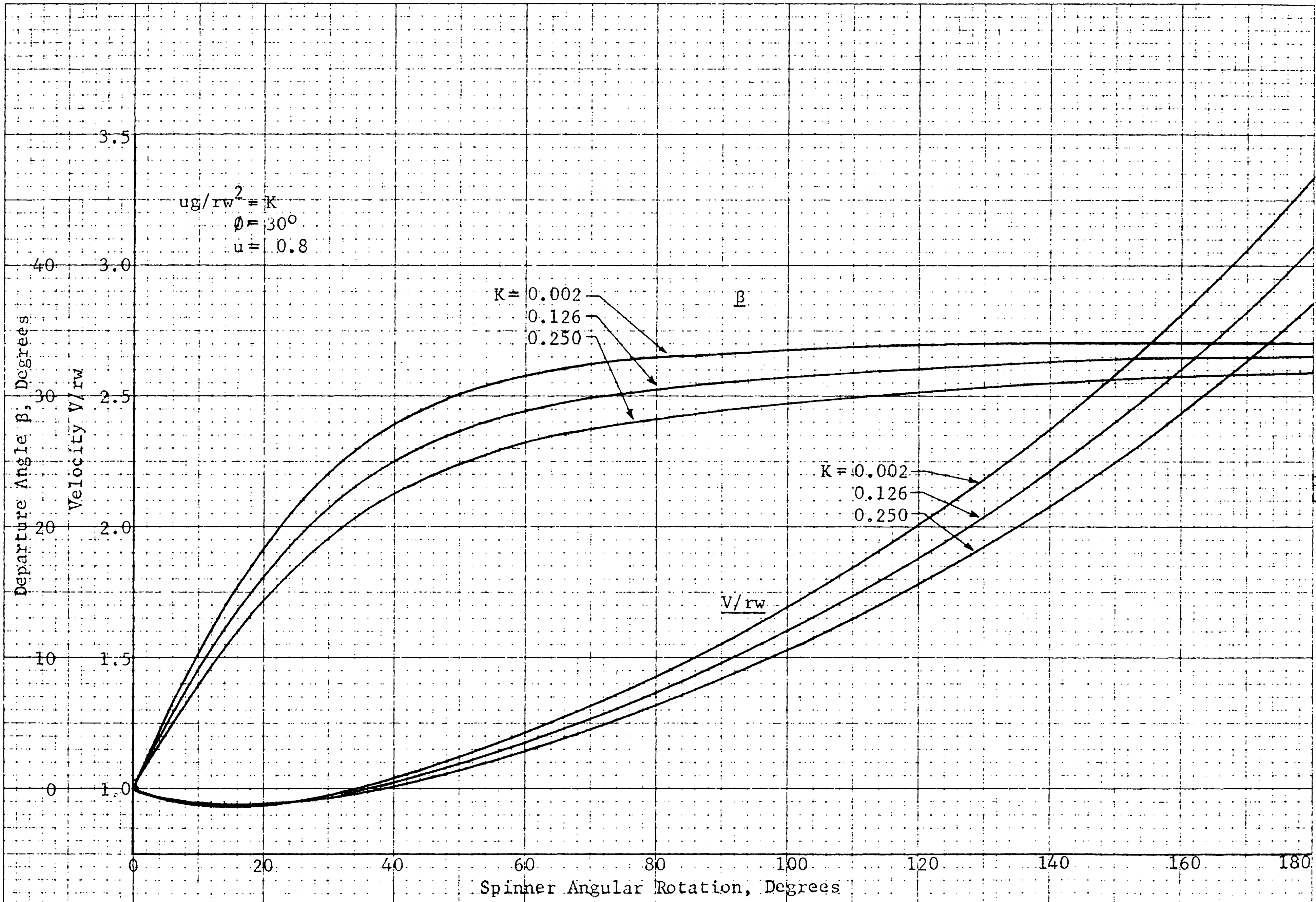

Figure 82 Dynamic Characteristics for Spinner with Backward-Curved Blades

Appendix IV

Dynamic Characteristics for Cone-Shaped Spinner

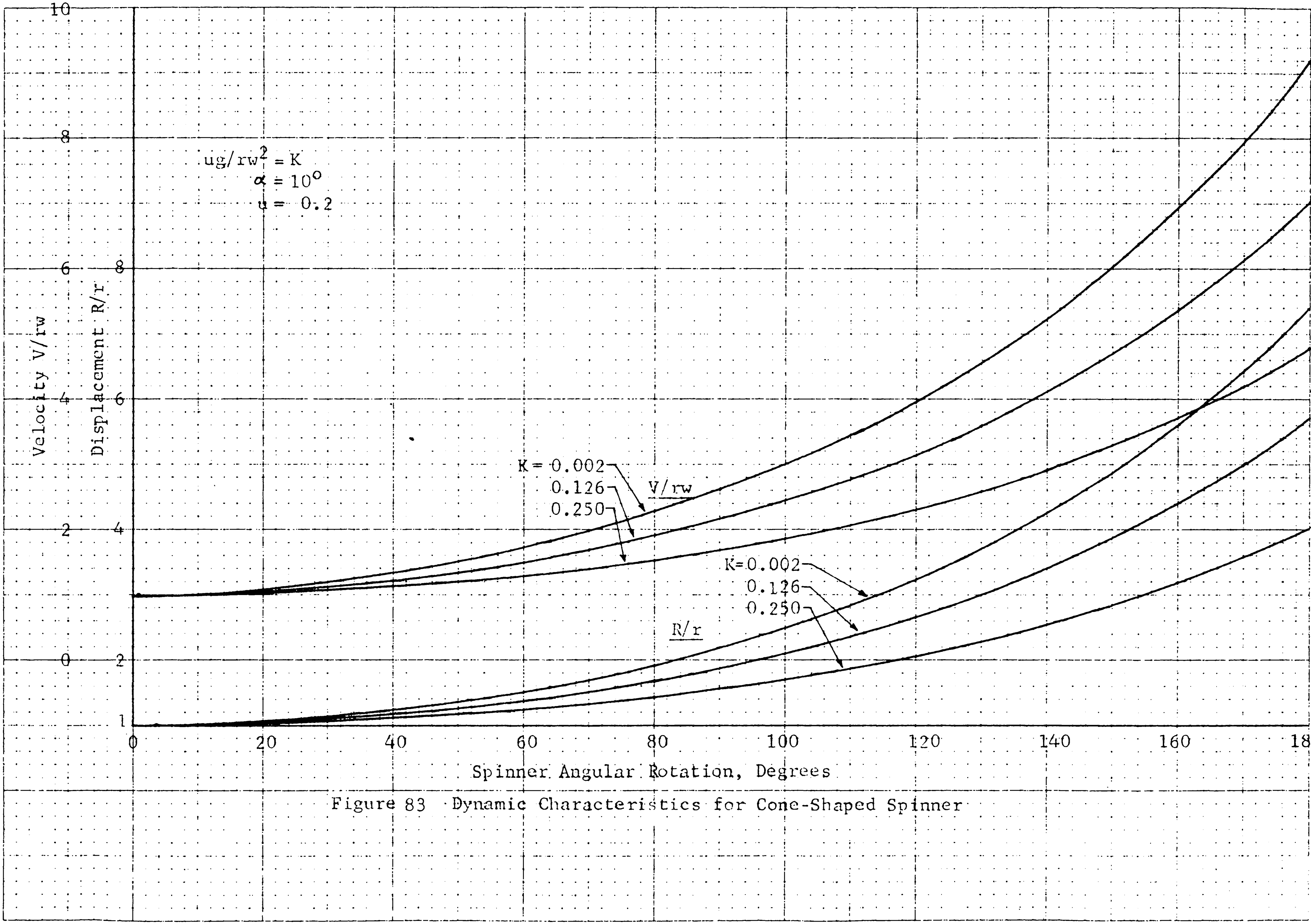

Figure 83 Dynamic Characteristics for Cone-Shaped Spinner

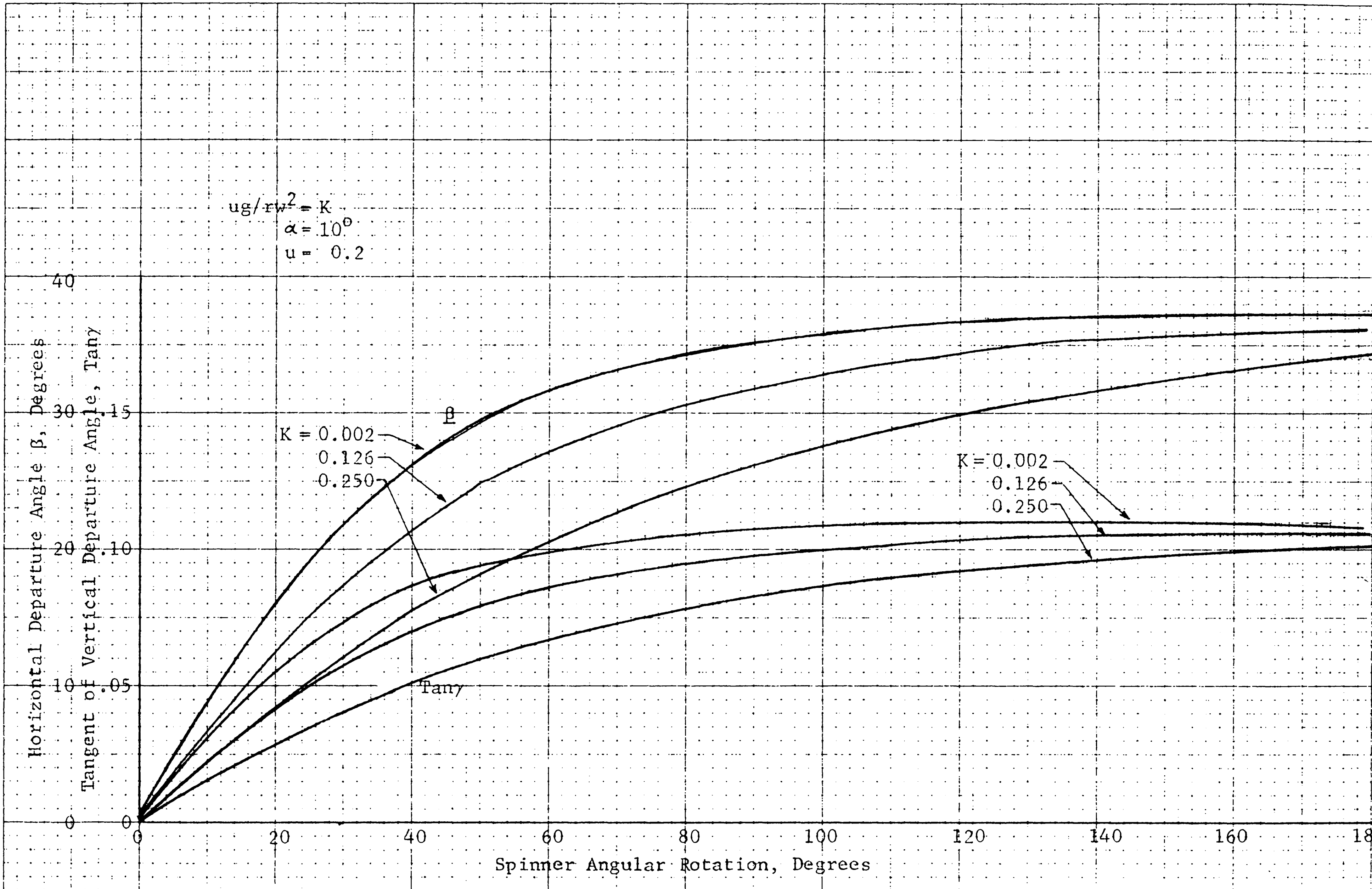

Figure 84 Dynamic Characteristics for Cone-Shaped Spinner

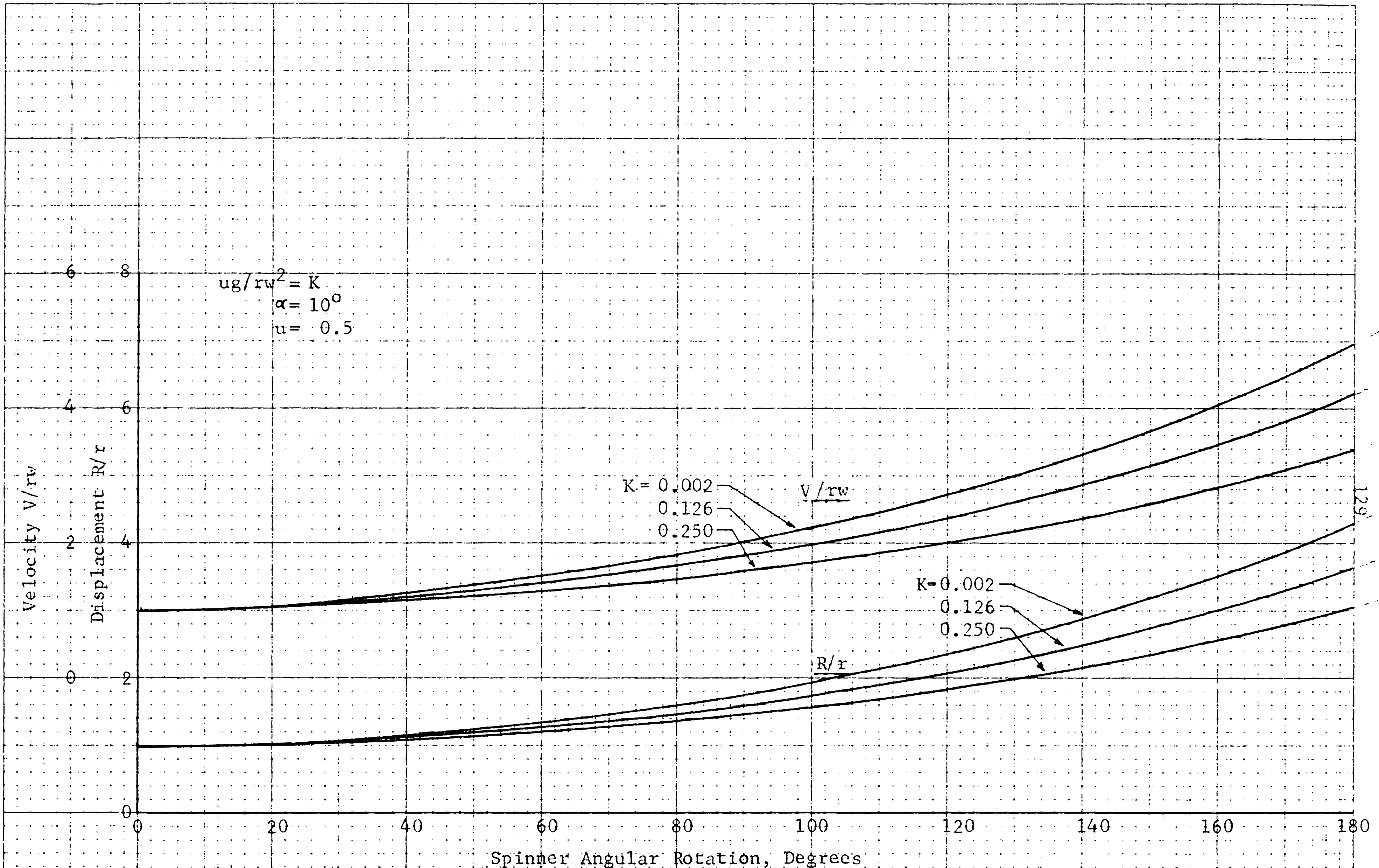

Figure 85 Dynamic Characteristics for Cone-Shaped Spinner

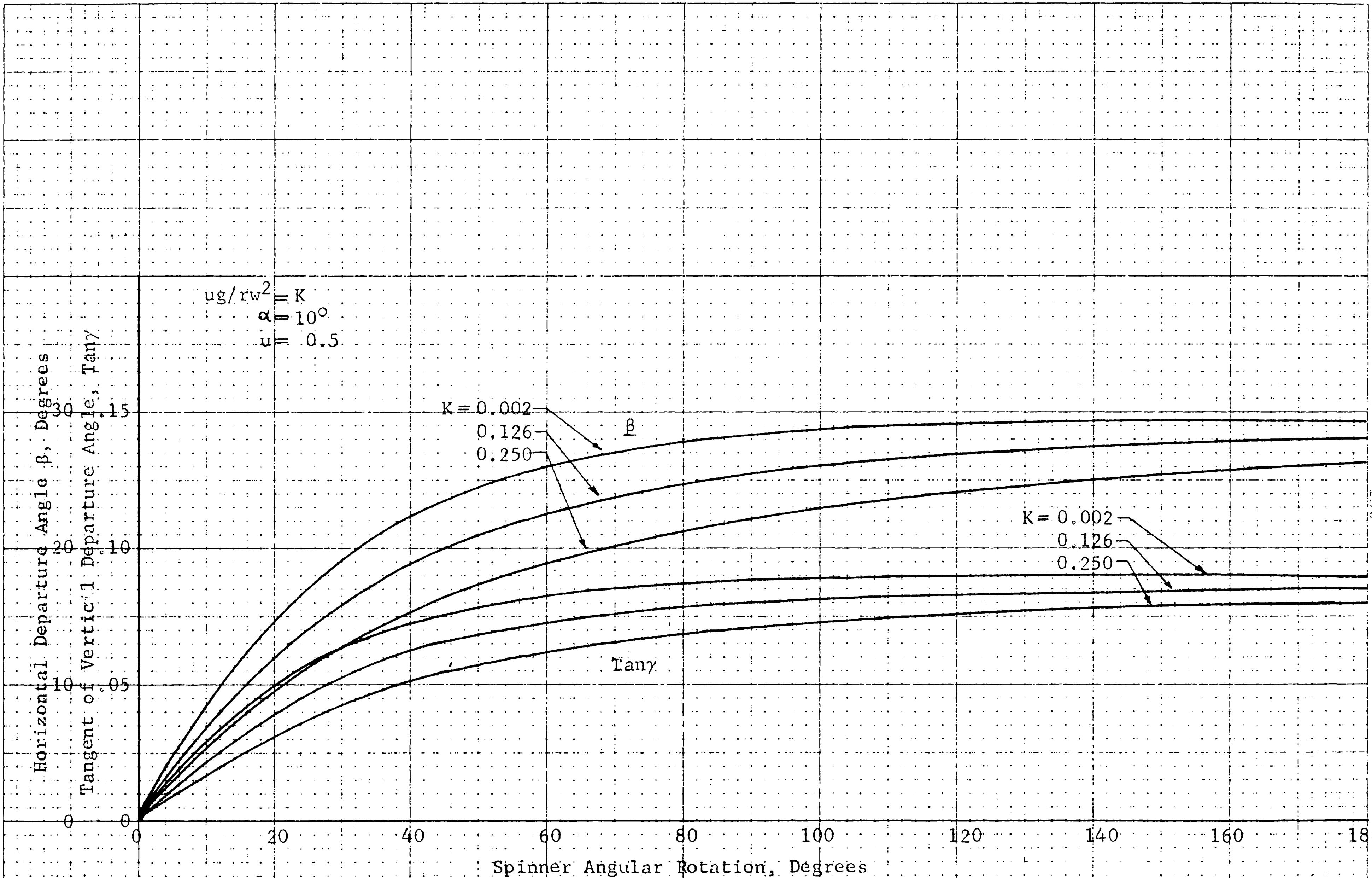

Figure 86 Dynamic Characteristics for Cone-Shaped Spinner

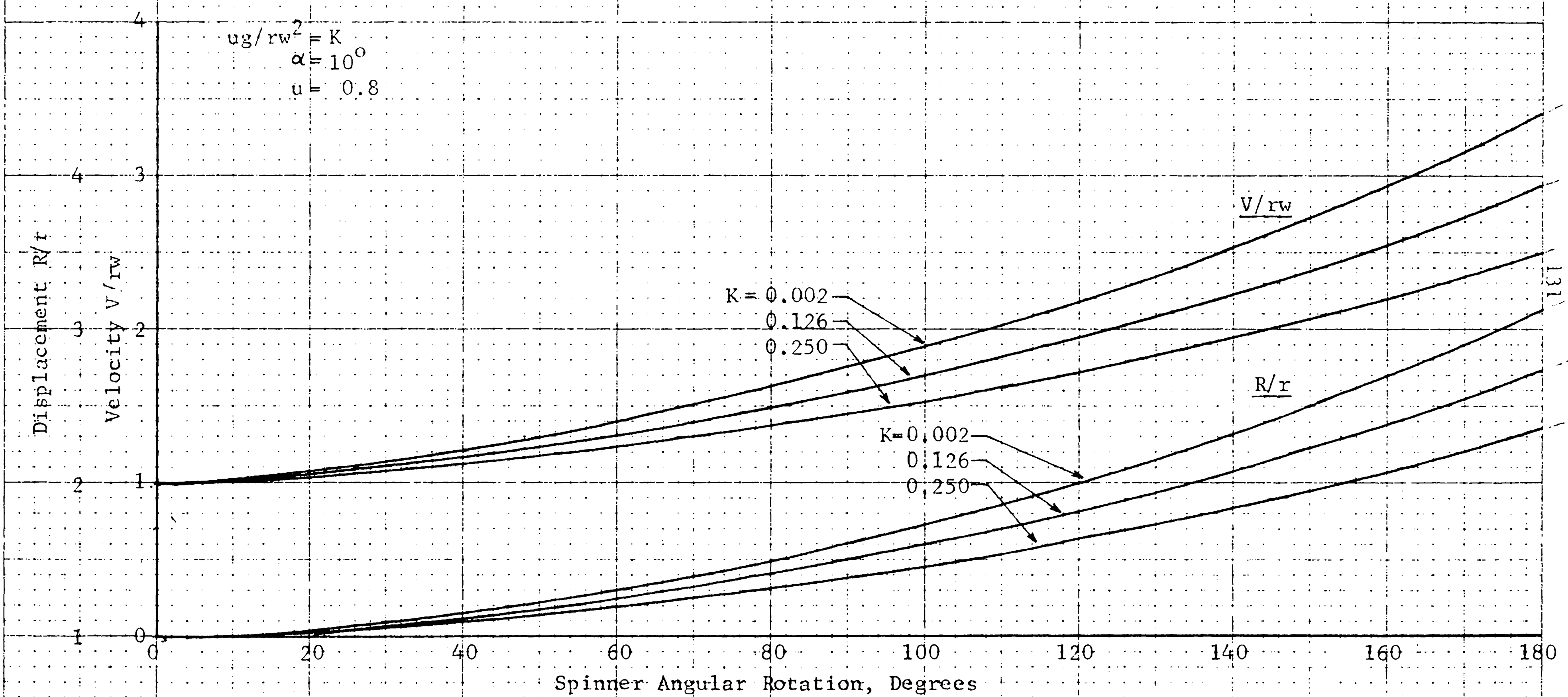

Figure 87 Dynamic Characteristics for Cone-Shaped Spinner

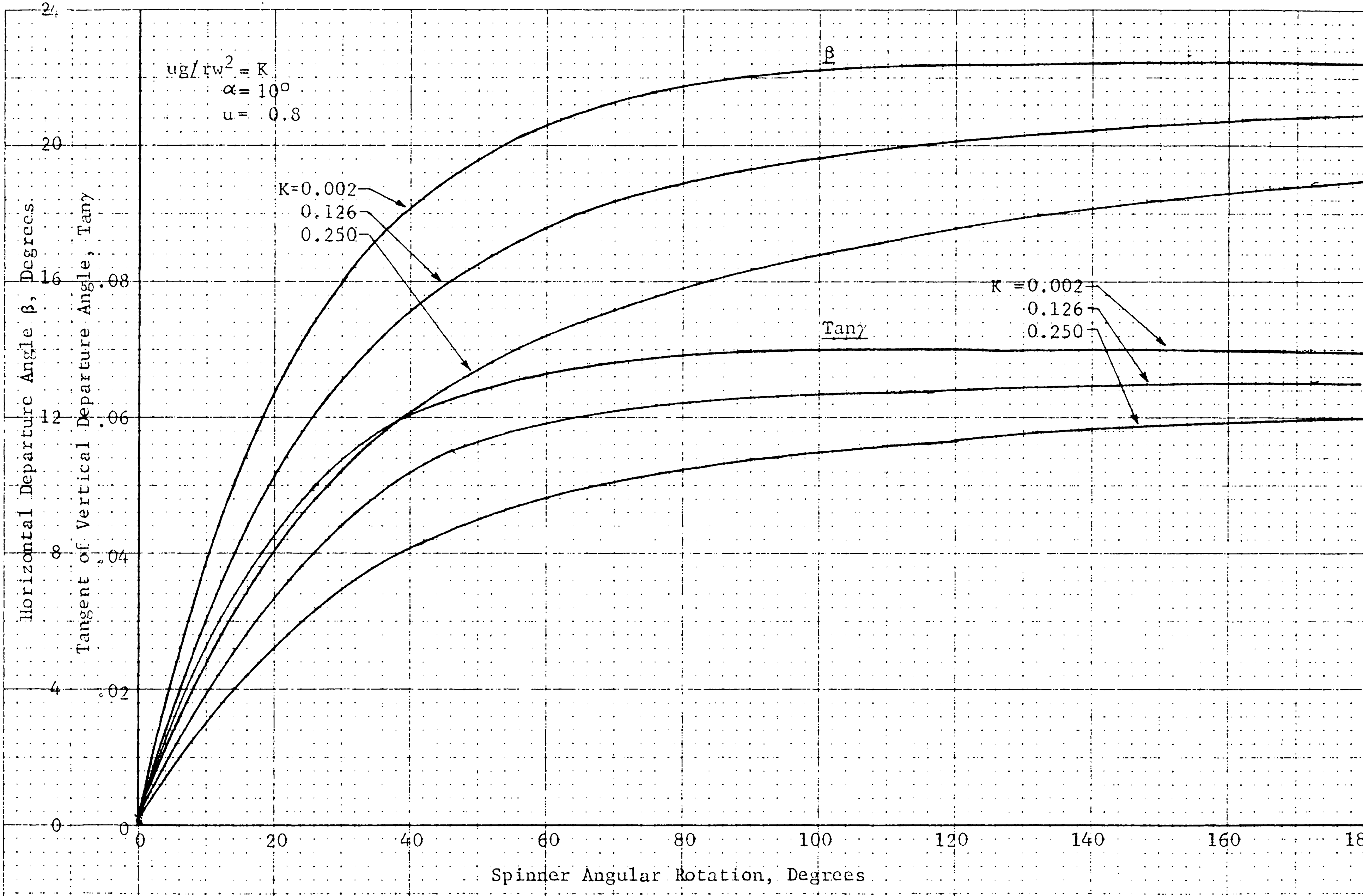

Figure 88 Dynamic Characteristics for Cone-Shaped Spinner

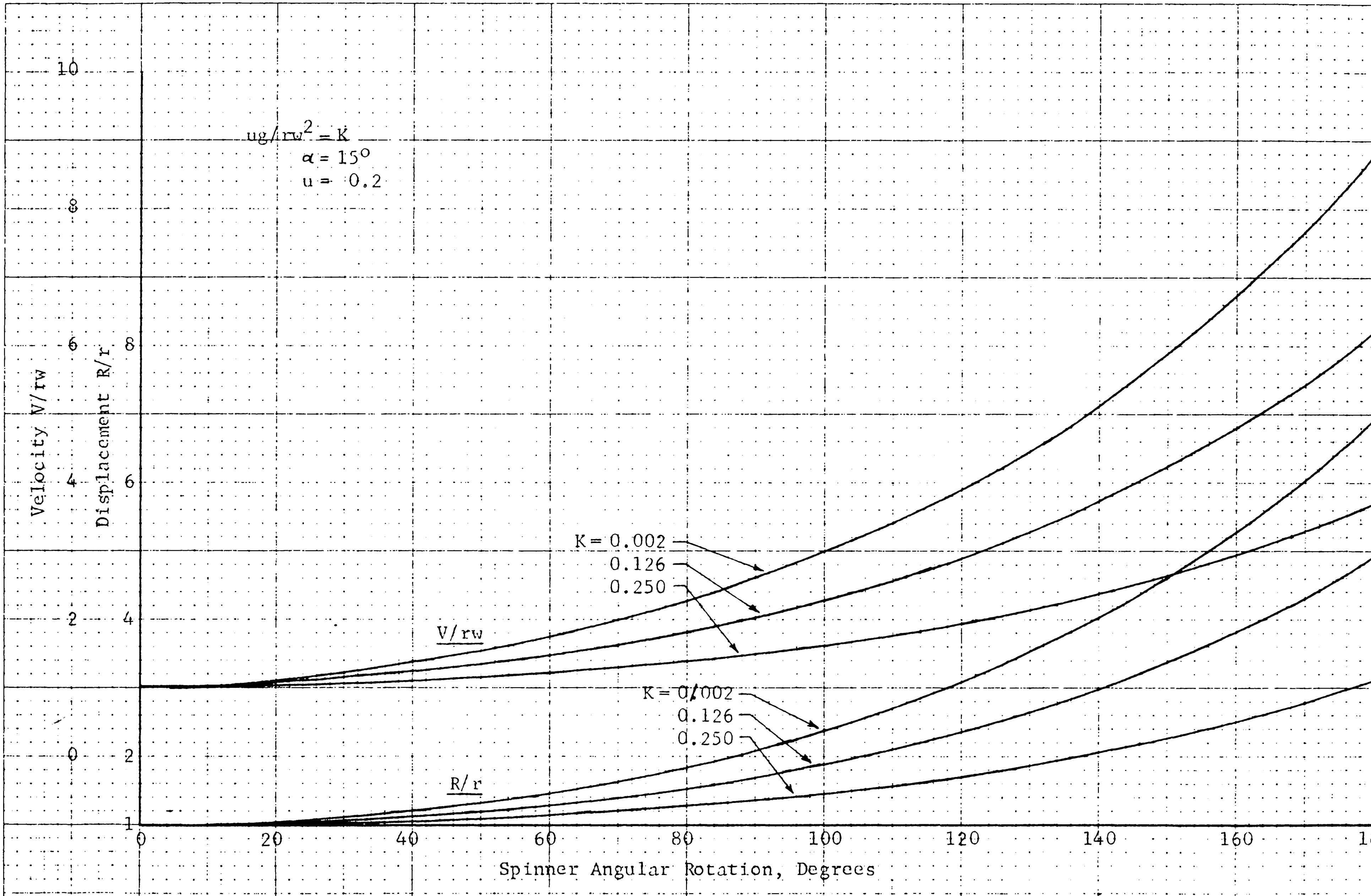

Figure 89 Dynamic Characteristics for Cone-Shaped Spinner

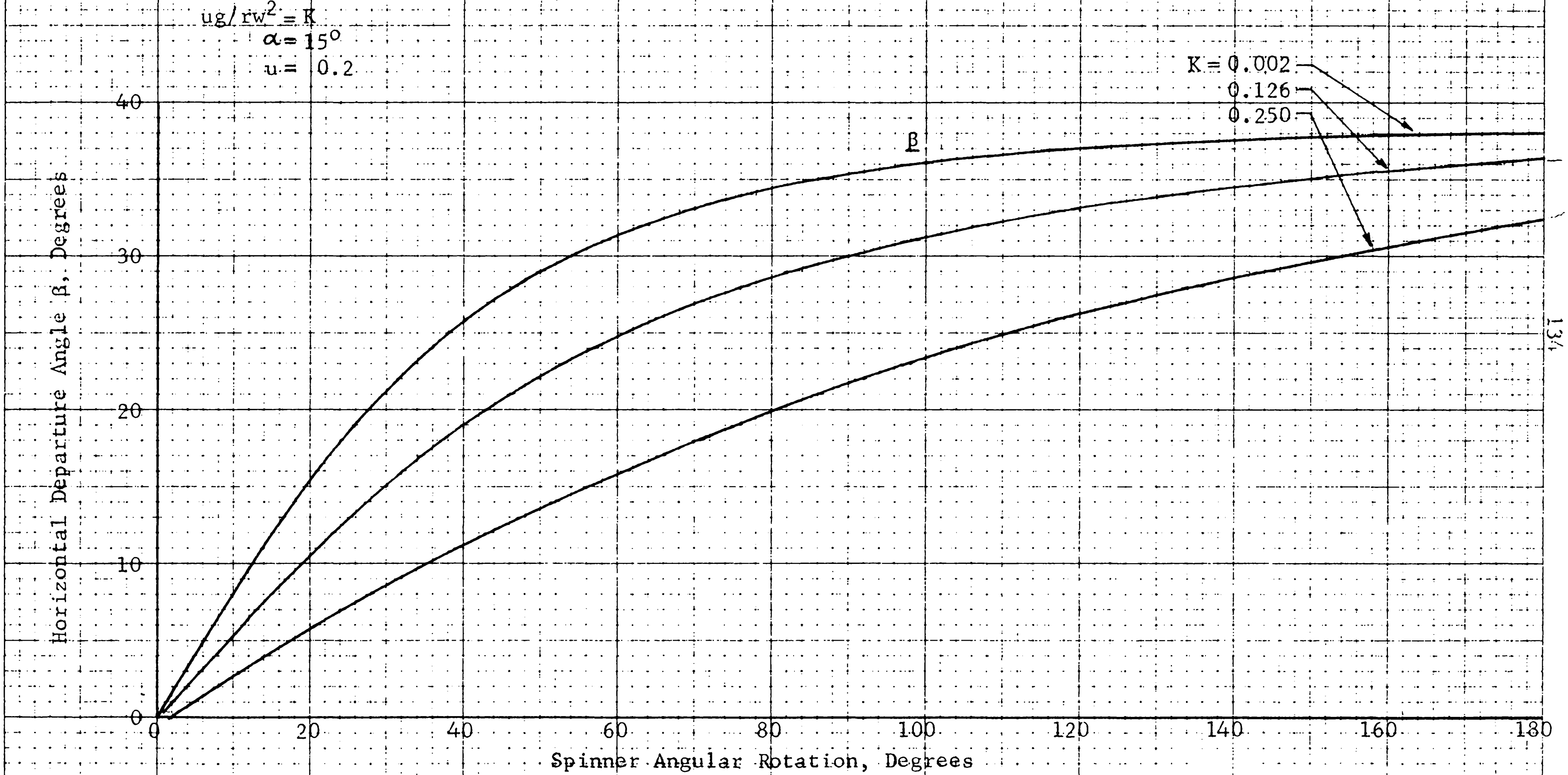

Figure 90 Dynamic Characteristics for Cone-Shaped Spinner

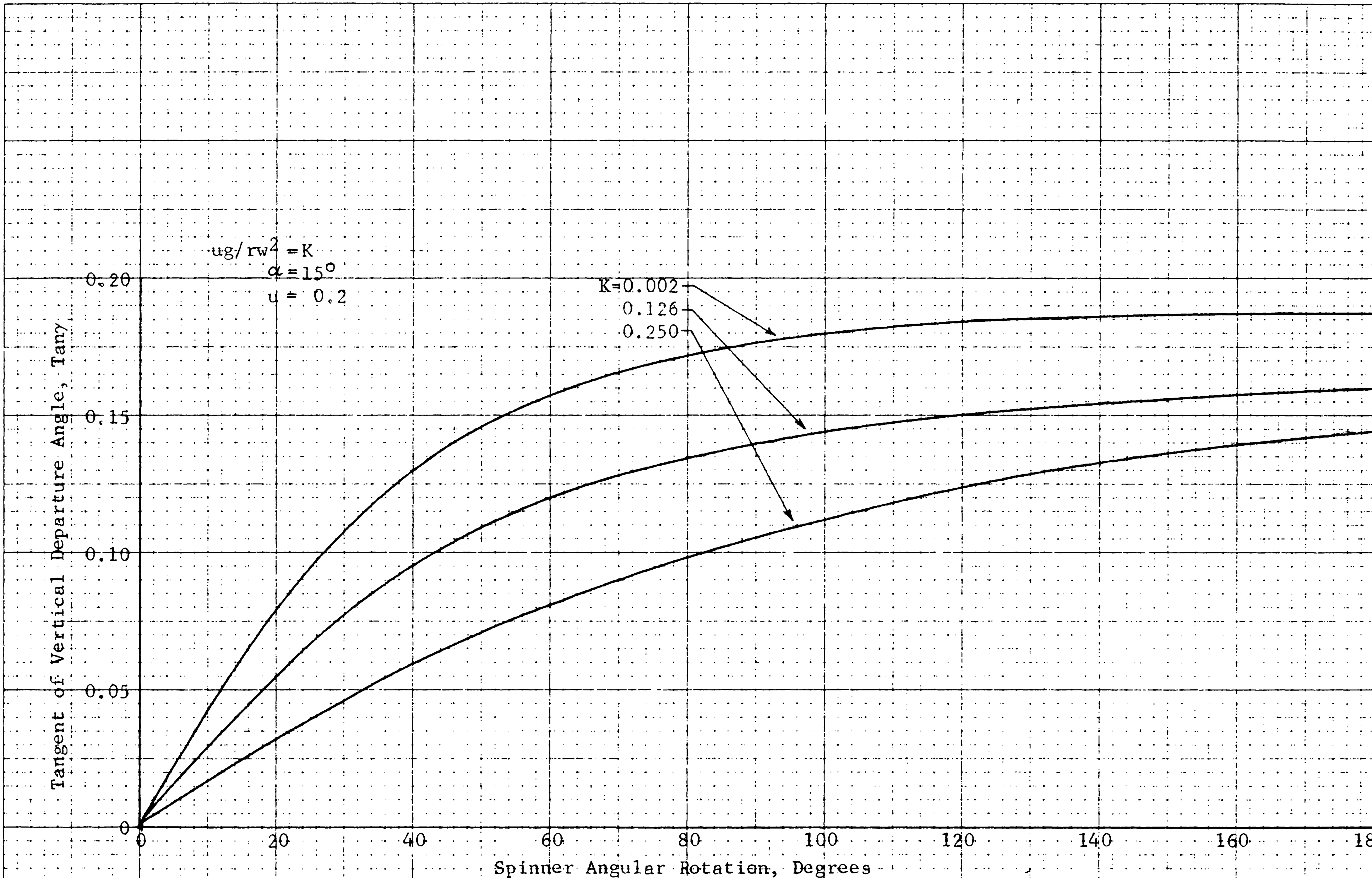

Figure 91 Dynamic Characteristics for Cone-Shaped Spinner

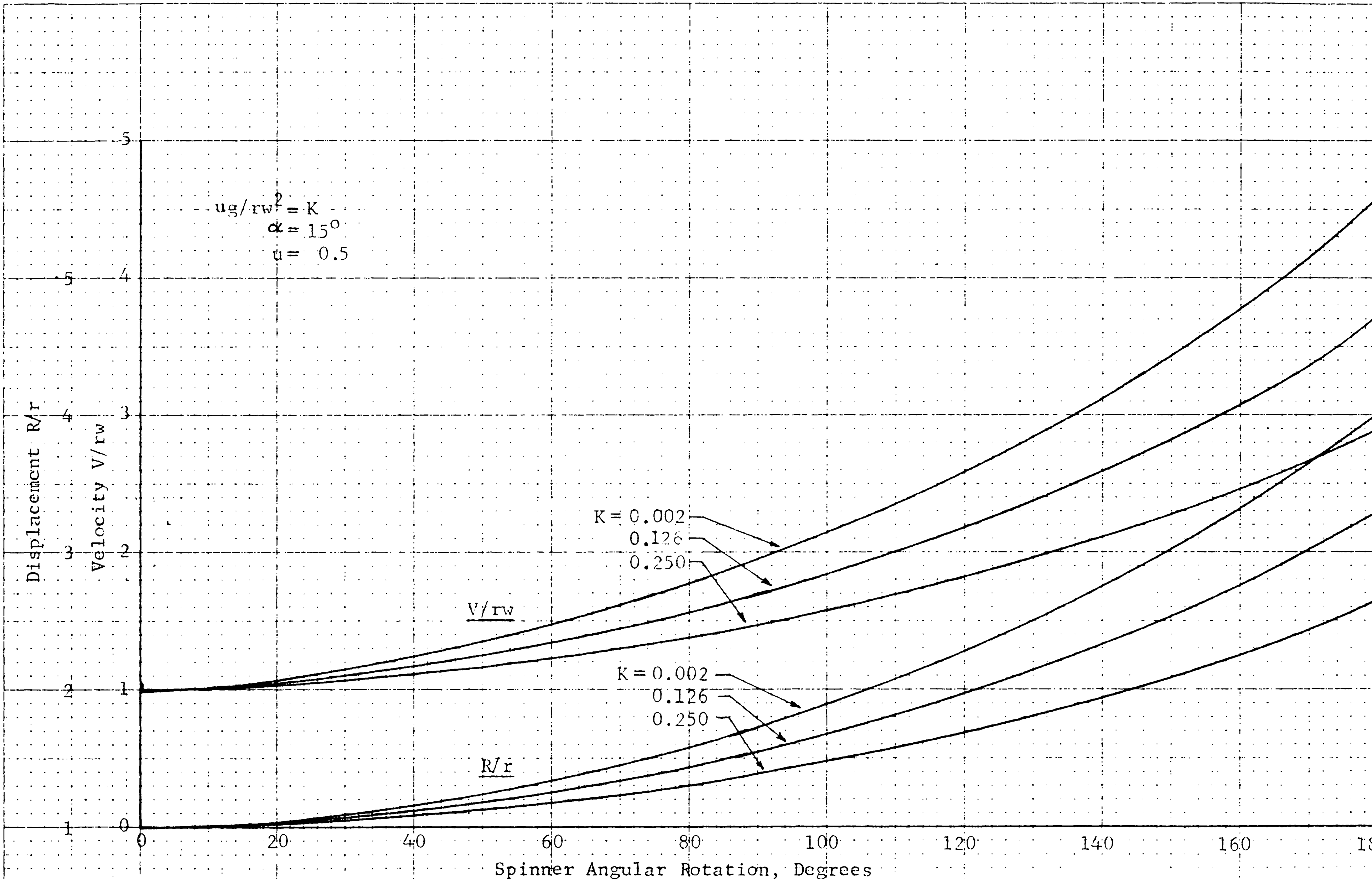

Figure 92 Dynamic Characteristics for Cone-Shaped Spinner

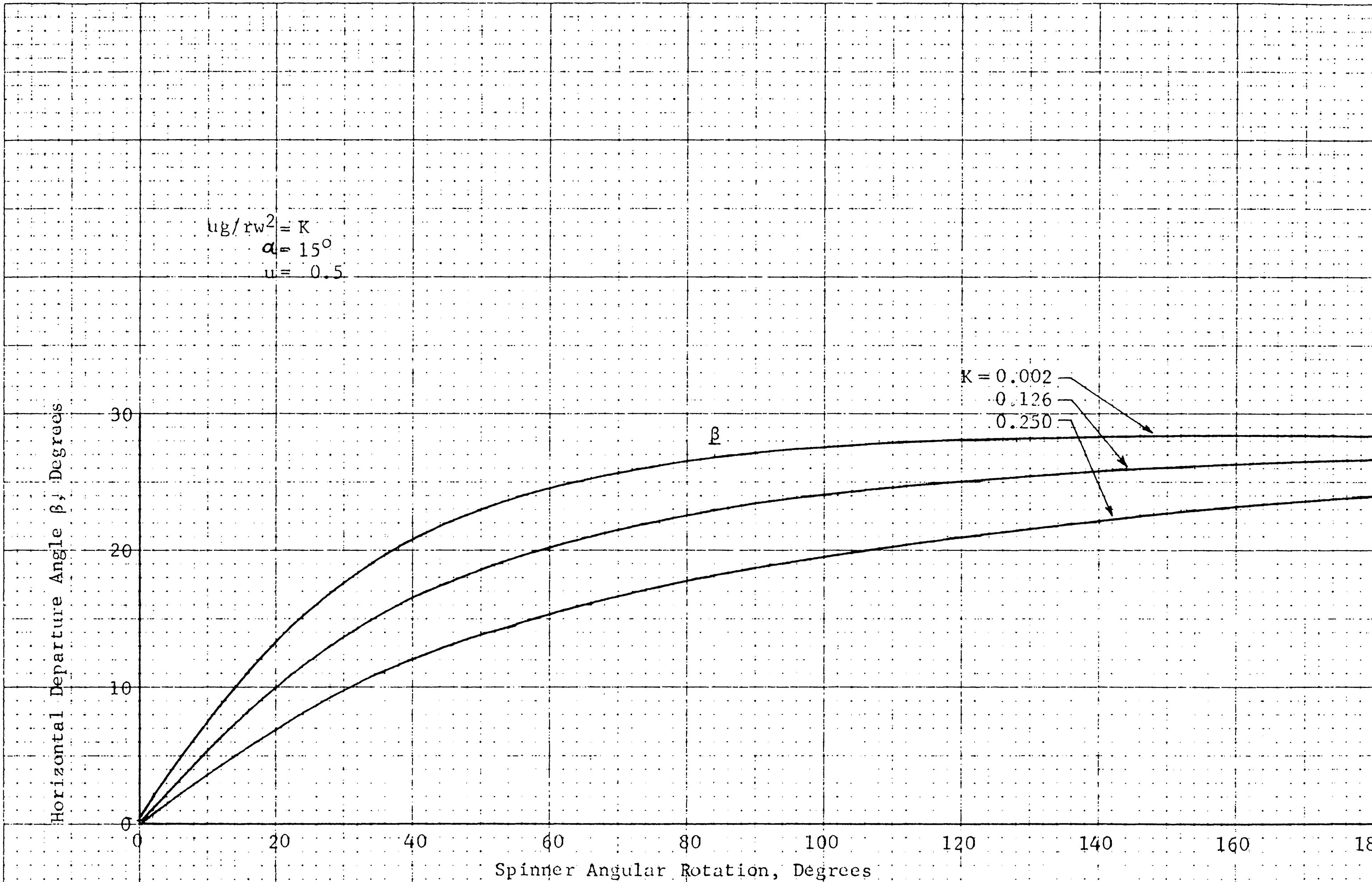

Figure 93 Dynamic Characteristics for Cone-Shaped Spinner

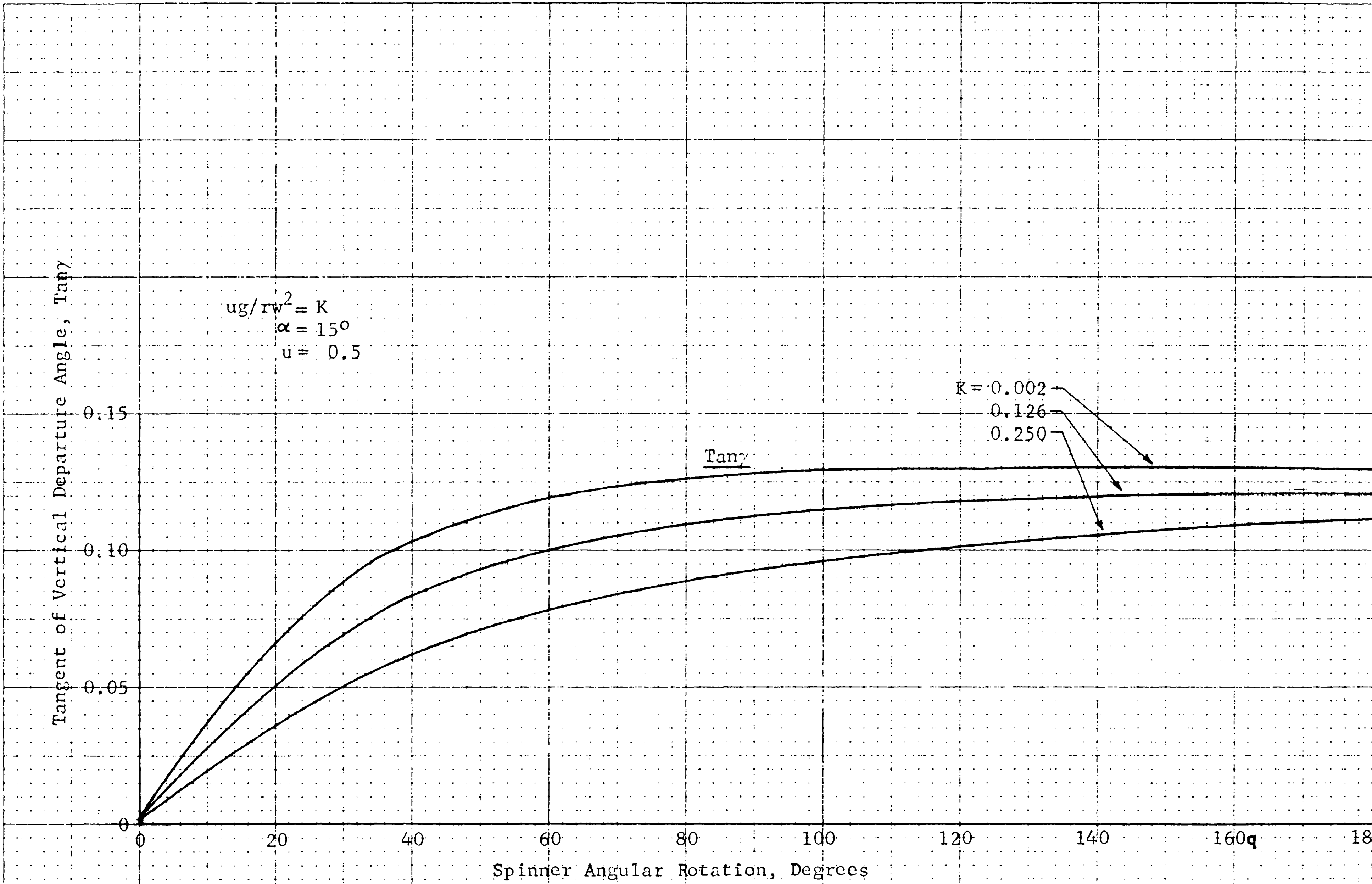

Figure 94 Dynamic Characteristics for Cone-Shaped Spinner

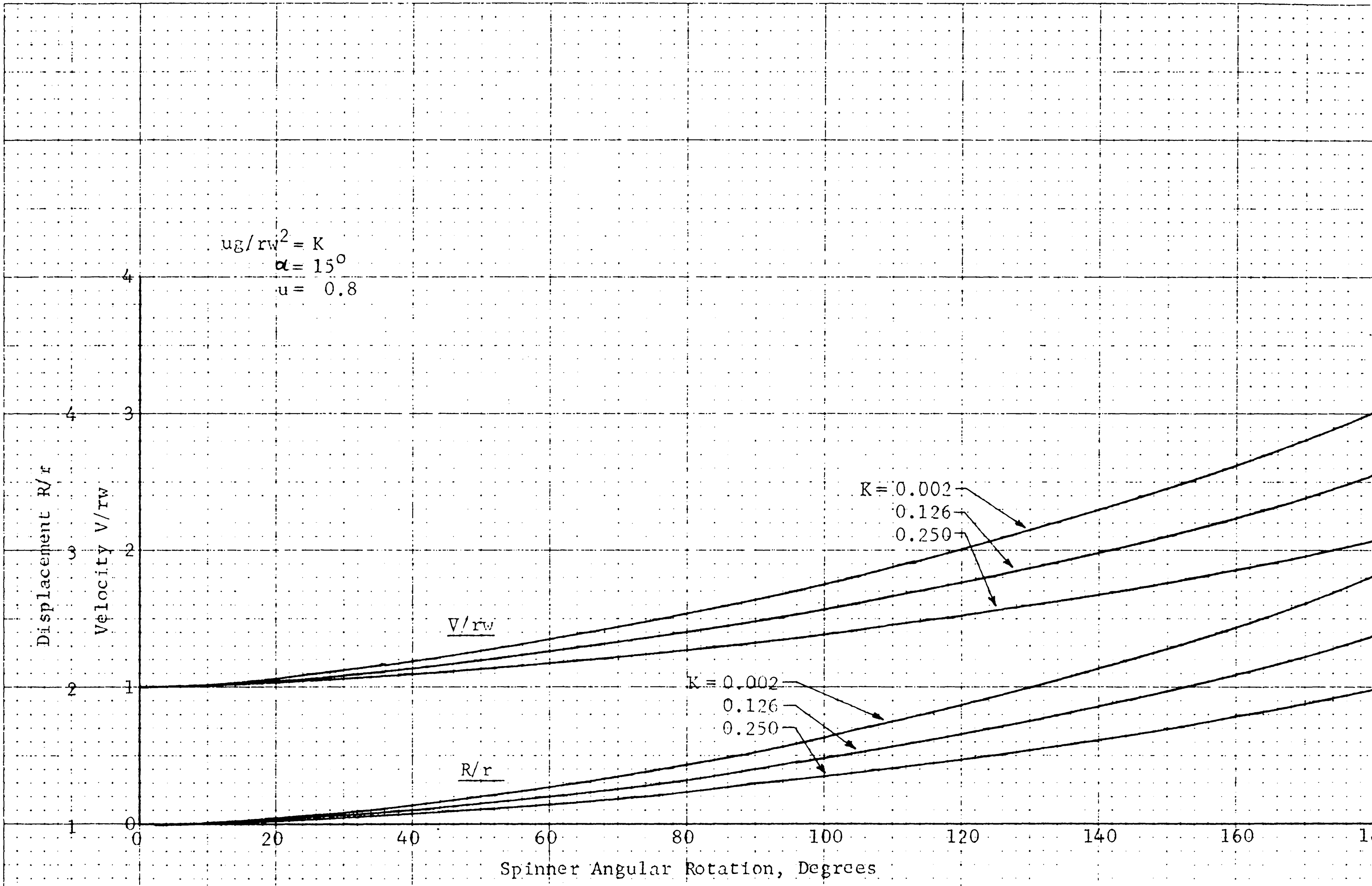

Figure 95 Dynamic Characteristics for Cone-Shaped Spinner

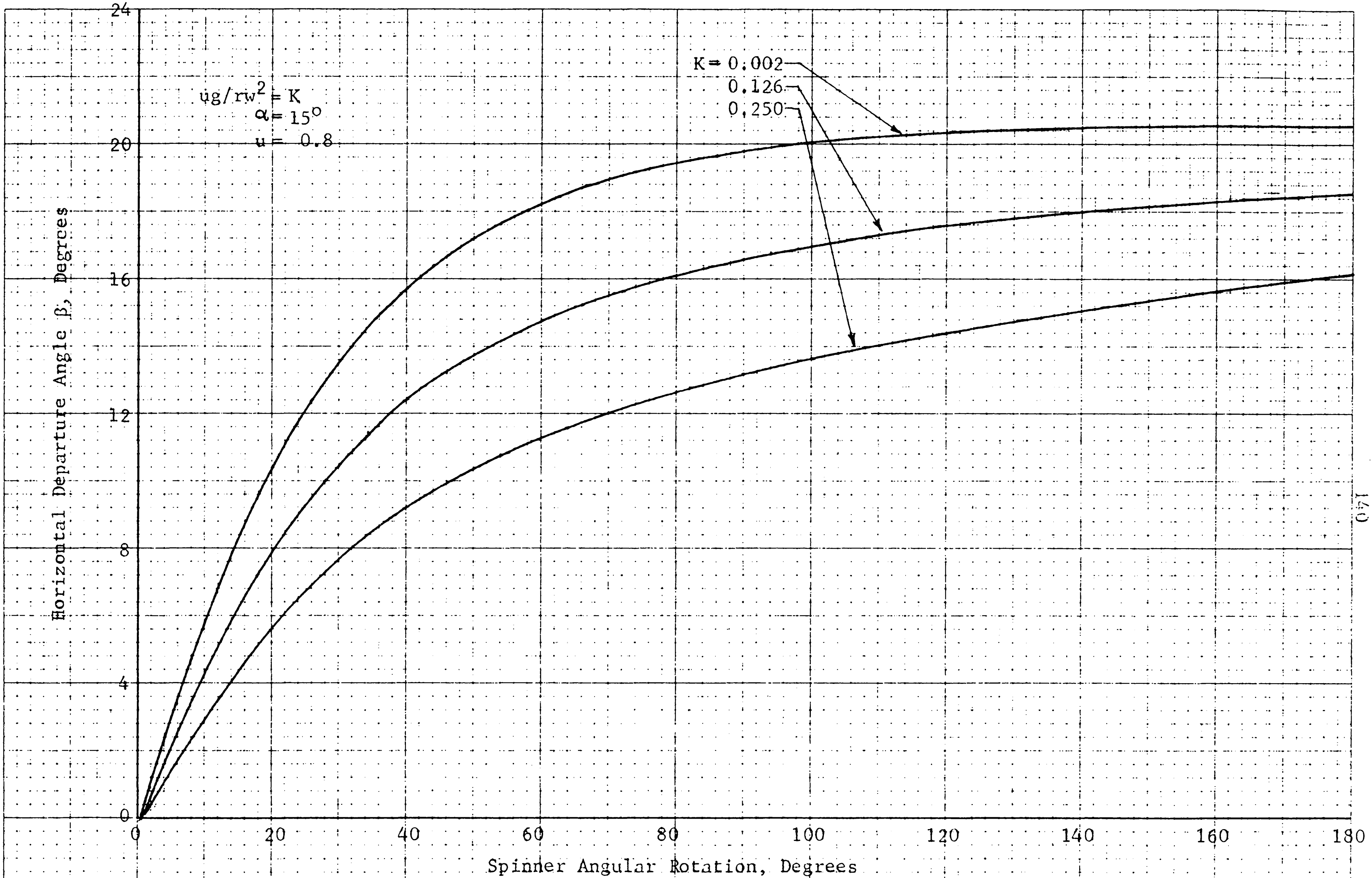

Figure 96 Dynamic Characteristics for Cone-Shaped Spinner

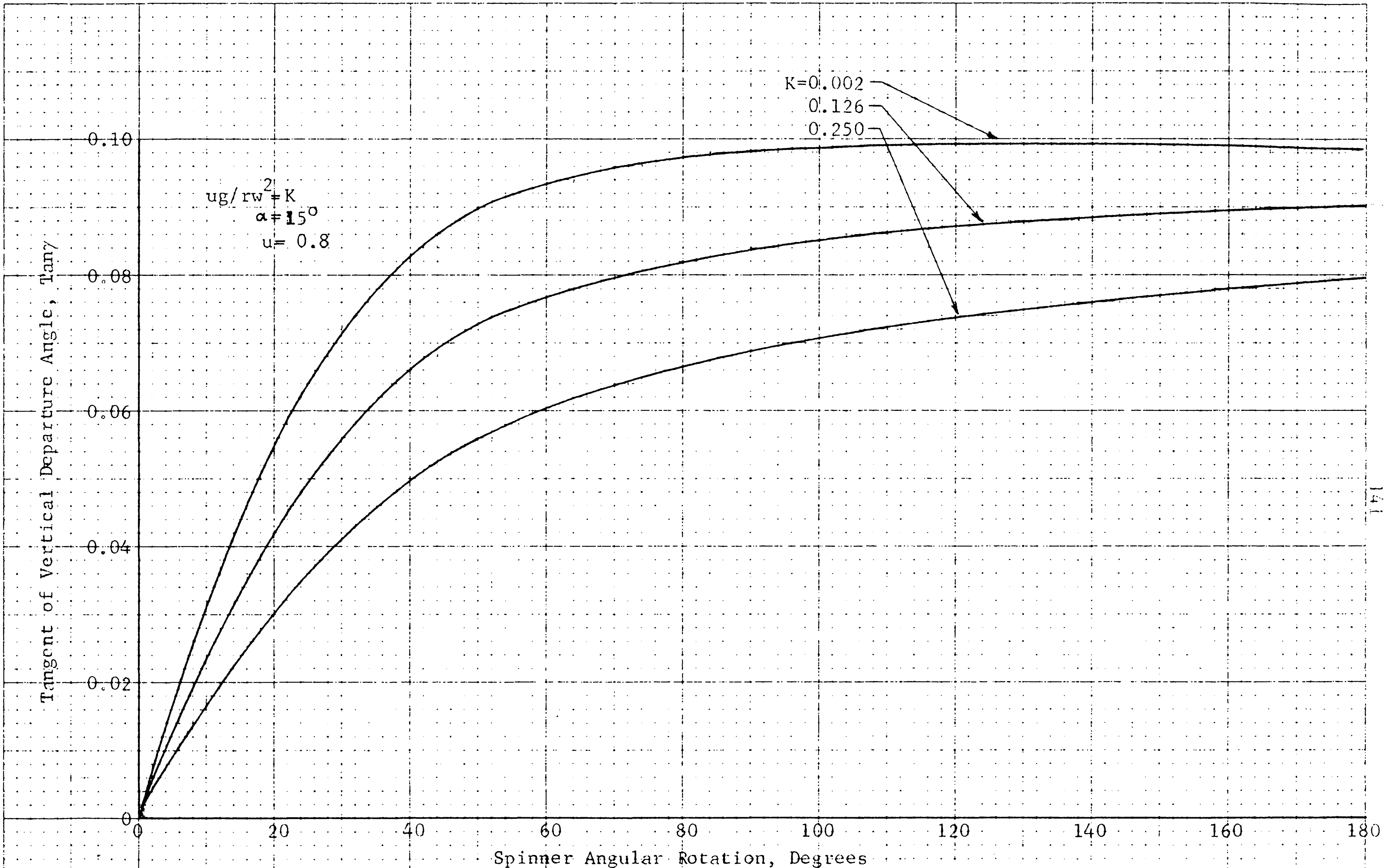

Figure 97 Dynamic Characteristics for Cone-Shaped Spinner

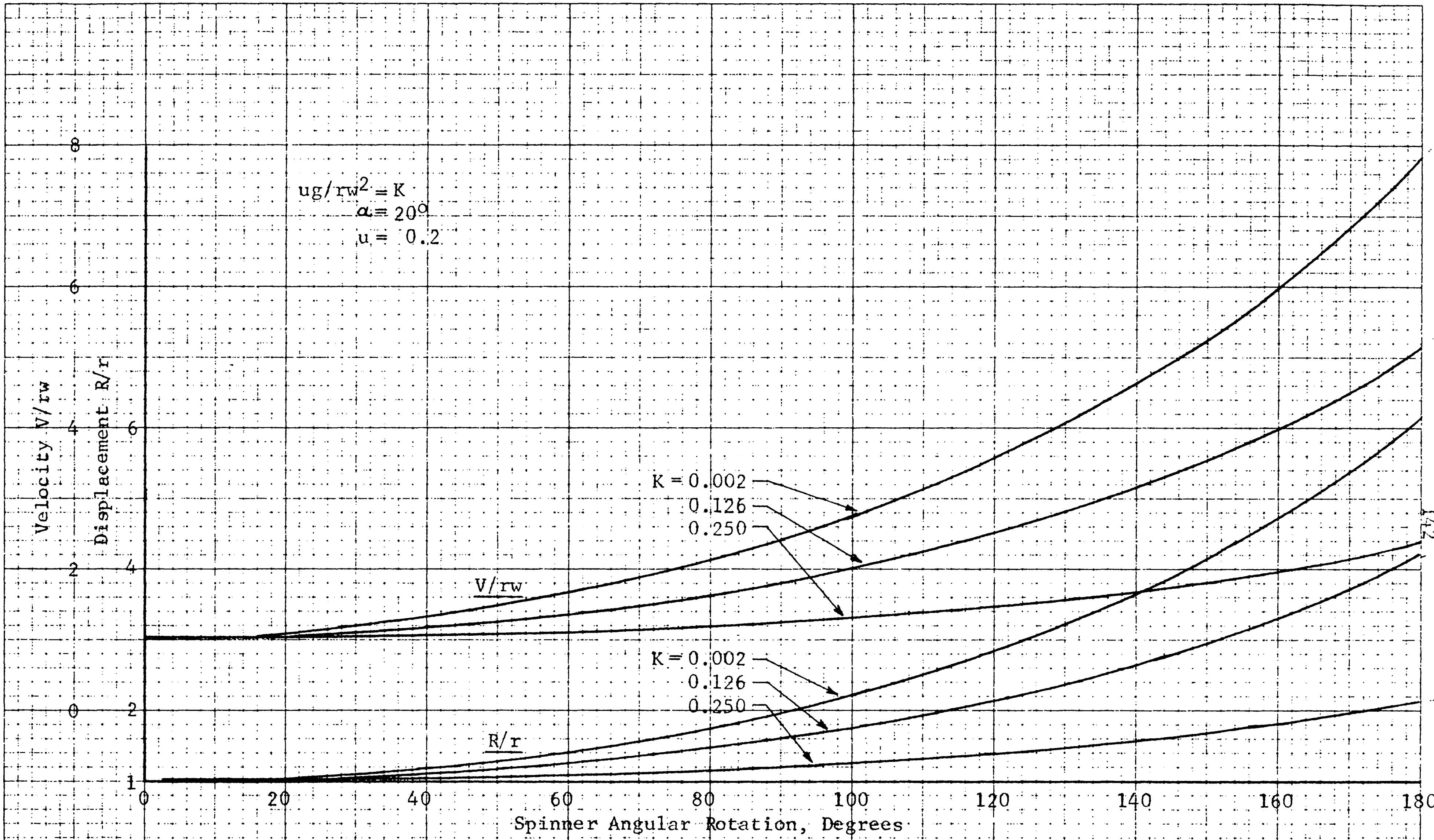

Figure 98 Dynamic Characteristics for Cone-Shaped Spinner

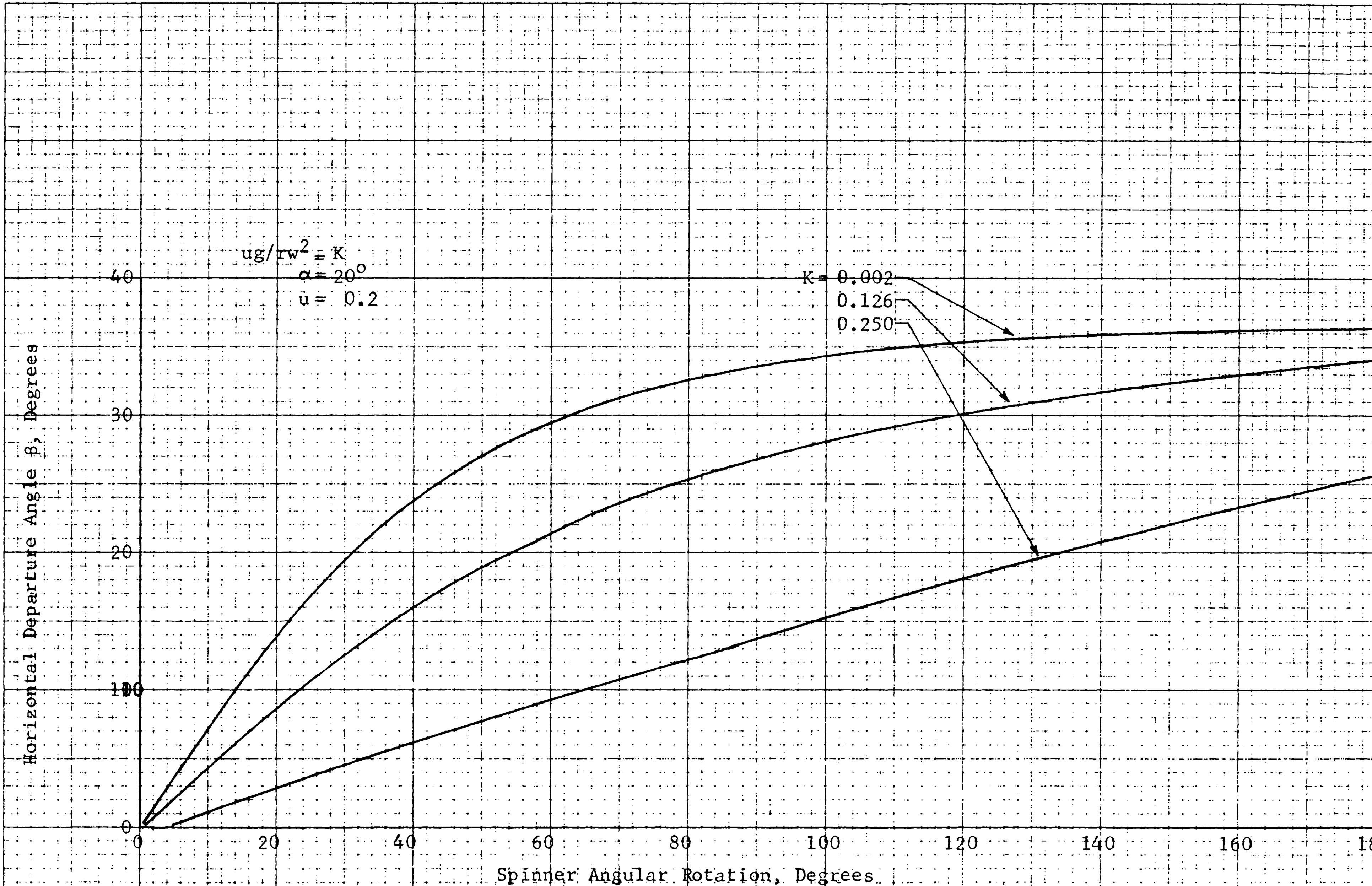

Figure 99 Dynamic Characteristics for Cone-Shaped Spinner

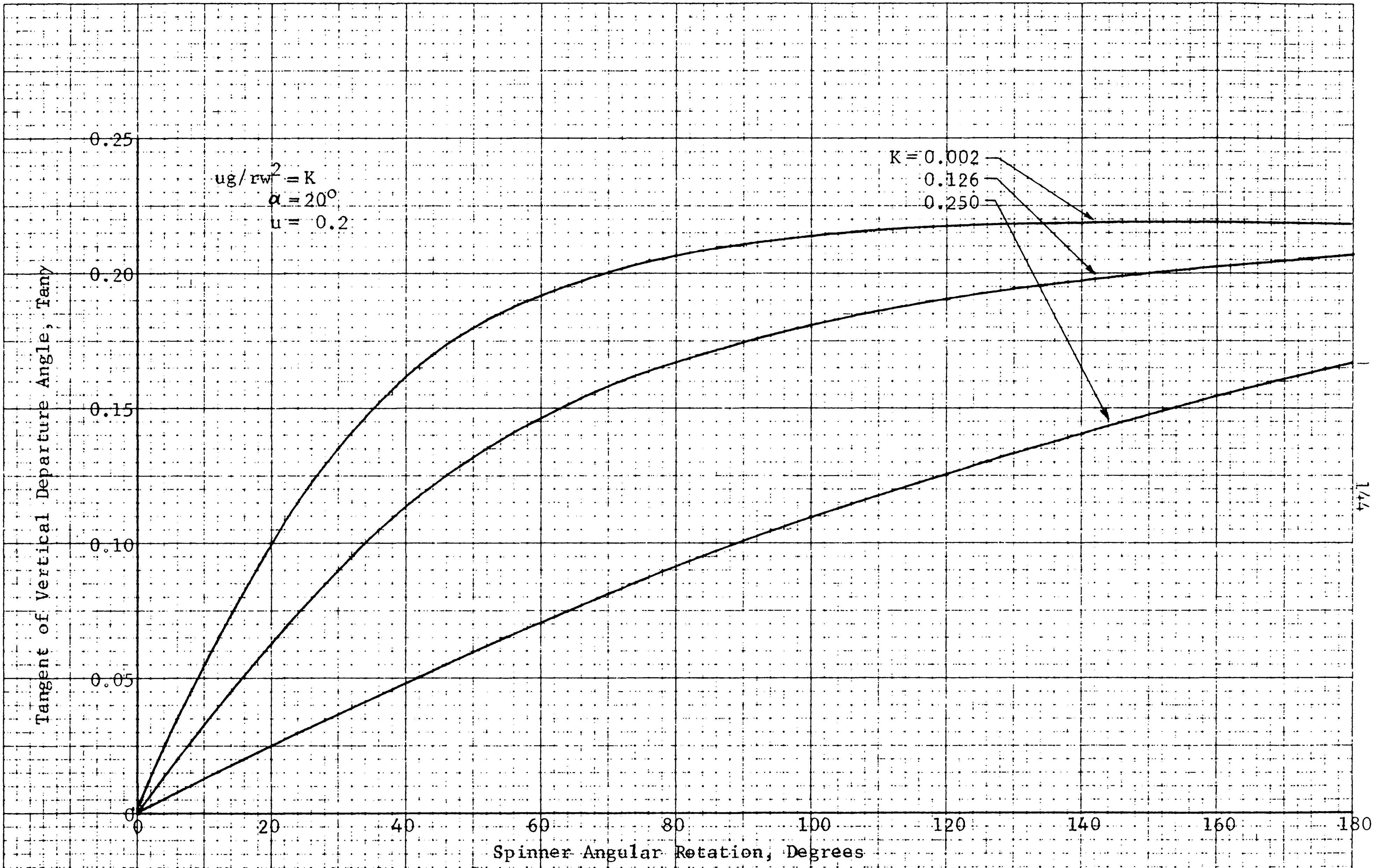

Figure 100 Dynamic Characteristics for Cone-Shaped Spinner

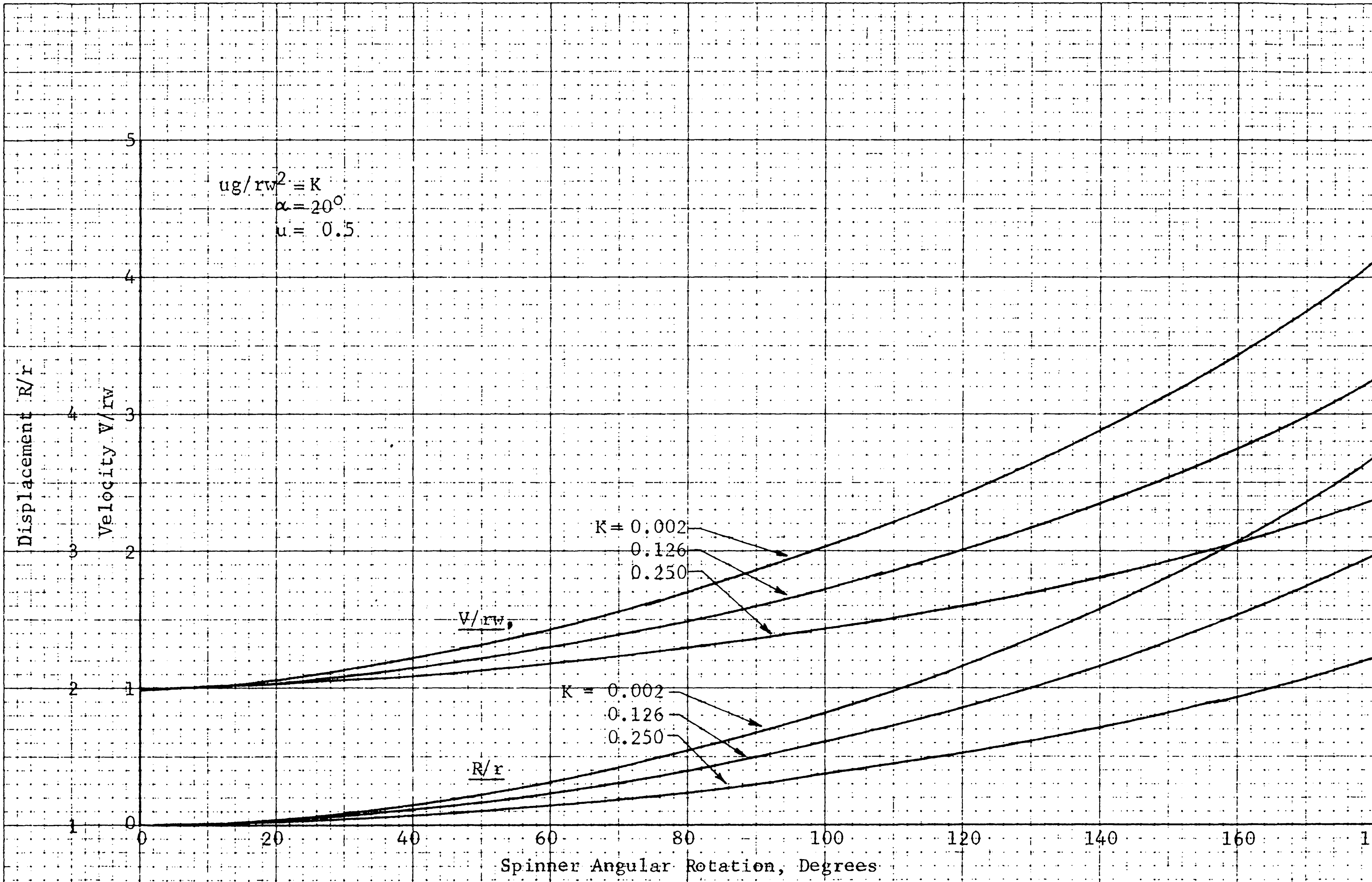

Figure 101 Dynamic Characteristics for Cone-Shaped Spinner

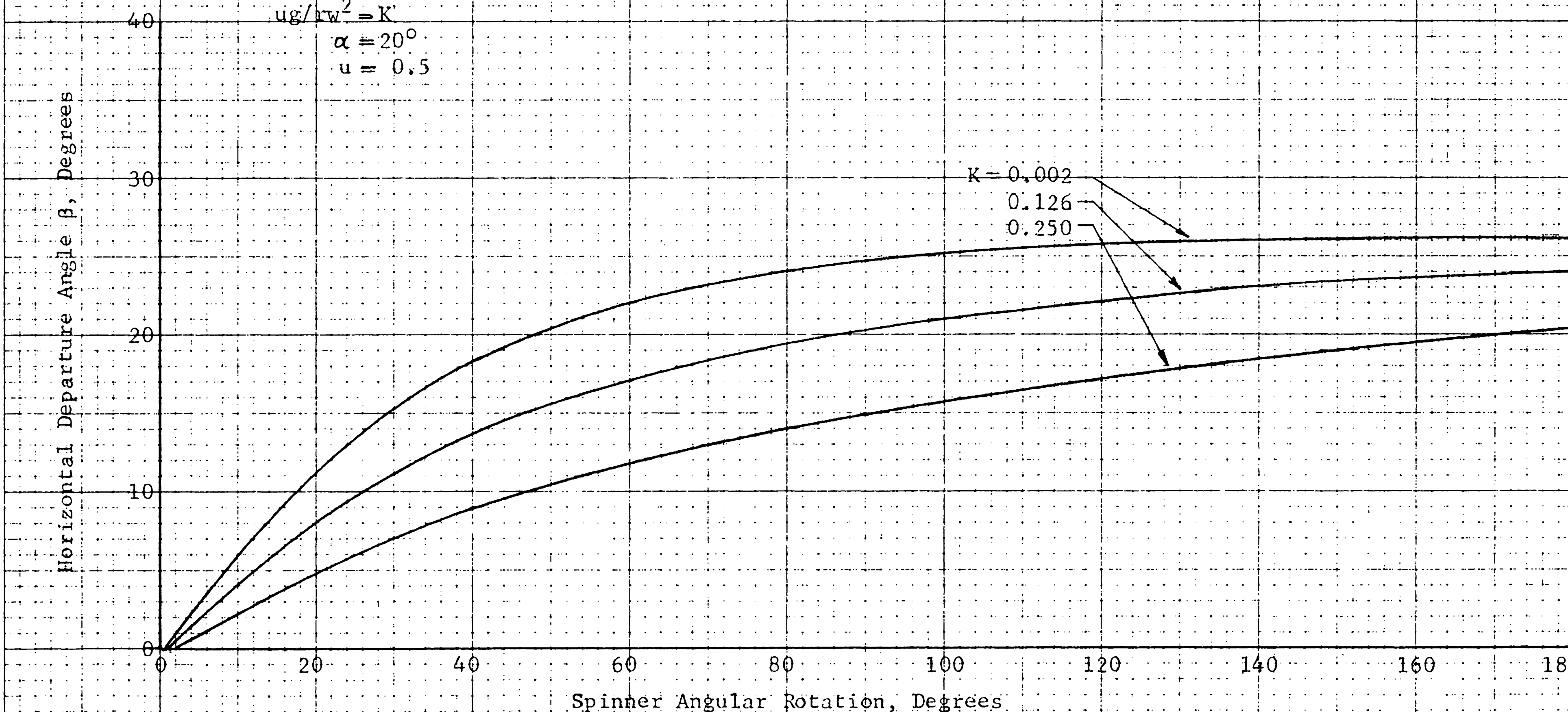

Figure 102 Dynamic Characteristics for Cone-Shaped Spinner

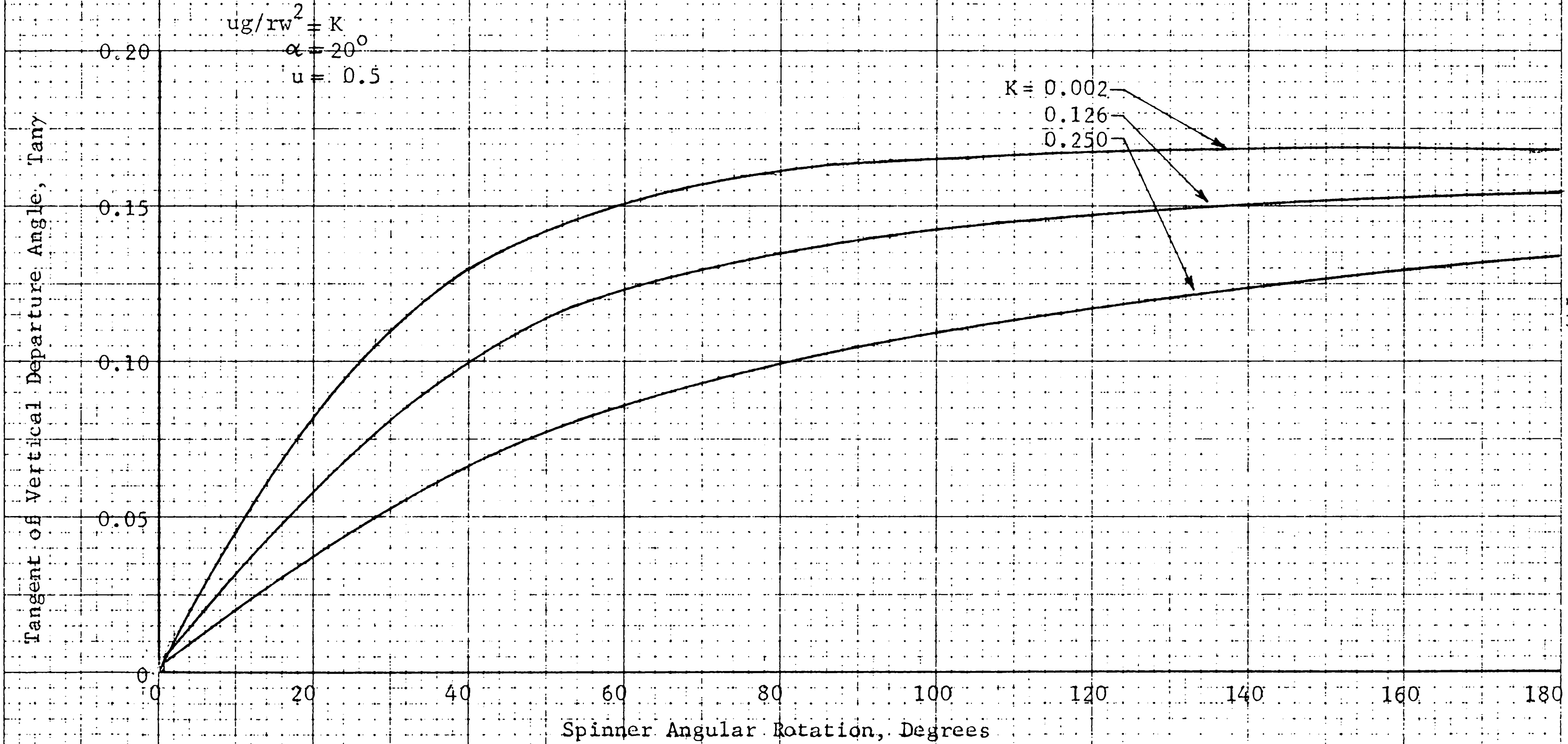

Figure 103 Dynamic Characteristics for Cone-Shaped Spinner

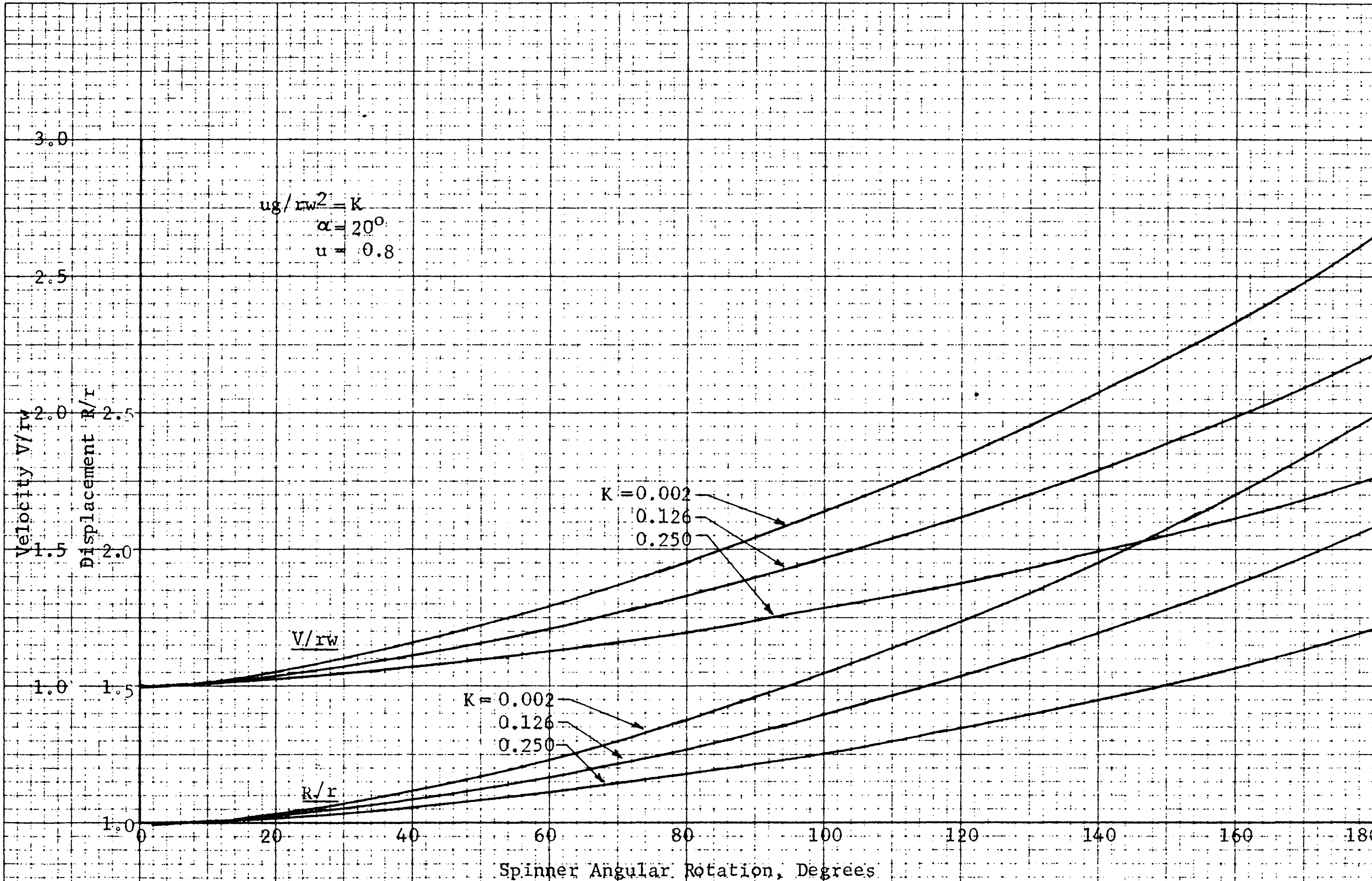

Figure 104 Dynamic Characteristics for Cone-Shaped Spinner

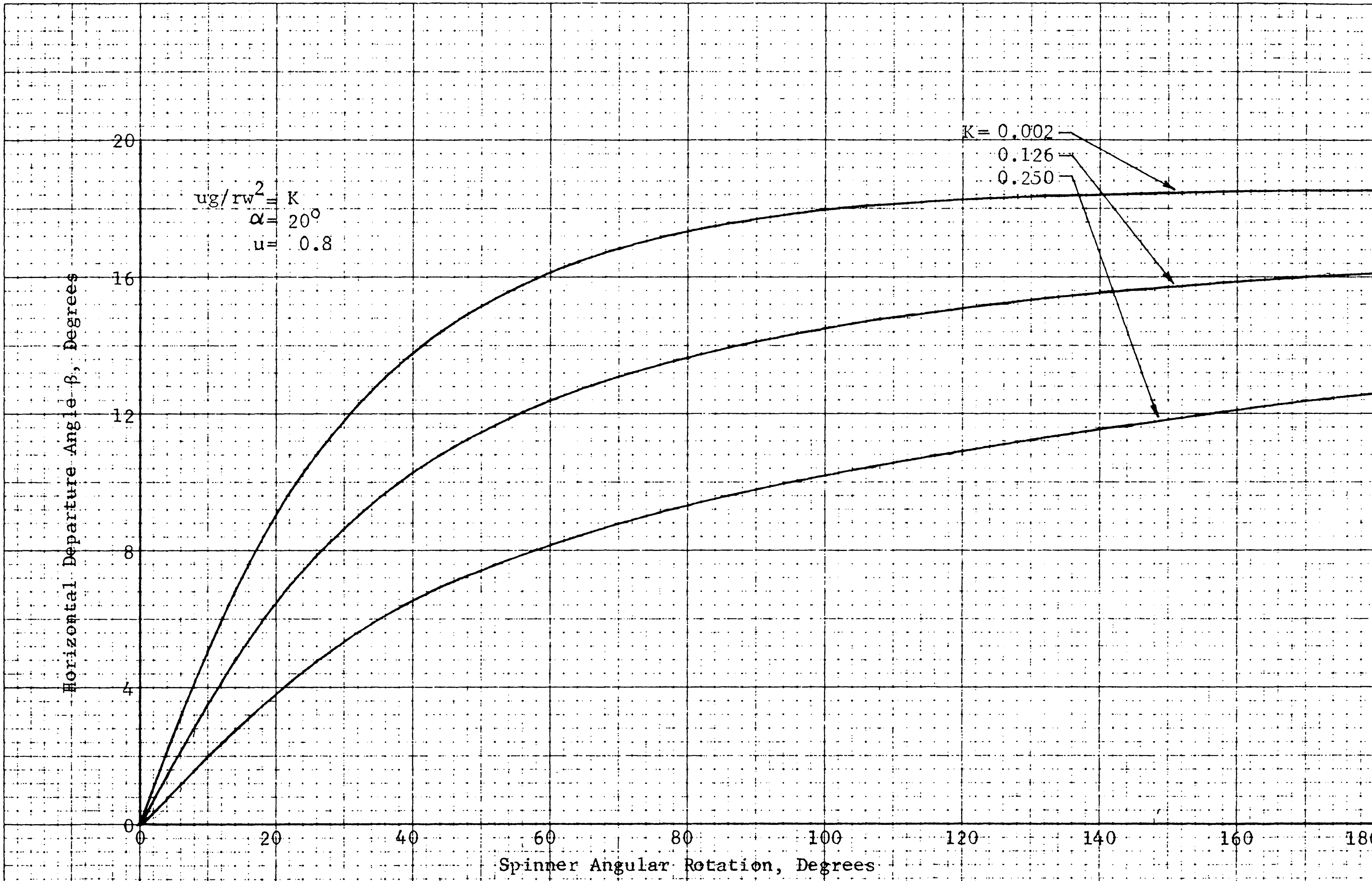

Figure 105 Dynamic Characteristics for Cone-Shaped Spinner

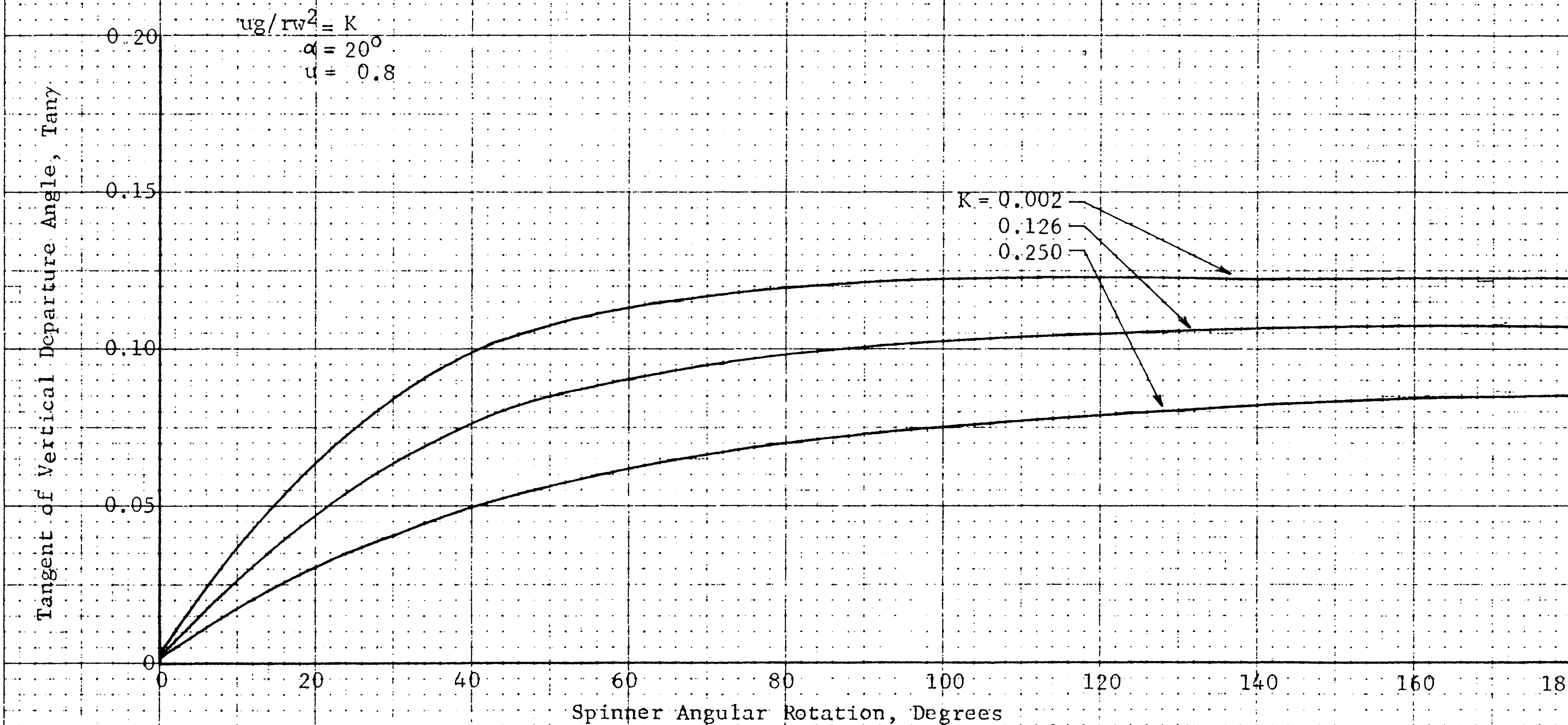

Figure 106 Dynamic Characteristics for Cone-Shaped Spinner

COMPUTER SOLUTION OF EQUATIONS FOR THREE CENTRIFUGAL DISTRIBUTOR CONFIGURATIONS

by

Hormoz Alizadeh

ABSTRACT

Centrifugal distributors are used extensively for the broadcast application of granular materials such as seed, granular fertilizer, and agricultural chemicals. A major problem with this equipment is nonuniform spreading which frequently results in reduced crop yield.

The object of this study was to provide information required for more satisfactory design of spreading equipment. The equations representing the motion of granular particles along the blades of three centrifugal distributor configurations were solved with the aid of an electronic analog computer. Straight, forward and backward-pitched blades and logarithmically spiraled blades, all on flat distributor bases, were studied. Straight radial blades on a concave, cone-shaped base were also investigated.

The results of this study were presented in graphs. Displacement, velocity, and departure angle versus the angular rotation of the distributor were plotted for a large range of parameters for each configuration. These variables were expressed in dimensionless form. From a study of the graphs it was noted that of all configurations investigated, the radial-blade arrangement requires the smallest rotational displacement of the distributor to impart a specified velocity to granular material. As the pitch is increased, greater rotation is required. For a given amount

of distributor rotation, higher values of the coefficient of friction cause a reduction in both displacement of the particle along the blade and its final velocity. The effect of increasing the ratio of gravity-induced friction force to centrifugal force is similar but smaller than the effect of increased friction alone.